PROVENANCE AND BASIN TECTONICS OF OLIGOCENE-

MIOCENE SEQUENCES OF THE BENGAL BASIN,

BANGLADESH

Except where reference is made to the work of others, the work described in this thesis is my own or was done in collaboration with my advisory committee. This thesis does not include proprietary or classified information.

_____

Khandaker Zahid

Certificate of Approval:

_____

Charles E. Savrda
Professor
Geology and Geography

_____

Ashraf Uddin, Chair
Associate Professor
Geology and Geography

_____

Willis E. Hames
Associate Professor
Geology and Geography

_____

Stephen L. McFarland
Dean
Graduate school

PROVENANCE AND BASIN TECTONICS OF OLIGOCENE-MIOCENE SEQUENCES OF THE BENGAL BASIN, BANGLADESH

Khandaker Zahid

A Thesis
Submitted to
the Graduate Faculty of
Auburn University
in Partial Fulfillment of the
Requirement for the
Degree of
Master of Science

Auburn, Alabama

December 16, 2005

PROVENANCE AND BASIN TECTONICS OF OLIGOCENE-MIOCENE SEQUENCES OF THE BENGAL BASIN, BANGLADESH

Khandaker Zahid

_____

Khandaker Zahid

_____

Date

Style Manual or journal used

Geology

Computer software used

Microsoft Word 2003

Microsoft Excel 2003

Adobe Photoshop 7

Rockwork 2004

Rockware Utilities 3

VITA

Khandaker Zahid was born on July 14th, 1976, in Bangladesh. He attended St. Xavier's elementary school and Chittagong Collegiate school before completing his B.Sc. (Honors) and M. Sc. in Geology from University of Dhaka, Bangladesh. He moved to Auburn University to pursue his second Masters in the Department of Geology and Geography in January 2003. Mr. Zahid's primary research interest lies mainly in syn- to post-orogenic sediments and orogenic history of mountain belts. He has been involved in research on a foreland basin in eastern Himalayas since his undergraduate years. He plans to continue his education and research on a Ph D. degree.

THESIS ABSTRACT

PROVENANCE AND BASIN TECTONICS OF OLIGOCENE-MIOCENE SEQUENCES OF THE BENGAL BASIN, BANGLADESH

Khandaker Zahid

Master of Science, December 16, 2005

162 typed pages

Directed by Dr. Ashraf Uddin

Oligocene and Miocene strata of the Bengal basin, Bangladesh, show significant changes in sediment composition and record sediment-input history from different sources adjacent to the basin. Oligocene Barail sands ($Qt_{70}F_2L_{28}$) are quartzolithic with rare to no feldspars. Dominance of quartz, presence of some lithic fragments and paucity of feldspar suggest erosion from a low-relief area under strong chemical weathering. The source area could have been the Indian craton. Minor contribution from the Indo-Burman ranges can not also be ruled out. Miocene Surma sandstones ($Qt_{59}F_{23}L_{18}$) are quartzolithic to quartzofeldspathic and have comparatively high feldspar and lithic contents. This change may represent the initiation of uplift and erosion of the Himalayas.

Oligocene heavy minerals are dominated by opaque and ultra-stable minerals, whereas the Miocene sediments show fewer opaque grains and contain garnets. Textural and mineralogical maturity of the heavy minerals along with the presence of

chrome spinel in the Oligocene sediments suggests a relatively short transport distance and a proximal source, which could be the Rajmahal Trap (located adjacent to the northwestern part of the basin). However, presence of epidote, garnet, and aluminum-silicate minerals (sillimanite) in Lower Miocene units indicate the possibility of input from an orogenic source from the eastern Himalayas and the Indo-Burman ranges. Detrital garnets in Miocene sediments are mostly almandine-rich with varied pyrope and low grossular content. These garnets indicate provenance from medium- to low-grade regionally metamorphosed rocks of the Higher Himalayas and high-grade metamorphic rocks of the Indian craton. Chrome spinel data of Oligocene sediments show that the spinels have high chromium content (average 42%) and wide range in TiO_2 wt% (0.3 to 3%). These spinels might have been derived from the Alpine-type ophiolites in the Indo-Burman ranges and the Rajmahal Trap. Tourmaline and calcic amphibole data from the Bengal basin also indicate a dominantly low-grade and metasedimentary provenance with minor contribution from granitoid and pegmatitic rocks.

High sedimentation rates, extremely low permeability of confining units, and very high compressibility are the main reasons for overpressure in Miocene strata at three of the studied structures (Titas, Bakhrabar, and Rashidpur). However, a combination of factors, including strong horizontal deviatoric regional stress from the advancing Indo-Burman ranges and uplift produced by fault propagation folding and concomitant shale diapirism are responsible for overpressure in the Sitakund structure of eastern fold belt. Absence of overpressure in the Oligocene strata in the Bengal basin indicates apparent lack of any significant orogeny in the east.

The transition from the Oligocene to Miocene strata records changes in sediment composition and input from additional sources to the basin depocenters. The basin received sediments mostly from the Indian craton during the Oligocene time with minor input from the Rajmahal Trap to the west and distant orogenic belts to the east. At the beginning of the Miocene time, the Bengal basin moved proximal to the encroaching Himalayan and the Indo-Burman orogenic belts, and started receiving sediments from the north and the east.

ACKNOWLEDGMENTS

Many people and organizations have made contributions without which this work would have been impossible. I would not have been able to complete this thesis without the support of my principal advisor Dr. Ashraf Uddin. He provided the opportunity to come to the United States, gave suggestions about a possible research topic, and guided me all the way through to the writing of this thesis. Dr. Uddin motivated me immensely to bring out the best in my research. His view of getting to the “bottom of the Himalayas” has kept me focused on the use of a rather regional project to a broader perspective of eastern and western Himalayas. In the present world of increasing specialization, his guidance helped me to stay open to the fields of sedimentary geology and tectonics and to accept the new ideas that are constantly evolving.

I would also like to express my gratitude to my other advisors, Drs. Charles E. Savrda and Willis E. Hames. My understanding of the subject has been greatly influenced by both of them. Dr. Savrda’a suggestions regarding sedimentary petrology and stratigraphy were very helpful and helped improve my writing. Dr. Hames helped tremendously with the mineral chemistry and geochronology.

Partial funding for this research came from National Science Foundation, Geological Society of America, and Auburn University. I would like to thank the Department of Geology and Geography at Auburn University for providing me support through a graduate teaching assistantship. I also would like to thank the faculty members of the geology department in University of Dhaka for their help during field investigations and sample collection. My gratitude also goes to Mr. Mir

Moinul Huq and Ms. Anwara Haque of Bangladesh Oil, Gas and Mineral Corporation (Petrobangla) for their support with data and reports. Thanks are due to my fellow graduate students, especially Pranav Kumar, Trent Godwin, and Wayne McDonald, for their support and friendship.

Last, but not the least, I express my devotion to my beloved parents and sister for their spiritual and moral support without which life would have been much harder. I thank God for the strength that made me able to finish this project, which is ‘dream come true’ for me.

TABLE OF CONTENTS

Page

LIST OF FIGURES

LIST OF TABLES

Page

CHAPTER 1. INTRODUCTION

1.0 INTRODUCTION

Sedimentary basins associated with mountain systems constitute an important repository of information on tectonic and erosional evolution. Provenance studies can provide important constraints on the processes and history of mountain building. Crustal thickening formed by convergence produces dramatic surface relief resulting in rapid erosion and accumulation of clastic detritus into subsiding flanking basins. Analysis of such basins provides the opportunity to analyze depositional environments, nature and timing of changes in composition and sedimentation style, and sediment sources.

Compositional analysis of detrital sediments is a powerful tool in tracing provenance (Dickinson, 1970, 1982; Ingersoll et al., 1984; Ingersoll et al., 1995). Petrofacies analyses can distinguish various tectonic settings and help understand and interpret plate interactions in the geologic past (Graham et al., 1976; Ingersoll, 1978; Dickinson and Suczek, 1979; Dickinson, 1982). Composition of detrital sediments is controlled by various factors, including source rocks, modes of transportation, depositional environments, climate, and diagenesis (Suttner, 1974; Ingersoll et al., 1984). Provenance studies that focus on certain key attributes of detrital mineralogy provide important constraints on basin evolution and unroofing history of mountain belts (Dorsey, 1988; Uddin and Lundberg, 1998a). Reconstruction of provenance from detailed mineralogical analyses is based on the assumption that depositional

environments, modes of transportation, climates, and diagenesis have not significantly altered detrital grain composition (Basu, 1976).

The Bengal basin in the northeastern part of Indian subcontinent, between the Indian Shield to the west and north and the Indo-Burman Ranges to the east, covers Bangladesh, parts of the West Bengal and Tripura states of India, and the Bay of Bengal (Fig. 1). The Bengal basin owes its origin to the collision of India with Eurasia and Burma, which built the extensive Himalayan and Indo-Burman Ranges and loaded the lithosphere to form flanking sedimentary basins.

The Sylhet trough is a sub-basin of the Bengal basin in northeastern Bangladesh. It is a tectonically complex province bounded by the Indian shield, Shillong plateau, and the Chittagong hills of the Indo-Burman ranges (Fig. 2). This is the only region where Paleogene sediments are exposed in the Bengal basin (Fig. 3). This trough contains a thick (12-16 km) fill of late Mesozoic and Cenozoic strata (Hiller and Elahi, 1988). Early Paleogene history of the Bengal basin was characterized by sedimentation on a passive continental margin formed during Mesozoic rifting and opening of the Indian Ocean (Sclater and Fisher, 1974). The Sylhet trough likely occupied a transitional setting on this margin between a shelf to the northwest and the basin to the southeast. Subsidence may have increased slightly during the Oligocene in response to crustal loading from the developing Indo-Burman Ranges (Brunnschweiler, 1974; Mitchell, 1993). Oligocene strata exposed on the northeastern margin of the Sylhet trough are fluvial, but probably grade basinward (to the southwest) over a short distance into deltaic and prodeltaic deposits (Johnson and Nur Alam, 1991).

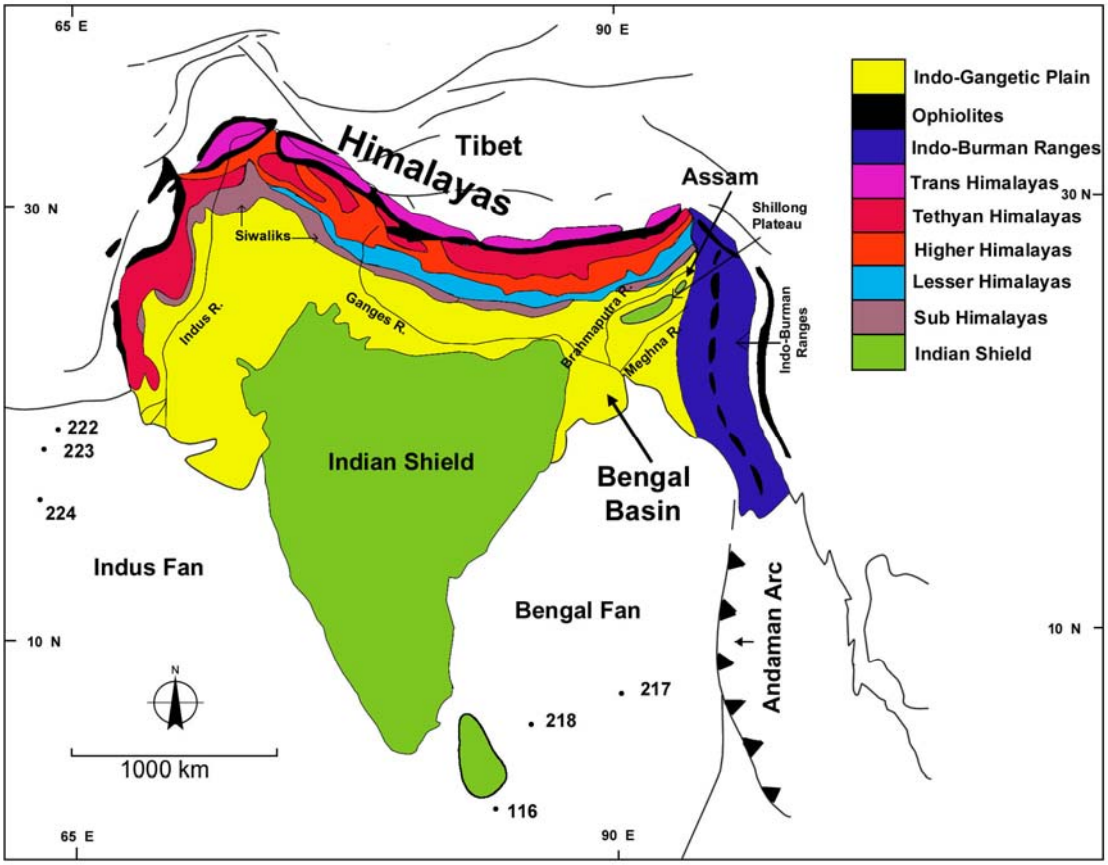

Figure 1. Map showing major tectonic elements near the study area, including the Bengal Basin, Assam Basin, and their possible source terrains, the Himalayas and the Indo-Burman ranges. This figure also shows locations of DSDP and ODP sites in the northern Indian Ocean (after Uddin and Lundberg, 1998a).

The provenance history of Paleogene sediments in the Bengal basin is not well known. There are currently two schools of thought regarding the provenance history of the Paleogene sediments of the Bengal basin. One holds that the sands were derived from the nearby Indian craton (Uddin and Lundberg, 1998a), while the other proposes that they were derived from the eastern Himalayas during their primary phase of uplift (Johnson and Nur Alam, 1991). Both ideas are based on evidence from only a limited number of samples from the Bengal basin. These studies also have suggested that the Bengal basin had been receiving orogenic detritus during Miocene time. The present stratigraphic framework of Bengal basin was developed based on the type area located in Assam, northeast India (Evans, 1964; Brunnschweiler, 1980). Bengal and Assam are, however, two separate basins with different tectonic and geomorphic histories (Kumar, 2004). Sedimentary packages that fill these two basins differ in thickness, composition, and inherent flow directions. A detailed petrographic study of provenance of Paleogene sediments of the Bengal basin was conducted for this study in attempt to better understand the provenance history. Transitional sediments of Paleogene-Neogene (Oligocene-Lower Miocene) age also have been studied to record critical changes in provenance and tectonic history (i.e., the change from pre-orogenic (?) to orogenic). Samples representing this significant time were widely available in exposed sections and sediment cores collected during petroleum exploration in the Bengal basin.

1.1 STUDY AREA

The main study area for this project is the Sylhet trough, which is a sub-basin of the Bengal basin in northeastern Bangladesh. Most of the samples for this study were collected from the Sylhet trough (Fig. 2). The trough lies in the frontal zone of

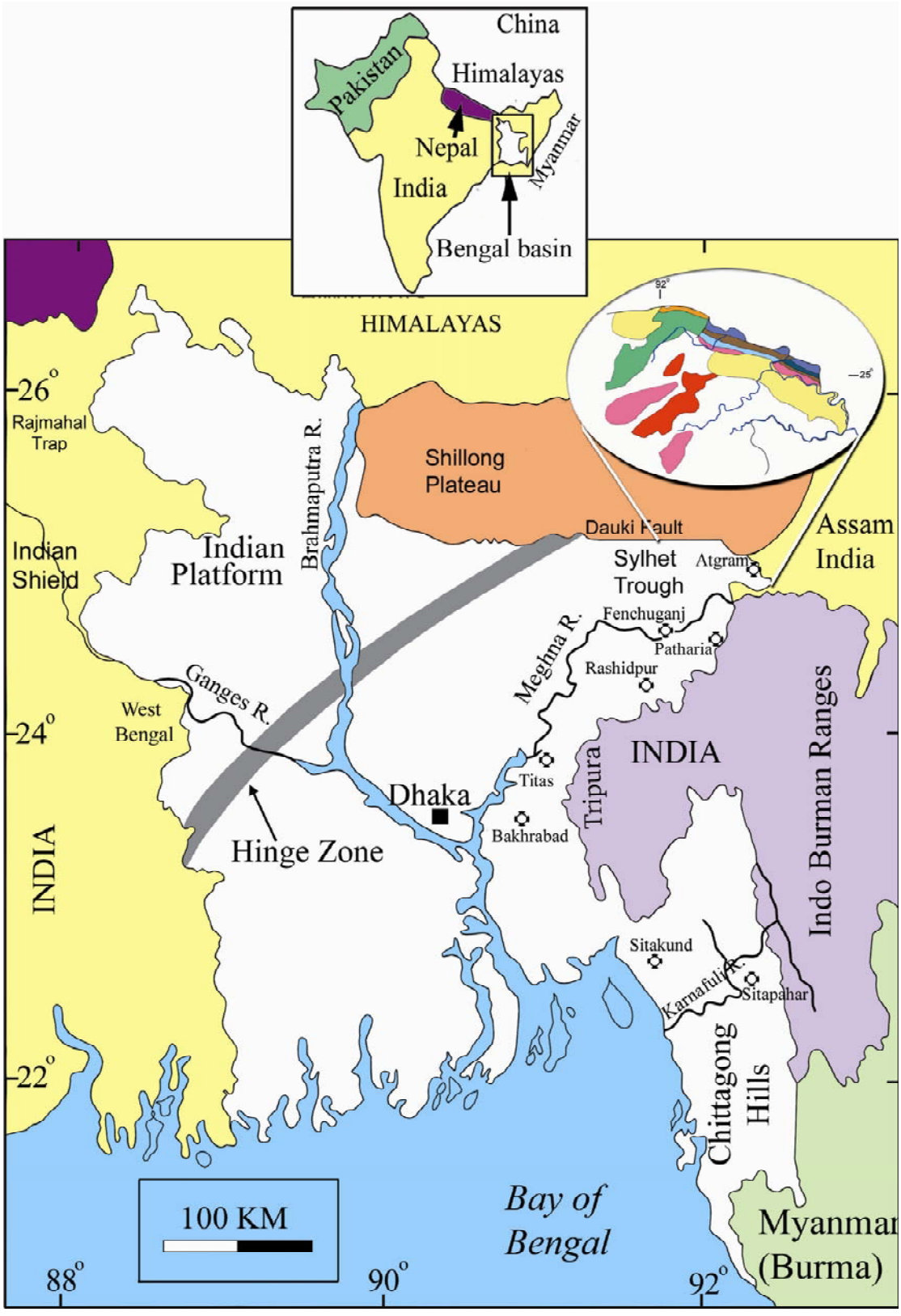

Figure 2. Map of the Bengal basin and the principal study area in the Sylhet trough (inset). A blown-up view of the inset is shown in figure 3. Most of the Lower Miocene core samples were collected from the Sitakund structure. Other samples of Miocene age are from Atgram, Patharia, Fenchuganj, and Titas structures (after Uddin and Lundberg, 1999).

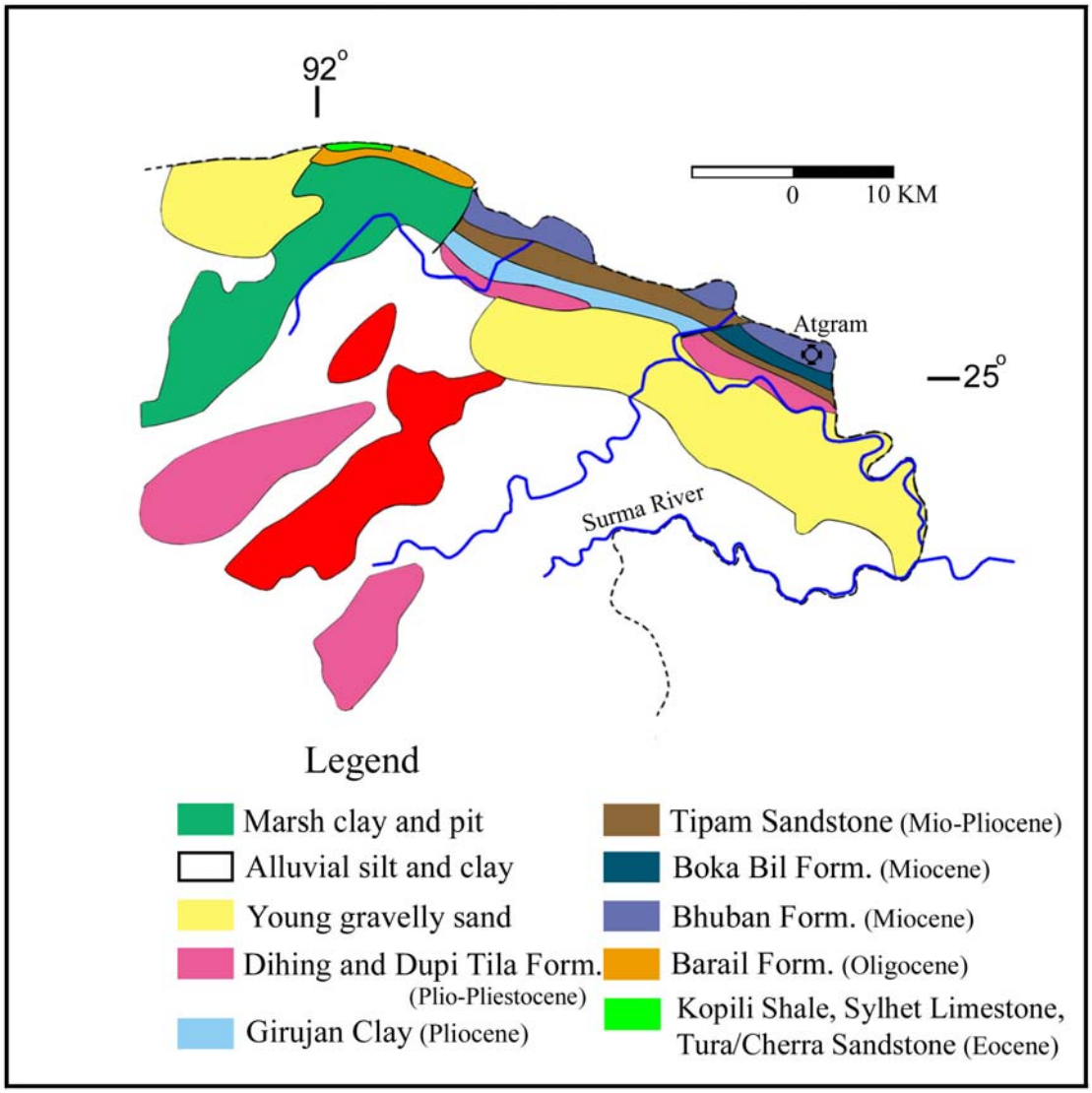

Figure 3. Outcrop map of the sequences exposed in northern Sylhet trough from which most of the samples have been collected from the Barail, Bhuban and Boka Bil formations (after Ahmed, 1983). Detailed stratigraphic position of these units is shown in Table 1.

the Indo-Burman ranges to the east. It is bounded to the north by the Shillong Plateau, which is underlain by a basement complex of Archean gneiss and greenstone and Late Proterozoic granite. Few core samples were collected from Sitakund, Titas, Patharia, Fenchuganj, and Atgram structures of the eastern folded belt (Fig. 2). Sampled cores were drilled by oil companies and were collected from their repositories.

1.2 PREVIOUS WORKS

Others have worked on various aspects of the Paleogene and Neogene sediments of the Sylhet trough. A geological study of the eastern and northeastern part of Sylhet trough was first carried out by the Geological Survey of Bangladesh in 1966. J.F. Holtrop and J. Keizer published a correlation of wells from the Sylhet trough in 1970 (Holtrop and Keizer, 1970). They mainly focused on the subsurface correlation scheme in the unexposed and poorly exposed parts of the trough and concluded that the delta built outward from east to west. Khan (1978) published a reconnaissance geological map that encompasses the entire Tertiary succession of the area, except the Sylhet Limestone. Ahmed (1983) mapped the Oligocene stratigraphy of Sylhet trough and proposed boundaries between stratigraphic units. Johnson and Nur Alam (1991) extensively worked on sedimentation and tectonics of the Sylhet trough for the Geological Survey of Bangladesh and funded by the Asian Development Bank. They predicted that incipient uplifts of the eastern Himalayas supplied sediments to Sylhet trough during the Oligocene. Uddin and Lundberg (1998a,b) worked on sand composition and heavy minerals of Cenozoic strata of the basin. In contrast to previous authors, they concluded that Oligocene sediments were derived from the Indian Craton instead of the eastern Himalayas. Their heavy mineral study (Uddin and Lundberg, 1998b) of the Bengal basin also shows a more cratonic

source for Eocene to Oligocene sediments and an orogenic source for the Miocene and younger sediments. Worm et al. (1998) evaluated sedimentation rates using magnetostratigraphy of part of Cenozoic successions in northeastern Bangladesh. They estimated average sedimentation rate and the rate of delta subsidence to have been ~1.2 km/m.y., which they noted to be one of the highest rates ever sustained for millions of years. Sikder and Alam (2003) worked on the structural development of the eastern fold belt and discussed the affect of convergence of the Indo-Burman plate on the development of the folds in that region. Uddin and Lundberg (2004) studied the Miocene sedimentation of Sylhet trough and southern Bengal basin. They demonstrated the timing of subsidence of Sylhet trough and direction of deltaic progradation during Miocene.

Rahman and Faupl (2003) studied detrital geochronology of sandstones of the Miocene Surma Group based on the stepwise-heating Ar^{40}/Ar^{39} method (McDougall and Harrison, 1988) for multigrain samples of white mica. They found that most samples yielded plateau age of ca. 24 Ma and concluded that sediments were derived from the eastern Himalayas.

Heavy-mineral studies have been done locally and regionally in the Himalayan system to assess the nature of source rocks, the routing of the ancestral fluvial systems, and the relationship of source rocks to unroofing history (Sinha and Sastri, 1973; Thompson, 1974; Johnson et al., 1985; Cerveny et al., 1989; Uddin and Lundberg, 1998b; Uddin et al., 2002; Kumar, 2004). Kumar (2004) noted low-diversity heavy-mineral assemblages in the Paleogene and high-grade, diverse assemblages in the Neogene of Assam. He attributed this change to orogen-scale unroofing of arc-type rocks in the Himalayas in the Neogene.

CHAPTER 2: TECTONIC SETTING AND REGIONAL GEOLOGY

2.0 INTRODUCTION

In order to comprehend the paleo-tectonic history of the basin, it is essential to view the greater Bengal Basin in its regional perspective. The dynamic nature of the basin can be attributed to the interaction of three plates; the Indian, Tibetan (Eurasian), and Burma (West Burma Block) plates. The intensity and pattern of plate-to-plate interaction varied with time, affecting the basin architecture and sedimentation style throughout the basin. Basin development began in the Early Cretaceous (about 127 Ma) when the Indian plate rifted away from Antarctica along an inferred northeast-southwest-trending ridge system (Sclater and Fisher, 1974). After plate reorganization at about 90 Ma, the Indian plate began migrating rapidly northward, leading to its collision with Asia, probably initiated during the Eocene between 55 to 40 Ma (Curray et al., 1982; Molnar, 1984; Rowley, 1996). Owing to the counter-clock wise rotation of the Indian plate (Lee and Lawver, 1995) some time after the initial convergence with Asia, the basin in the east gradually started to close from north to south (oblique subduction). In the eastern part of the basin, the subduction complex of the Indo-Burman arc emerged above sea level, although major uplift of Himalayas may not have begun until the Miocene (Gansser, 1964).

2.1 INDIAN CRATON

Despite some debate about initial collision of the Indian plate with Eurasia, the Cretaceous has widely been considered as the time of initial rifting of the Indian continent from the East Gondwana block (Curry and Moore, 1974; Acharyya, 1986; Hutchison, 1989). There were two episodes of extensive continental flood basalt extrusion, namely, Rajmahal (~118 Ma; Kent et al., 2002) and Deccan (70-65 Ma, Mahoney et al., 1985). The Rajmahal trap comprises two units: trap flows and intertrappean sediments. The trap flows are basaltic in composition; they are hard, crystalline to cryptocrystalline, usually porphyritic, and vesicular. The intertrappean sediments consist of fine-to medium-grained massive sandstones, and medium to dark gray, micaceous and carbonaceous shales with thin bands of shaly coal and coal (Bhattacharji and Bhattacharji, 2002). The Deccan trap exposed in west-central India is a thick (~2000 m exposed) sequence of flat-lying tholeiitic lava flows that presently cover an area of nearly 500,000 km^2. The eruption of this large volume of basaltic rocks took place within a short time span, from the end of Cretaceous to the very Early Tertiary (Mahoney et al., 1985). Rift-drift episodes associated with the Paleo-Mesozoic break-up of Gondwanaland created continental blocks, which were located within the Tethyan Ocean (Curry et al., 1982). These Gondwanic blocks were accreted to the Asian collage by collisional processes. The Indian block collided terminally with the Tibetan block during Early-Middle Eocene, initiating the Himalayan orogenesis (Dasgupta and Nandy, 1995).

The Bengal Basin is bounded by the Indian Craton to the west (Fig. 4). The Indian crust has a composite mosaic-type structure that includes remnants of an Archean gneissic complex (Rahman, 1999). The Bengal basin is bounded to the north by the northeastern extension of Indian craton, the Shillong plateau. This plateau was

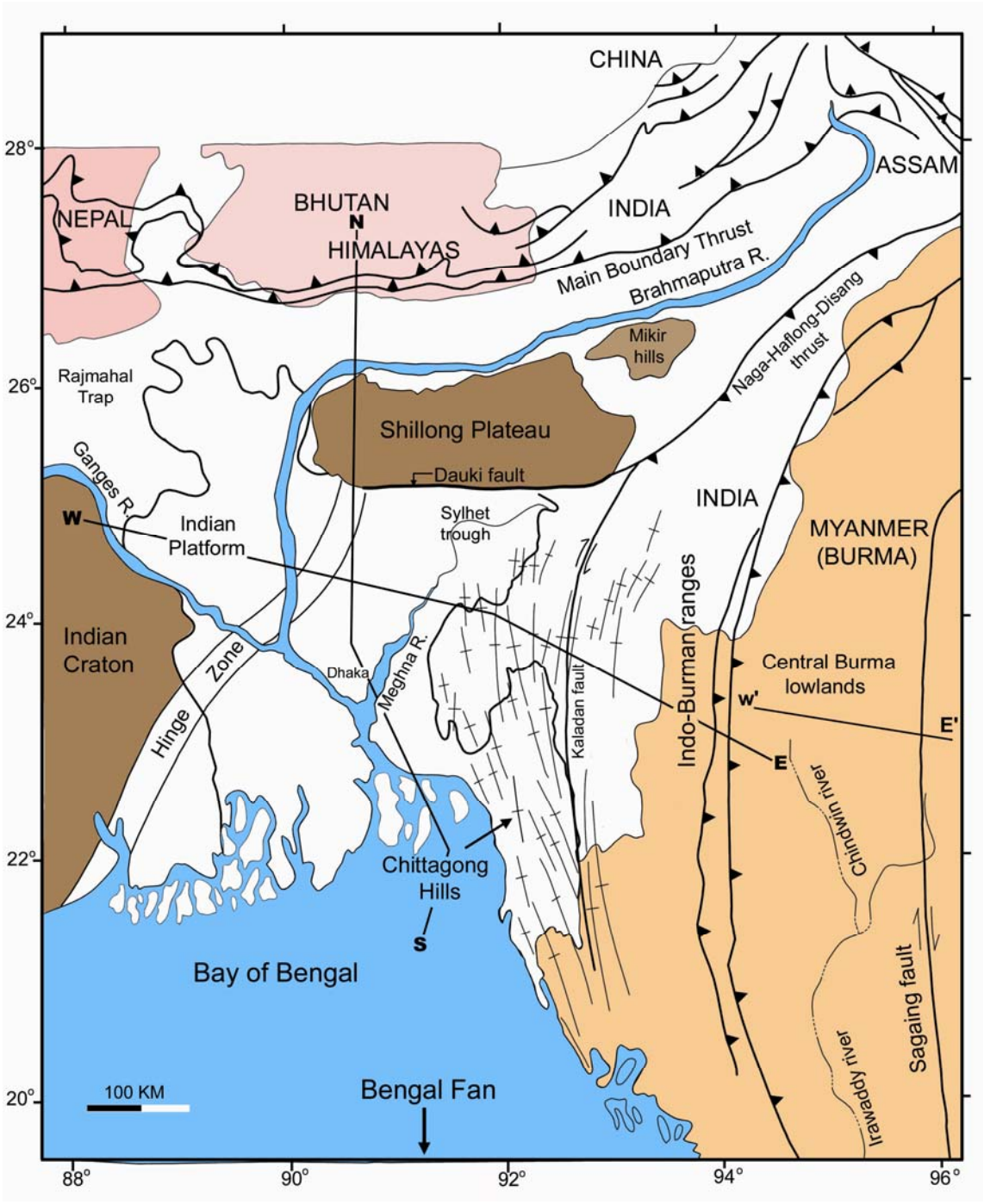

Figure 4. Map showing major tectonic elements in and around the Bengal basin. The Dauki fault separates the Sylhet trough from the uplifted Shillong Plateau to the north. Cross-sections along E′-W′, N-S, and E-W are shown in figures 5, 8 and 9 (after Uddin and Lundberg, 1998b).

uplifted to its present height (average 1 km, maximum 2 km) in the Pliocene (Johnson and Nur Alam, 1991).

The Shillong plateau is bounded to the west by the Garo-Rajmahal trough fault and to the south by the Dauki fault (Johnson and Nur Alam, 1991). Late Mesozoic and Cenozoic sedimentary rocks drape portions of the southern Shillong plateau and generally dip south in a monocline. As much as 15-18 km of structural relief between the Shillong plateau and the basement of the Sylhet trough has been postulated (Murthy et al., 1976; Hiller and Elahi, 1988). The poorly exposed Dauki fault forms the contact between the Shillong plateau and the Sylhet trough (Fig. 9). This fault has a nearly straight face across essentially flat topography. The 5-km-wide fault zone is characterized by extensive fracturing (Evans, 1964) and near vertical (85˚) dips of Pliocene and Pleistocene strata (Khan, 1978). The Precambrian rocks of the Shillong plateau belong to two groups: (1) an Archean gneissic complex; and (2) the Proterozoic Shillong Group. The gneissic complex, exposed in the northern and western part of the plateau, consists of quartzo-feldspathic gneiss and schists (Rahman, 1999). The boundary between the Gneissic complex and Shillong Group is marked by a lithologic as well as structural break. The Proterozoic rocks have undergone regional metamorphism up to garnet-grade prior to the igneous activity in the area. The Shillong Group was overlain by Mesozoic to Miocene rocks prior to the Pliocene uplift of the Shillong plateau (Johnson and Nur Alam, 1991).

2.2 INDO-BURMAN RANGES

The collision of the Indian and Eurasian plates is represented by the Indo-Burman Ranges along the eastern margin of the Indian sub-continent. The Indo-Burman Ranges consist principally of early Tertiary synorogenic sequences, which

have been deformed into imbricate thrust zones, and is a prominent geotectonic element of South Asia. The generally north-south-trending Indo-Burman Ranges is an active orogenic belt that comprises a folded, thrusted and wrench-faulted outer arc complex, or accretionary prism, that accreted to the edge of the Eurasian Plate beginning the Jurassic (Graham et al., 1975; Rangarao, 1983). The ranges extend from the southern tip of the Mismi Hills into southwest China and have an average width of 230 km. Mitchell (1981) divided the ranges into two orogenic belts: the western belt, comprising the Cretaceous to Eocene sedimentary rocks; and the eastern belt, consisting of schists and turbidites (Mitchell, 1993; Fig. 5). The eastern belt is locally overthrust by serpentinized harzburgites with pillow lavas and hornblende gabbros. Miocene sediments unconformably rest on the Eocene rocks along the west coast of Arakan in the eastern belt of Indo-Burman Ranges. Several authors (Mitchell, 1993; Dasgupta and Nandy, 1995) have suggested that the Indo-Burman Ranges were trench deposits containing ophiolitic mélanges scrapped off the Indian plate.

2.3 BENGAL BASIN

The Bengal basin, formed by rifting from passive continental margin, is gradually closing due to plate collision and orogeny along its eastern and northern margins (Rowley, 1996). The basin has been filled by an extremely thick accumulation of mostly clastic sediments which reach a maximum thickness of 20 km in the deeper part of the basin. The Bengal basin has two broad tectonic provinces: (1) the Indian platform, where thin sedimentary strata overlie rocks of the Indian craton in the northwest (in northwestern part of Bangladesh); and (2) a very thick basin-fill that overlies deeply subsided basement of undetermined origin in the south and east (Bakhtine, 1966; Khandoker, 1989). These two provinces are separated by a northeast

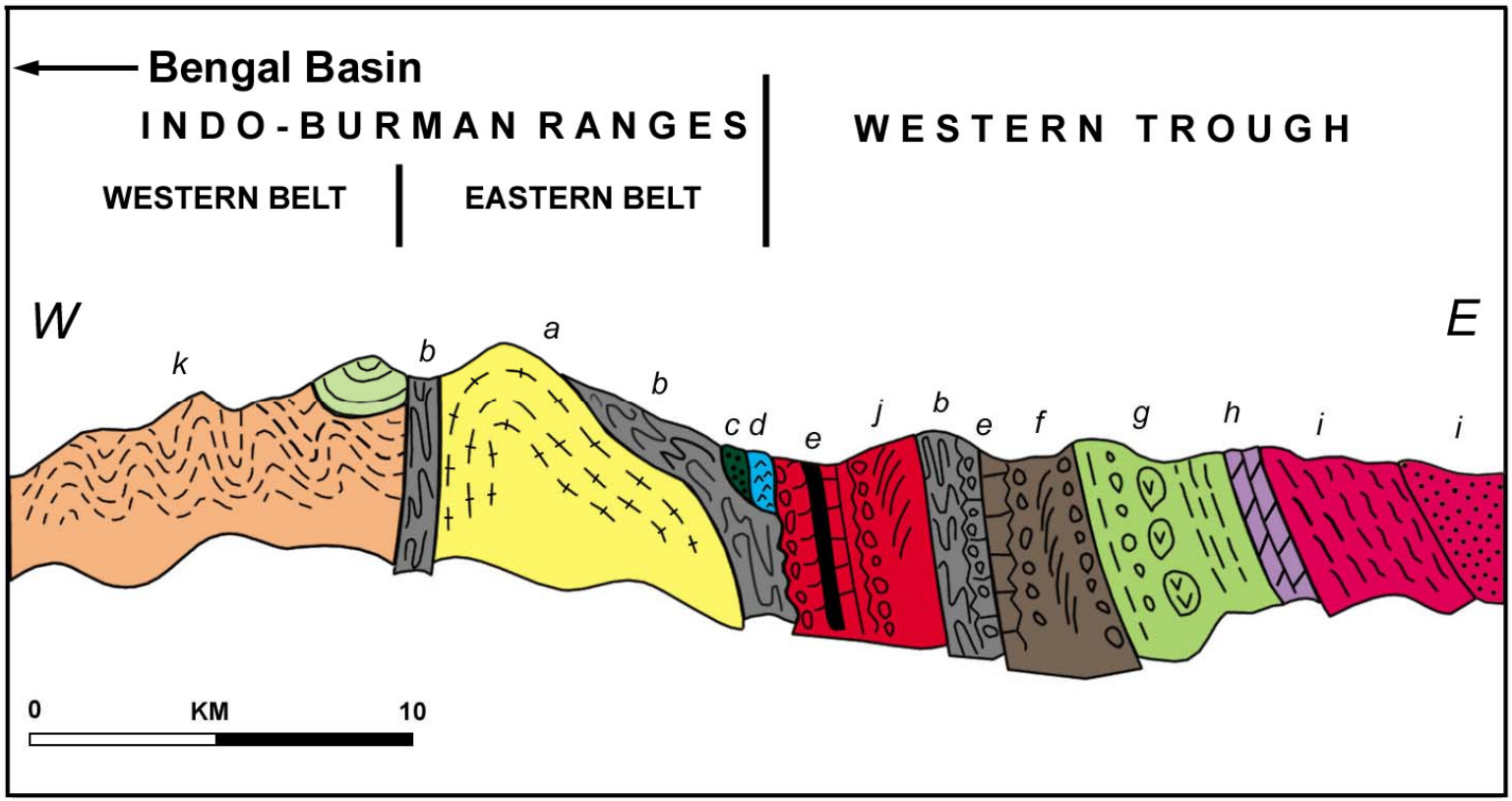

Figure 5. Schematic composite cross-section, through Mt. Victoria in eastern Indo-Burman Ranges and part of western limb of fore-arc basin syncline, Western Trough. a) Biotite- and biotite-graphite schists; b) Carnian quartzose turbidites, carbonaceous mudstones, minor limestone, recumbently folded and mostly forming broken beds; c) serpentinized harzburgite; d) pillow basalt with included blocks of Triassic flysch; e) ammonite-bearing carbonaceous limestones, pyritic mudstones; f) Maastrichtian Paunggyi Conglomerate overlying Albian limestone, serpentinite and Triassic rocks; g) boulder beds with granodiorite, dacite clasts; h) Lower Eocene shallow marine limestones; i) Lower Eocene Laungshe shales and Tilin sandstones; j) house-size blocks of Triassic sandstone, Senonian micritic limestone, bedded chert, basalt, gabbro, within Paunggyi Conglomerate zone; k) Lower Eocene feldspathic turbidites, grits, mudstones, with blocks of j, l) felspathic sandstone and shale, with post-Palaeocene fossils, occupying syncline (Modified from Mitchell, 1984).

-trending hinge zone (Fig. 2). Indian continental crust extends beyond the hinge zone toward the southeast (Khandoker, 1989).

The eastern fold belt marks the outermost part of the zone of compression between the west Burma block and the Indian plate (Fig. 6). The north-south-trending folds in this belt decreases in amplitude and become broader and less complex westwards. Intensity of folding rapidly attenuates westwards; the central and western parts of the basin are relatively undeformed. Some structures show evidence of more than one phase of deformation. The age of folding ranges from the Pliocene to Recent.

The Sylhet trough is a sub-basin of the Bengal basin in northeastern Bangladesh. It is characterized by a large, closed, negative gravity anomaly (as low as -84 milligals; Mirkhamidov and Mannan, 1981; Fig. 7). The Sylhet trough has minimal topography and is actively subsiding (Holtrop and Keizer, 1970). Estimates of the sediment thickness in the Sylhet trough range from about 12 to 16 km (Hiller and Elahi, 1984). The eastern part of the Sylhet trough lies in the frontal zone of the Indo-Burman Ranges.

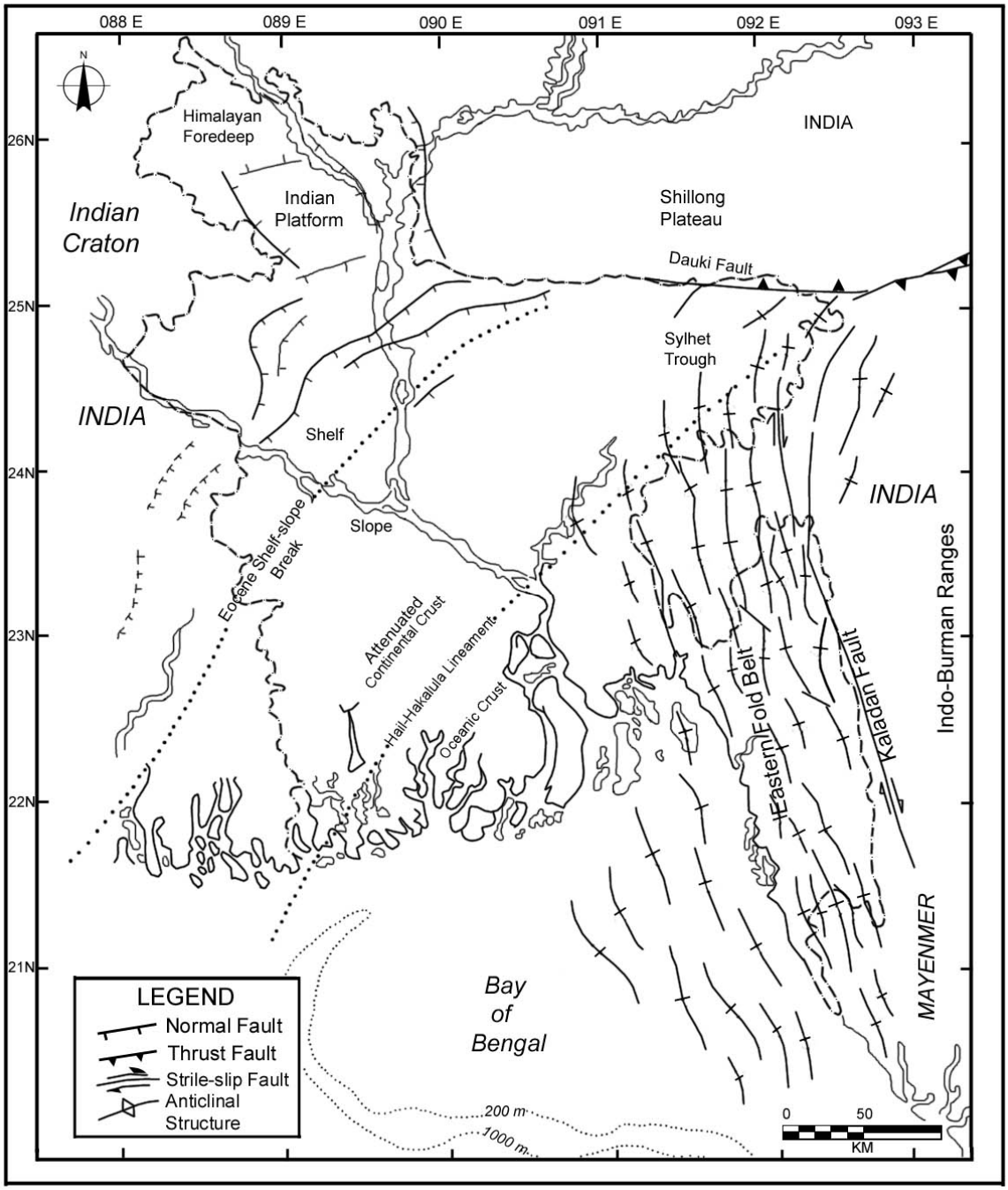

Figure 6. Structural elements of Bengal basin showing extents of continental and oceanic crusts, Eocene shelf-slope break, Dauki fault separating Shillong plateau and Sylhet trough, and anticlinal trends in eastern Bengal basin (after Hoque, 1982).

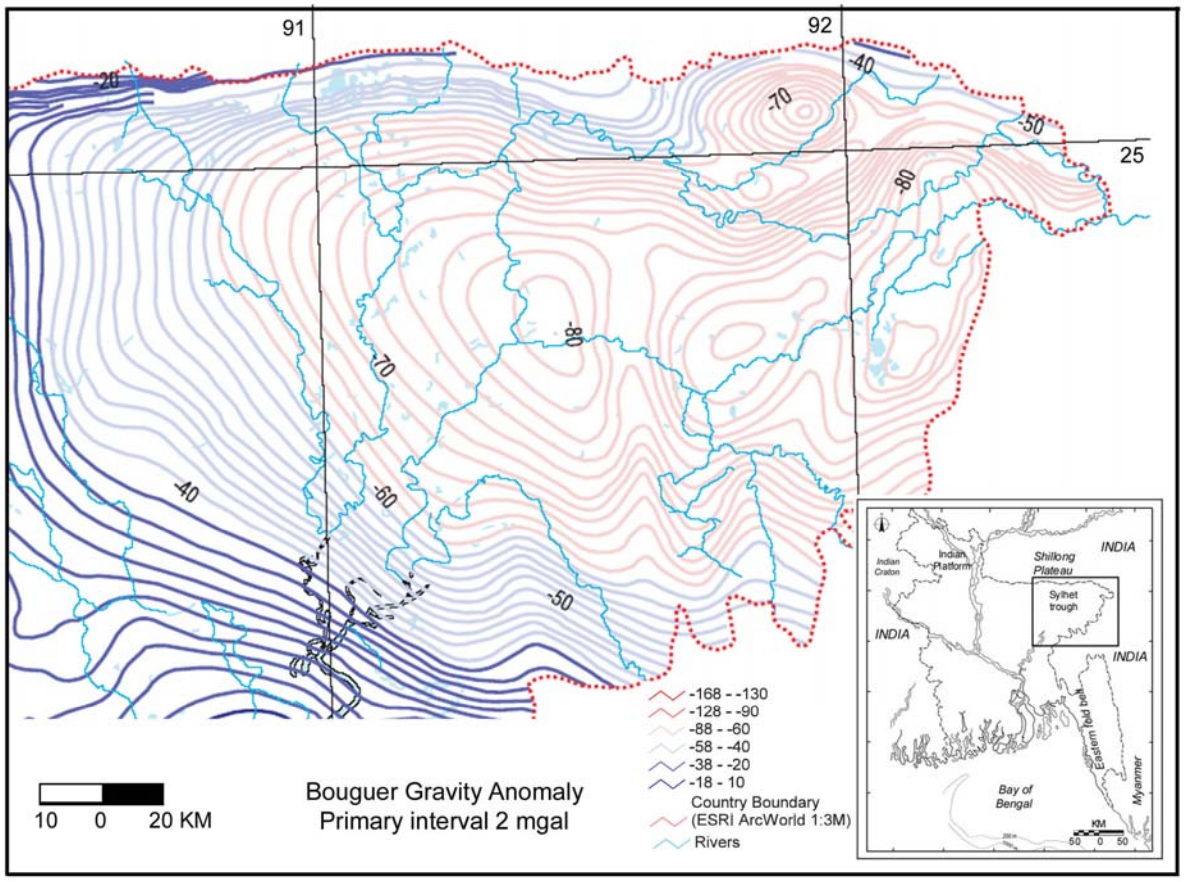

Figure 7. Bouguer gravity-anomaly map of the Sylhet trough of Bengal basin (after Geological Survey of Bangladesh, 1990).

CHAPTER 3: STRATIGRAPHY AND SEDIMENTATION

3.0 INTRODUCTION

The stratigraphic framework of Bengal basin was initially established by lithostratigraphic correlation to type sections in the Assam basin, northeastern India (Evans, 1964; Holtrop and Keizer, 1970; Khan and Muminullah, 1980). Seismostratigraphic correlations have subsequently refined the conventional stratigraphic framework for most parts of the Bengal basin (Salt et al., 1986), including the Sylhet trough (Hiller and Elahi, 1984). The Bengal basin received sediments from several areas: (1) the Barail and Naga Hills entering to the northeast, (2) the Indo-Burman to the east (Roy, 1986), (3) the eastern Himalayas, and (4) the Shillong plateau. The complete sedimentary succession of the Bengal basin is only known from northwestern Bangladesh. It can be broadly divided into (1) pre-rift Gondwana deposits, (2) post-rift, pre-collision Lower Cretaceous to Middle Eocene deposits, and (3) syn-orogenic Upper Eocene to Recent shelf-slope-fan sequences.

3.1 PRE-RIFT LOWER GONDWANA DEPOSITS

Permian pre-rift Gondwana rocks are found in the western platform of the Bengal basin. They are mostly fluvio-deltaic sediments that form a series of N-S and NNE-SSW trending half-grabens that correspond to older Precambrian basement lineation. Elongated grabens of similar age and structural style were described from several basins in eastern India and probably represent pre-rift “failed arms” or

aulocogens extending inland from the rifted basin margin. The more prominent grabens are indicated by closed Bouguer gravity anomaly lows (Fig. 8).

3.2 POST-RIFT PRE-COLLISION DEPOSITS

The Cretaceous to Middle Eocene rocks of western Bangladesh represent a post-rift, pre-collision phase of basin development. These consist of (1) the Paleocene Tura Sandstone (also known as Cherra Formation), a shallow marine sequence of poorly-sorted sandstone, mudstone, fossiliferous marl, and impure limestone interpreted as shallow-marine to marine deposits (170–360 m thick); (2) the Middle Eocene Sylhet Limestone, a shallow marine nummulitic limestone with minor interbeds of sandstone (250-m-thick); and (3) the overlying Upper Eocene Kopili Shale, the lithologies and fossil content of which indicate deltaic to slope depositional environments (40-90 m thick; Table 1; Reimann, 1993). Parts of the Kopili Shale also may have been deposited in a deep-sea fan environment (Reimann, 1993). On seismic sections, the Tura Sandstone and Sylhet Limestone show progressive onlap of the rifted continental margin, culminating in maximum transgression during the Middle Eocene when platform limestones covered most of the western shelf (Johnson and NurAlam, 1991).

3.3 SYN-OROGENIC SHELF-SLOPE-FAN SEQUENCES

The Oligocene strata, informally referred to as the Barail Group, are exposed along the northern fringe of the Sylhet trough near the Dauki fault area. These strata range in thickness from 800 meters (Johnson and Nur Alam, 1991) to 1600 meters (Ahmed, 1983). The Barail equivalent rocks (the Bogra Formation; Khan and Muminullah, 1980) in the Platform area are less than 200 m thick (Table 1). The

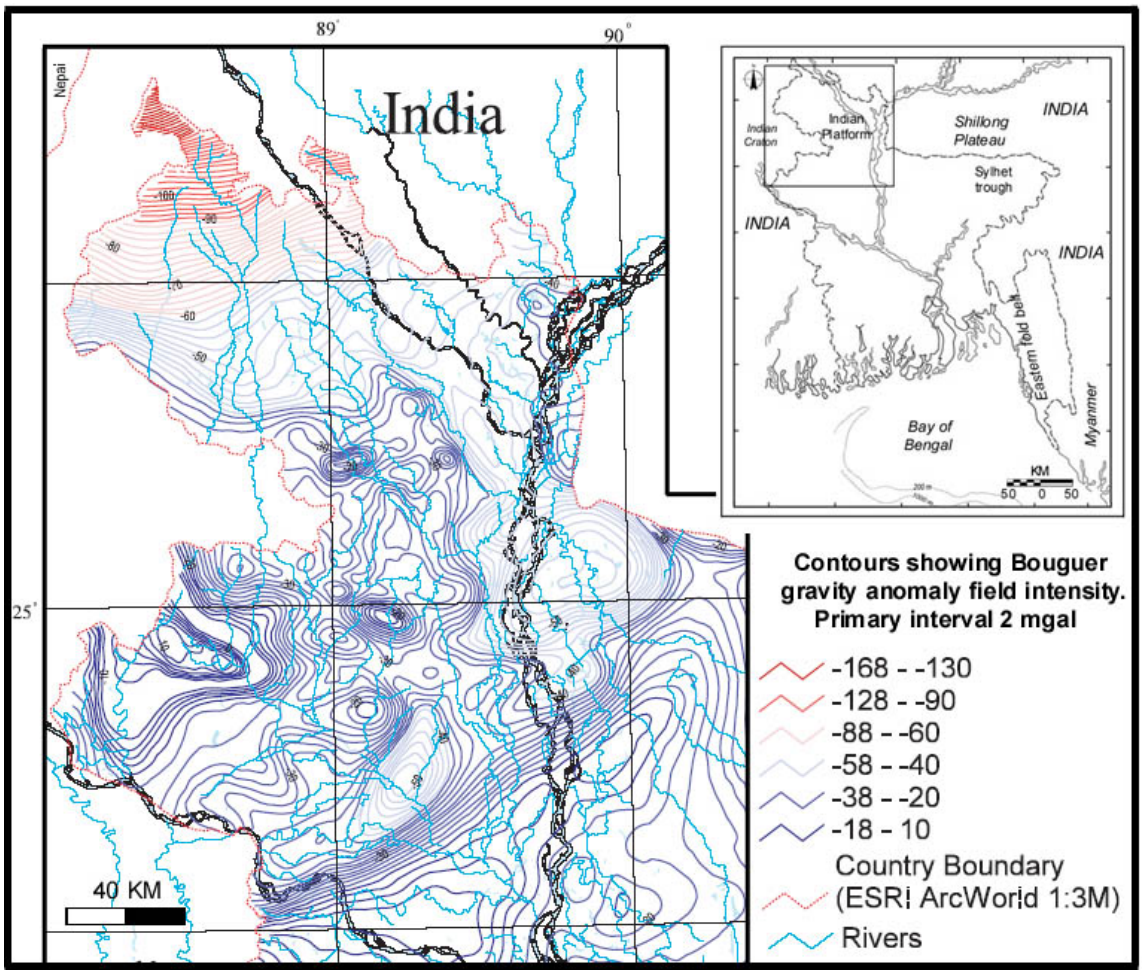

Figure 8. Bouguer gravity-anomaly map of the northwestern stable shelf part of Bengal basin showing closed gravity lines along the grabens (after Geological Survey of Bangladesh, 1990).

	Age	Group	Formation	Thick-ness (m)	Lithology
	Holocene	Alluvium			
Syn-orogenic Shelf-slope Fan Sequence	Pleistocene	Dihing	Dihing	129	Yellow and gray, medium grained, occasionally pebbly sandstone
		Dupi Tila	Upper Dupi Tila	2393	Medium to coarse grained, gray to yellow sandstone with clay balls
			Lower Dupi Tila		
	Pliocene	Tipam	Girujan Clay	3500	Red, brown, purple mottled clay with sand lenses
			Tipam Sandstone		Gray to brown, coarse grained, cross-bedded, massive sandstone
	Miocene	Surma	Boka Bil	3100	Alternation of shale, siltstone and sandstone
			Bhuban		Sandstone, siltstone, shaly sandstone, shales and lenticular conglomerate
	Oligocene	Barail	Renji	800-1600	Coarse grained sandstone, carbonaceous shale intercalation, lenses of coal
			Jenam		Dark gray silty and sandy shale
Post-rift	Paleocene-Eocene	Jaintia	Kopili Shale	15-150	Alternating dark-gray calcareous shale, thin limestone band
			Sylhet Limestone	148	Gray to dark gray highly fossiliferous limestone
			Tura/Cherra Sandstone	240	White, pink to brown, coarse grained, cross-bedded, carbonaceous sandstone
Pre-rift Lower Gondwana	Pre-Paleocene	Undiff-erentiated Sediment-tary rock			

Table 1. Stratigraphic succession of Bengal basin (Johnson and Nur Alam, 1991; Uddin and Lundberg, 1998a, 1999).

Barail sediments in the Sylhet trough, which are not formally subdivided, have been interpreted as deposits of predominantly tide-dominated shelf environments (Alam, 1991). In contrast Dasgupta (1977) has interpreted the Barail Group in the lower Assam Basin, India, as deposits of a progradational submarine fan complex. Fan sedimentation also is manifested in the overlying Miocene Surma Group (Dasgupta, 1977). The contact of the Surma Group with the Barail Group in Assam appears to reflect transgressive onlap (Banerji, 1981; Salt et al., 1986). This marine transgression on the shelf may be the result of major upthrust movement along the Dauki fault (Fig. 9) in the Early Miocene or subsidence associated with the approach of the subduction zone (Murthy et al., 1976; Fig. 10).

The Miocene Surma Group traditionally has been divided into two units; the Lower Bhuban and the Upper Boka Bil formations (e.g., Holtrop and Keizer, 1970; Hiller and Elahi, 1984, 1988; Khan et al., 1988) which occur throughout the Bengal basin. Some consider Surma Group as a single stratigraphic unit because there are no significant lithologic and petrologic differences between these formations (Johnson and Nur Alam, 1991). The Surma Group is overlain unconformably by the upper Miocene to Pliocene Tipam Group, consisting of the Tipam Sandstone and Girujan Clay formations. The Tipam Sandstone comprises coarse-grained, cross-bedded sand and pebbly sand, with common carbonized wood fragments and coal interbeds. These sediments are interpreted as deposits of bed-load dominated, braided-fluvial systems (Johnson and Nur Alam, 1991). The Girujan Clay, composed mainly of mottled clay, accumulated as lacustrine and fluvial overbank deposits (Reimann, 1993). The Dupi Tila Group, unconformably overlying the Tipam Group, comprises a sandy lower unit and an upper argillaceous unit (Hiller and Elahi, 1984). Khan et al. (1988) noted that

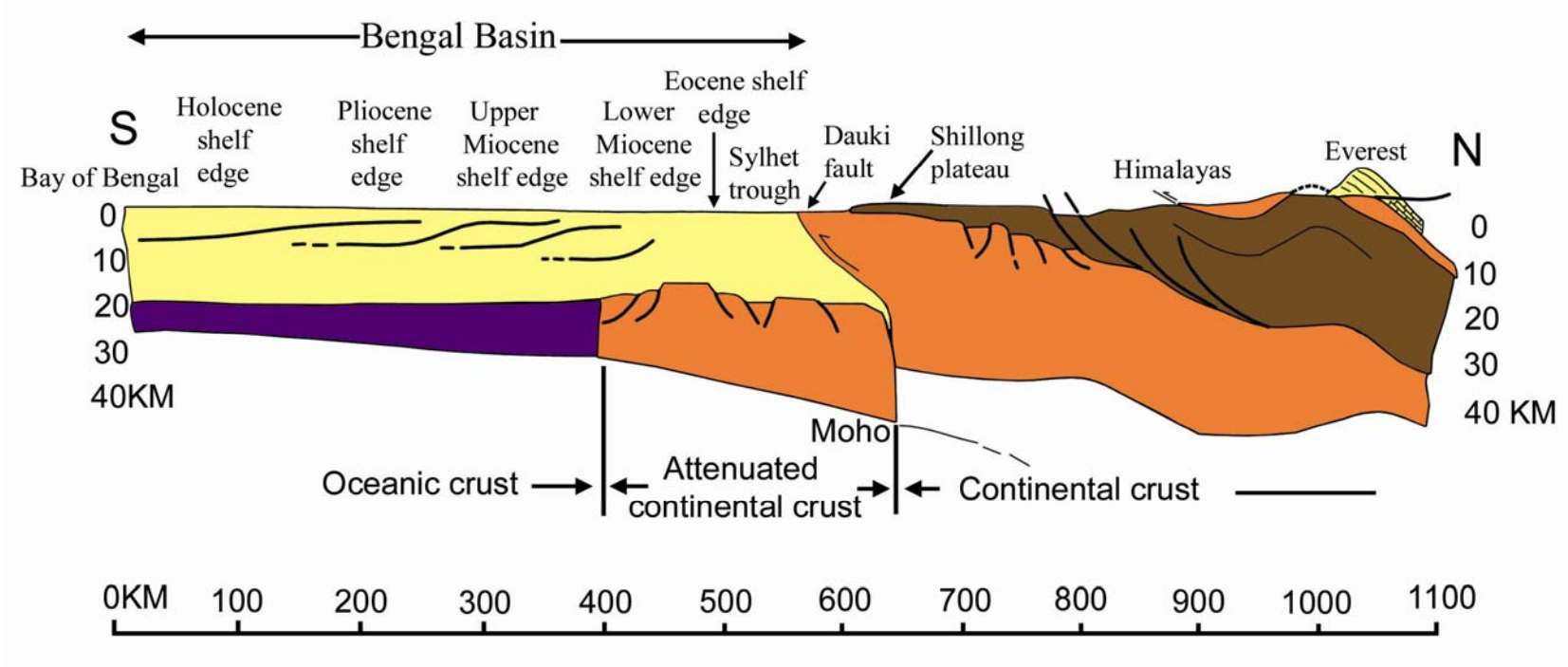

Figure 9. Schematic cross-section of the Bengal Basin (N– S) through the Shillong plateau. This section shows sediment progradation to the south (after Murphy, 1988; Uddin and Lundberg, 2004)

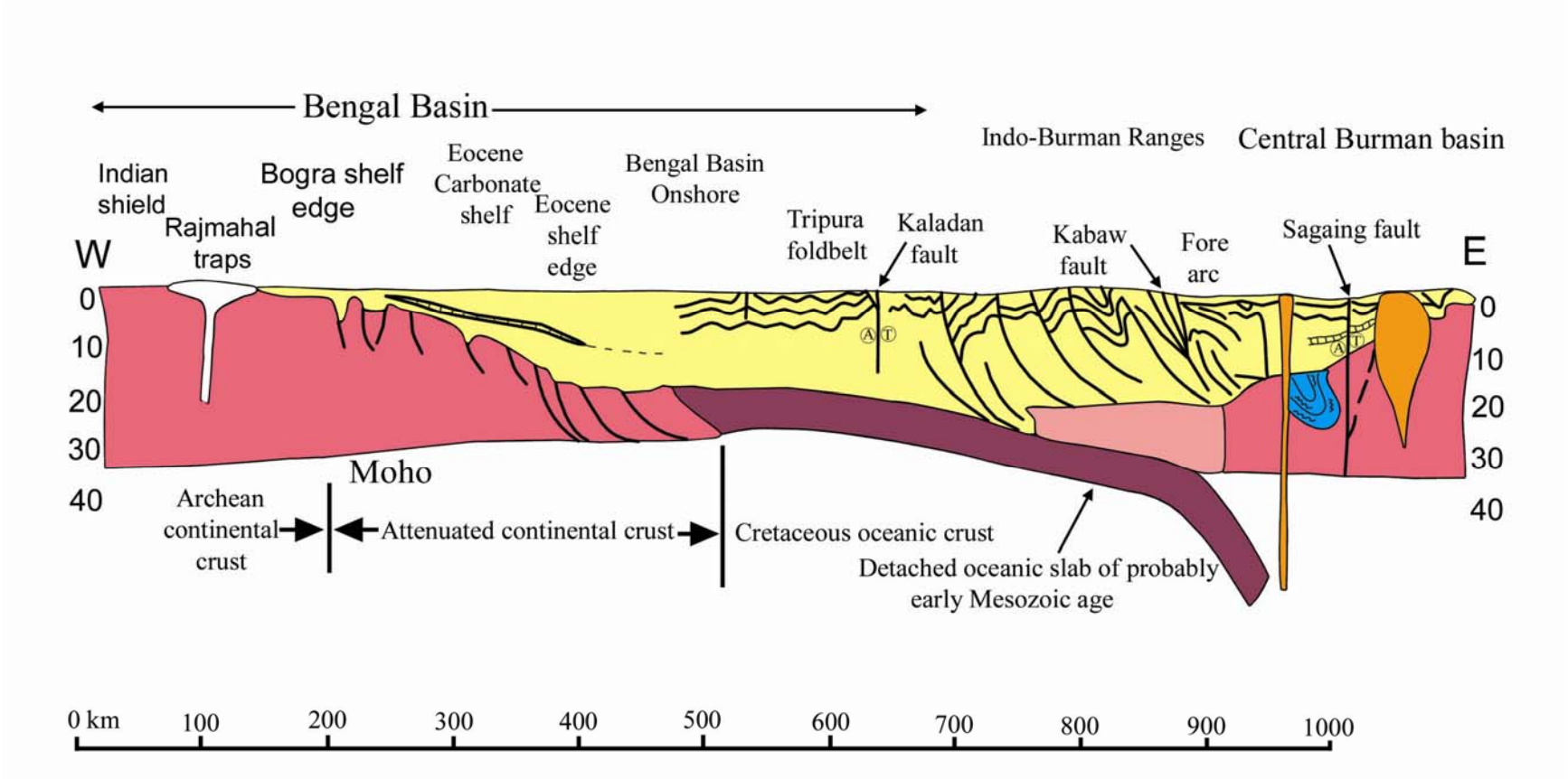

Figure 10. Schematic cross-section of the Bengal basin (E–W) through the northern Chittagong Hill region. This section shows sediment thickening towards the east (after Murphy, 1988; Uddin and Lundberg, 2004)

sediments of the Plio-Pleistocene lower Dupi Tila Formation are similar to the Tipam Sandstone, except that they tend to be poorly consolidated. The upper Dupi Tila Formation is characterized by fine- to medium-grained sandstones. These are commonly silty, contain lignitic wood fragments, and are intercalated with mottled clays. The fining-upward sequences of the lower Dupi Tila Formation, with alternating channel and floodplain deposits, have been interpreted to represent meandering river environments (Johnson and Nur Alam, 1991). The younger Pleistocene sediments of the Dihing Formation have been identified only locally as relatively thin subaerial deposits unconformably overlying the Dupi Tila Group. It is apparent from Table 1 that a large thickness of sediment (nearly 7 km) has been deposited in the Sylhet trough from Middle Pliocene onward. That could be due to Mio-Pliocene uplift of the Chittagong hills.

3.4 SUMMERY OF DEPOSITIONAL ENVIRONMENTS

The Sylhet Limestone in western Bengal basin is a strong seismic marker and is the most reliable correlative unit in the basin. The presence of nanno-fossils and foraminifera indicate marine deposition (Ismail, 1978; Chowdhury, 1982; Wallid, 1982; Chowdhury et al., 2003). Strong freshwater inputs are evident from the presence of abundant terrestrial and coastal miospores. During the Late Eocene to Oligocene time, the eroded and block-faulted basement surface was onlapped by a sequence of fluvial-delta plain sandstones and shales in the Himalayan foreland basins known as the Barail Group. Sequences of Oligocene strata (Fig. 11) in wells in western Bengal basin contain broadly regressive lithofacies that grade up from inner-shelf and delta-front to mixed-energy carbonaceous delta-plain lithofacies. In eastern

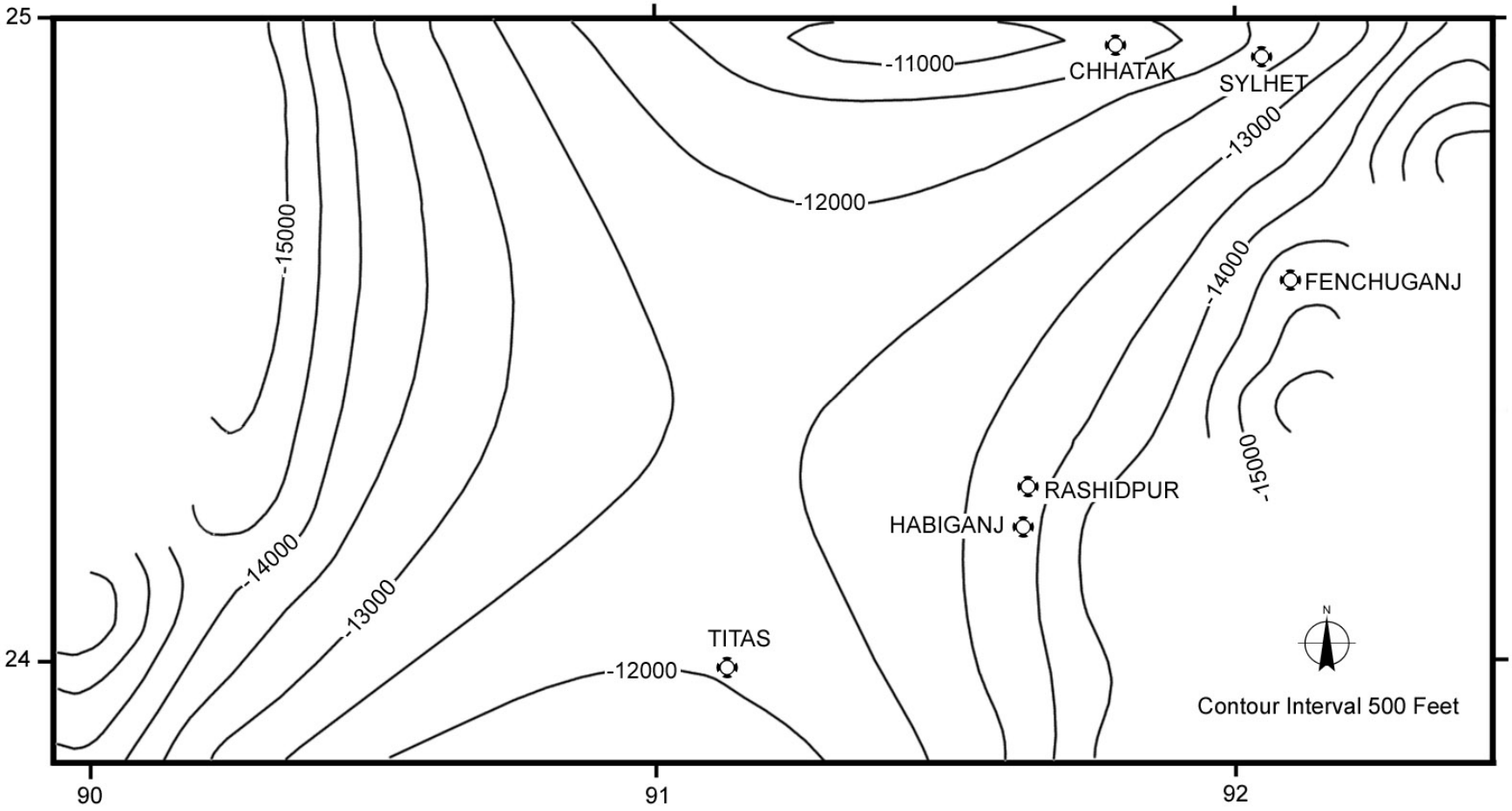

Figure 11. Structure contour map of top of Oligocene Barail unit in Sylhet trough (after Hoque, 1982)

Bangladesh, Oligocene sediments have been penetrated by only one well (Atgram IX) which largely comprises mixed energy delta-plain lithofacies.

The lower part of the Surma Group (Bhuban Formation) was deposited in a delta plain to delta front and comprises a progradational sequence. In western part of the basin, it is characterized by high-amplitude, shelf and clinoform reflectors of variable continuity (Alam, 1989). However, in the deeper part of the basin, the banded and clinoform seismic facies are replaced by low-amplitude, low-continuity channeled seismic facies, representing mainly argillaceous outer-shelf and slope lithofacies. The upper part of Surma Group (Boka Bil Formation) was deposited during the Late Miocene when a major progradational cycle in connection with Himalayan uplift resulted in the development of a very broad delta front, inner shelf, and outer shelf. The Lower Pliocene Tipam Group and Plio-Pliestocene Tipam Group are dominated by fluvial, alluvial floodplain, and delta-plain lithofacies that represent a significant shift to more proximal paleoenvironments. The Girujan Clay, the upper part of Tipam Group, represents upper delta-plain deposits with a higher proportion of mudstone than the overlying Dupi Tila Formation (Fig. 12).

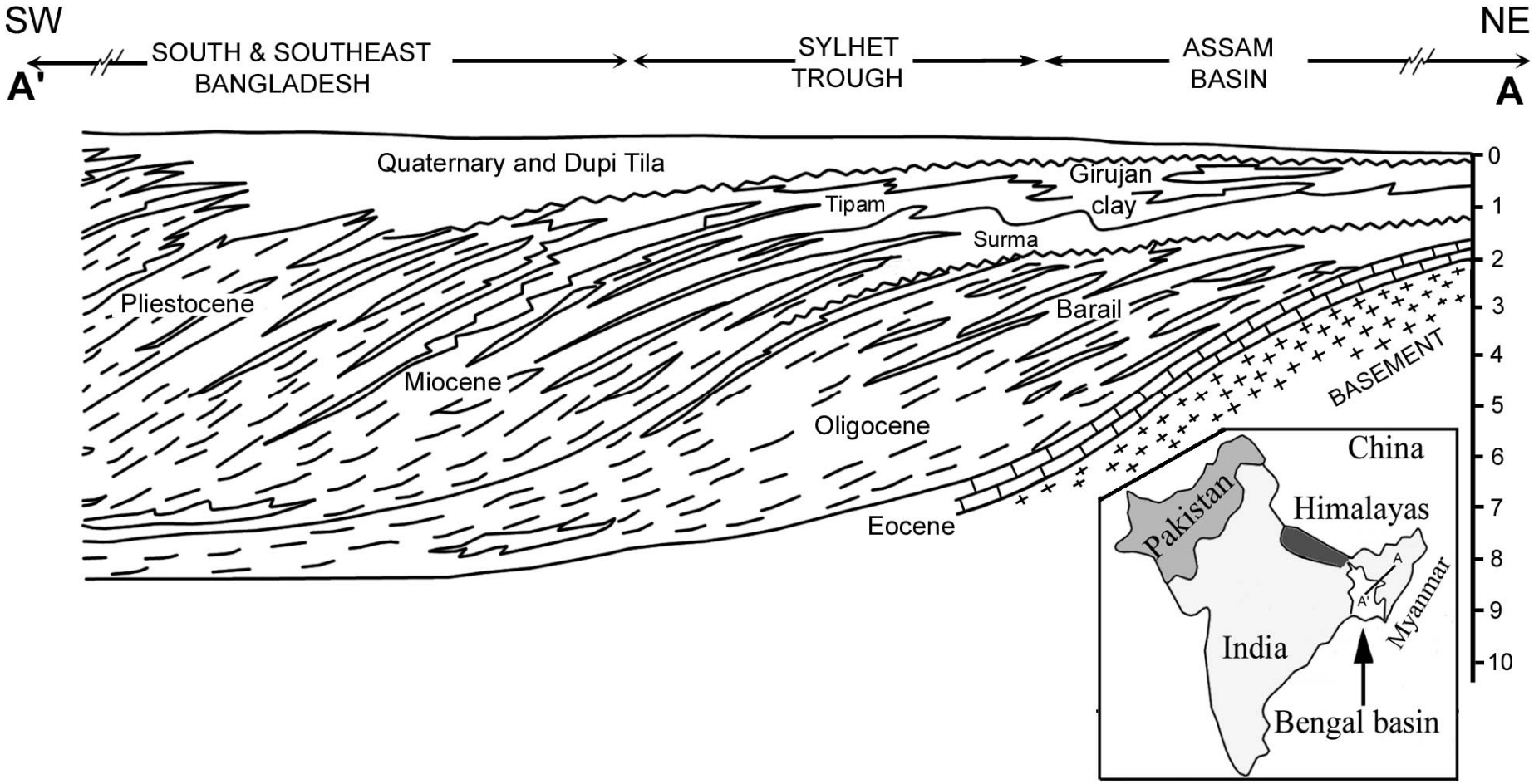

Figure 12. Facies correlation and depositional setting of Cenozoic rocks of Bengal Basin along A' – A in inset (after Petrobangla, 1983).

CHAPTER 4: SANDSTONE PETROGRAPHY

4.0 INTRODUCTION

It has been a common practice by sedimentary petrologists to quantify relative abundance of mineralogic and textural components of a rock to determine the provenance history of sandstones. The abundance of various components can be determined by extrapolating directly the result of a two-dimensional analysis, in which an orthogonal grid of points is constructed on a surface and the components are identified at each grid point. Considerable work has focused on modal analysis of sandstones, generally with the ultimate objective of evaluating detrital mineralogy of source rocks (Suttner et al., 1981; Basu, 1981, 1985; McBride, 1985). Provenance of sandstone has a well-established relationship with petrography and tectonic setting (Dickinson and Suczek, 1979; Ingersoll and Suczek, 1979; Dickinson, 1985; Garzanti et al., 1996; and many others). Despite various other sedimentological factors, detrital modes of sandstone assemblages primarily reflect the different tectonic settings of provenance terranes. Petrofacies analysis, the results of which are plotted on various compositional ternary diagrams, helps in understanding and interpreting plate interactions in the geologic past (Graham et al., 1976; Ingersoll, 1978; Dickinson and Suczek, 1979). Evolutionary trends in sandstone composition within sedimentary provinces commonly indicate erosional modification of provenance and changes in tectonic setting through time.

This chapter deals with the petrology and modal analysis of Paleogene and some Paleogene-Neogene transitional sediments deposited in the Sylhet trough and southeastern Bengal basin. This kind of petrographic study focuses on some key attributes of detrital mineralogy that provides important constraints on basin evolution and unroofing history of mountain belts (Dorsey, 1988; Uddin and Lundberg, 1998a).

Choosing appropriate categories of grains in modal analysis is a critical step, and thus deserves particular attention. For example, this study involves both mono- and polycrystalline framework grains in order to understand tectonic evolution and provenance (Dickinson, 1970a, 1982; Dickinson and Suczek, 1979; Ingersoll et al., 1984; Ingersoll et al., 1995). In practice, clastic petrologists generalize grain type into certain groups for comparison with other studies although there are no limits to the types of grains that have to be counted. Polycrystalline grains are described based on their overall mineralogical and textural association and are counted as lithic fragments (Basu et al., 1975).

4.1 METHODS

Thirty-five Paleogene-Neogene samples were analyzed for this study. Oligocene samples (Barail Group) were collected from the Sylhet trough, the only location in Bengal basin where rocks of that age are well exposed at the surface (Figs. 2 and 3). Almost all the Lower Miocene samples (Lower and Middle Bhuban) were collected from an anticlinal structure (Sitakund anticline) from the southeastern part of the Bengal basin (Fig. 2). However, three were collected from cores of wells located in the northeastern part of the basin. Middle Miocene samples (Upper Bhuban) were collected from well cores located in the same area. Modal analyses were conducted following the Gazzi-Dickinson method, whereby sand-sized minerals

included in lithic fragments are counted as the mineral phase rather than the host lithic fragment in order to normalize for grain-size variation (Table 2; Dickinson, 1970b; Ingersoll et al., 1984). Thin sections were stained for plagioclase and potassium feldspars. A minimum of 300 points were counted per sample. Point-counting data are presented in Table 3. Modal sandstone compositions have been plotted on standard ternary diagrams (QtFL, QmFLt, QmPK, LsLvLm, $LsLm_1Lm_2$, etc.) and used to assess temporal changes in provenance (Dickinson, 1970a; Dorsey, 1988). The following compositional parameters were evaluated: Qt = total quartz; Qm = monocrystalline quartzose grains; Qp = polycrystalline quartz grains, including chert grains; F = total feldspar grains; P = plagioclase feldspar grains; K = potassium feldspar grains; L = lithic fragments; Lt = total lithic fragments; Ls = sedimentary lithic fragments; Lv = volcanic lithic fragments; Lm =metamorphic lithic fragments; Lsm = sedimentary and metasedimentary lithic fragments; Lvm = volcanic, hypabyssal, metavolcanic lithic fragments; Lm_1 =very low- to low-grade metamorphic lithic fragments; and Lm_2 = low- to intermediate-grade metamorphic lithic fragments (Tables 2 and 3).

4.2 PETROGRAPHY

Sandstones from Oligocene Barail Group are mostly quartzolithic with rare to no feldspars. In contrast, those from Lower Miocene are mostly quartzolithic to quartzofeldspathic. Sandstone modal analyses of the Paleogene-Neogene units are presented in Table 3 and ternary diagrams of those sands are plotted in figures 13 through 17.

Table 2. Recalculated modal parameters of sand and sandstones (Uddin and Lundberg, 1998a).

1. Primary parameters
(Dickinson and Suczek, 1979; Dorsey, 1988)

Qt = Qm + Qp, where
Qt = total quartzose grains
Qm = monocrystalline quartz (> 0.625 mm)
Qp = polycrystalline quartz (or chalcedony)

Feldspar Grains (F = P + K)
F = total feldspar grains
P = plagioclase feldspar grains
K = potassium feldspar grains

Unstable Lithic Fragments (Lt = Ls + Lv +Lm)
Lt = total unstable lithic fragments
Lv = volcanic/metavolcanic lithic fragments
Ls = sedimentary/metasedimentary lithic fragments

2. Secondary parameters
(Dickinson, 1970a; Uddin and Lundberg, 1998a)

P/F = Plagioclase/ total feldspar
Lm_1 = Very low- to low-grade metamorphic lithic fragments
Lm_2 = Low- to intermediate-grade metamorphic lithic fragments

Table 3. Normalized modal compositions of sandstones from the Oligocene and Miocene units of the Bengal Basin, Bangladesh.

Oligocene – Barail Formation

Sample no.	Qt	F	L	Qm	F	Lt	Qm	P	K	Ls	Lv	Lm	Ls	Lm1	Lm2
Bsr 3.1	68	0	32	66	0	34	100	0	0	64	0	36	64	26	10
Bsr 5.1	75	1	23	72	2	26	98	0	2	69	0	31	69	16	16
Bsr 6.1	71	2	27	66	2	32	97	0	3	53	0	47	53	19	28
Bsr 8.2	77	3	21	74	3	23	96	0	4	88	0	13	88	13	0
Bsr 9	57	1	42	56	1	43	98	0	2	94	2	5	95	2	3
Bsr 13	67	4	29	66	5	30	94	0	6	78	0	22	78	22	0
Bsr 14	62	2	36	60	2	38	97	0	3	96	0	4	96	4	0
Bsr 16	63	3	34	61	3	36	96	0	4	95	0	5	95	5	0
Bsr 18	73	7	20	71	7	22	90	0	9	54	7	39	58	39	4
Bsr 19	67	2	32	64	2	34	97	0	3	57	1	42	57	37	5
Bsr 22	84	1	15	82	1	18	99	0	1	44	33	22	67	0	33
Bsr 1.2	72	0	28	71	0	29	100	0	0	42	0	58	42	0	58
Mean Value	70	2	28	67	2	30	97	0	3	69	4	27	72	15	13
Std. deviation	7	2	8	7	2	7	3	0	3	20	6	18	17	13	14

Lower Miocene – Bhuban Formation

Sita 1	71	12	17	69	13	18	84	8	7	61	0	39	61	18	21
Sita 5	54	22	24	51	23	26	69	12	19	66	0	34	66	29	6
Sita6	53	28	19	44	33	22	57	20	23	48	24	28	64	36	0
Sita 7 new	64	24	12	56	30	15	65	18	17	75	0	25	75	25	0
Sita 7	69	20	11	66	22	12	75	24	1	67	0	33	67	33	0
Sita 8 new	67	23	10	61	28	12	69	13	18	88	0	13	88	13	0
Sita 8	52	23	25	50	24	26	67	16	17	69	0	31	69	31	0
Sita 8 new	61	29	10	52	36	12	59	21	21	79	0	21	79	21	0
Sita 10	55	26	19	52	28	21	65	18	17	86	0	14	86	14	0
Sita 12	62	27	10	62	28	11	69	18	13	57	0	43	57	43	0
Sita 19	58	20	23	54	21	25	72	17	11	55	0	45	55	45	0
Sita 20	50	25	25	48	26	26	65	16	19	59	0	41	59	31	10
Sita 21 new	55	20	25	51	22	28	70	9	21	76	0	24	76	24	0
Sita 22	52	27	20	51	28	21	64	16	20	58	0	42	58	42	0
Sita 23 new	55	20	25	46	24	29	66	11	23	60	0	40	60	40	0
Sita 23	59	24	17	57	25	18	69	12	19	60	0	40	60	40	0
Sita 24	59	22	19	55	25	20	69	15	16	55	0	45	55	45	0
Sita 25 new	60	23	18	55	25	20	69	10	22	96	0	4	96	4	0
Patha 5-5	65	22	13	59	25	15	70	13	17	85	0	15	85	15	0
Path 5-3	54	27	19	42	34	24	55	28	17	89	0	11	89	11	0
ATGR 1-7	64	14	23	55	17	28	77	3	21	42	0	58	42	47	11
MEAN:	59	23	18	54	26	20	68	15	17	68	1	31	69	29	2
Std. deviation	6	4	5	7	5	6	6	6	5	15	5	14	14	13	5

Middle Miocene – Bhuban Formation

Sample no	Qt	F	L	Qm	F	Lt	Qm	P	K	Ls	Lv	Lm	Ls	Lm1	Lm2
Titas 1	63	22	14	58	26	16	69	12	19	57	20	23	71	29	0
Path 5-2	65	27	8	60	31	9	66	11	23	75	0	25	75	25	0
Mean Value	64	25	11	59	28	13	67	12	21	66	10	24	73	27	0
Std. dev	1	3	5	1	4	5	3	0	3	13	14	1	3	3	0

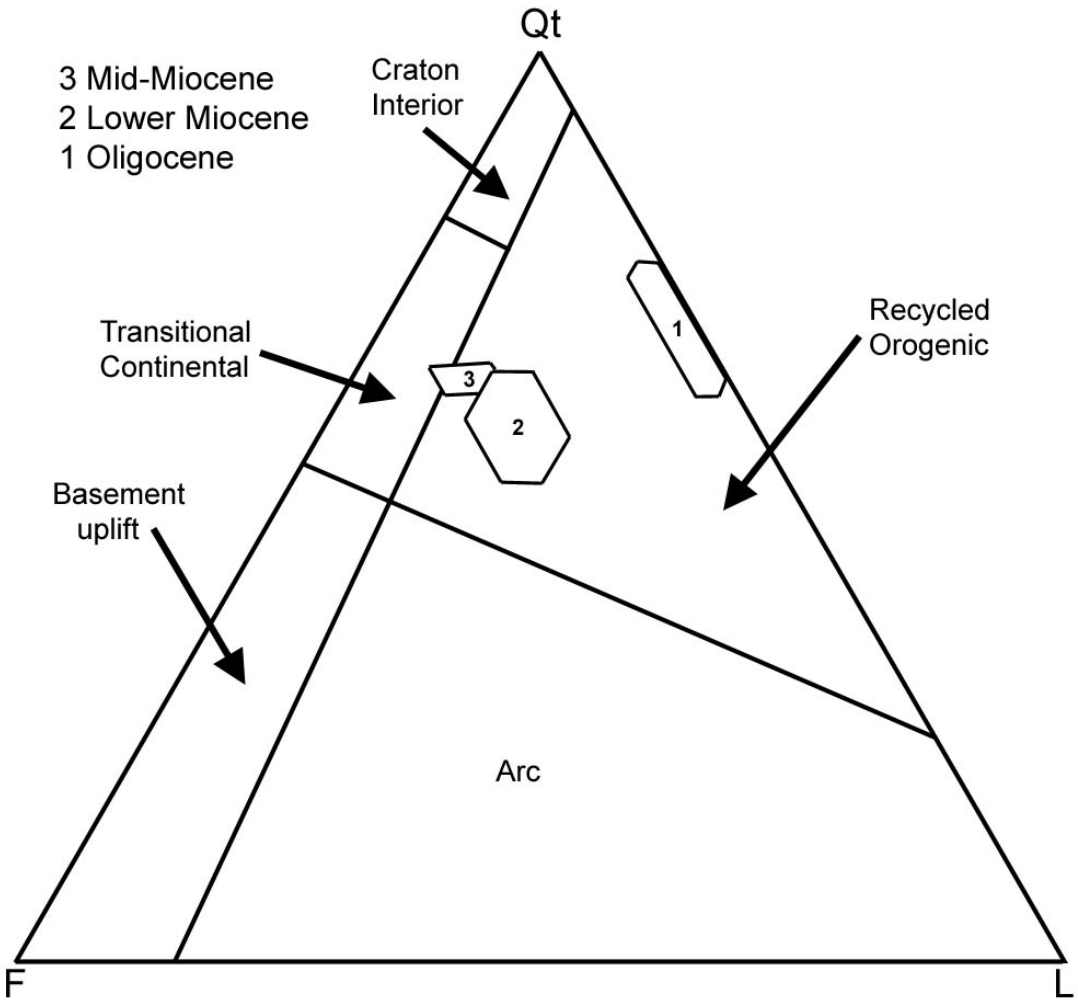

Figure 13. QtFL plot showing composition of Bengal basin sandstones. Provenance fields are from Dickinson (1985).

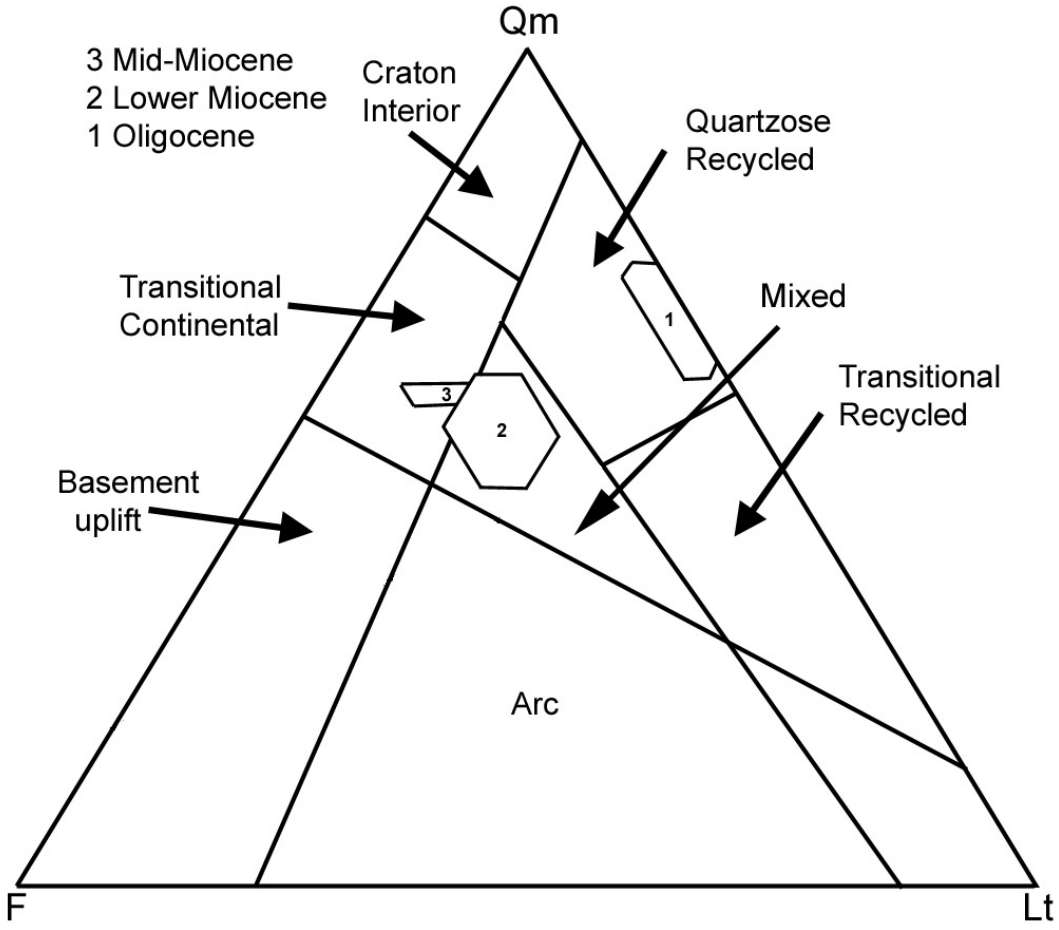

Figure 14. QmFLt plot of Bengal basin sandstones, showing mean and standard deviation polygons for each stratigraphic unit, along with appropriate provenance fields from Dickinson (1985). Cherts and other polycrystalline quartz grains are included in the total lithic counts (see Table 2).

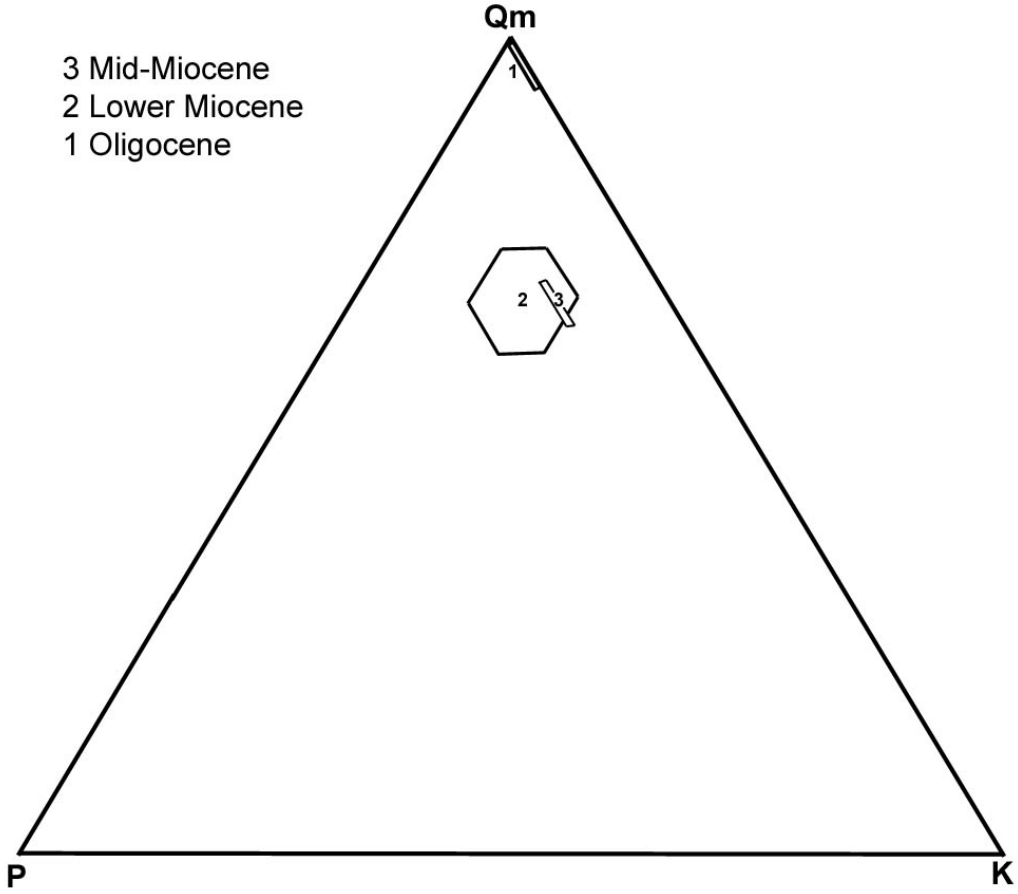

Figure 15. QmPK plot of mean values for the Bengal basin sandstones, showing mean and standard deviation polygons for each stratigraphic unit.

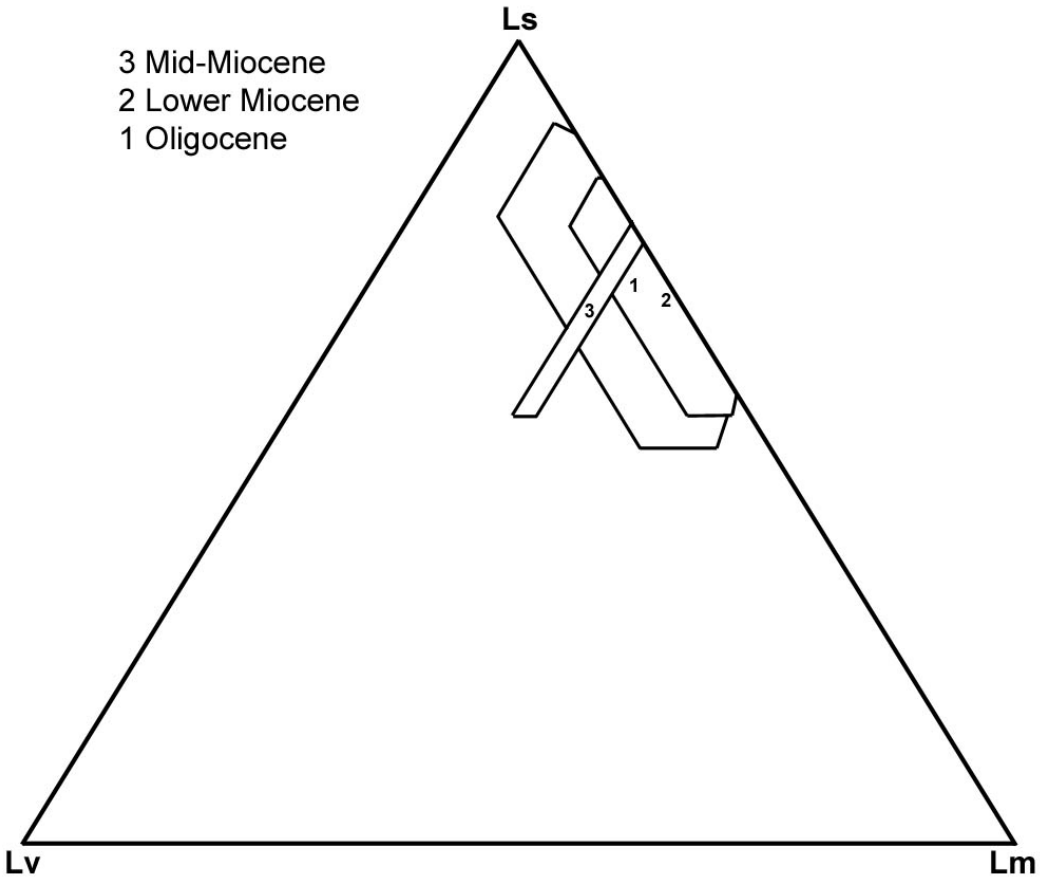

Figure 16. LsLvLm plot showing variation in the composition of lithic fragments in Bengal basin. Ls = sedimentary lithic fragments, Lv = volcanic lithic fragments, and Lm = low- to intermediate-grade metamorphic rock fragments.

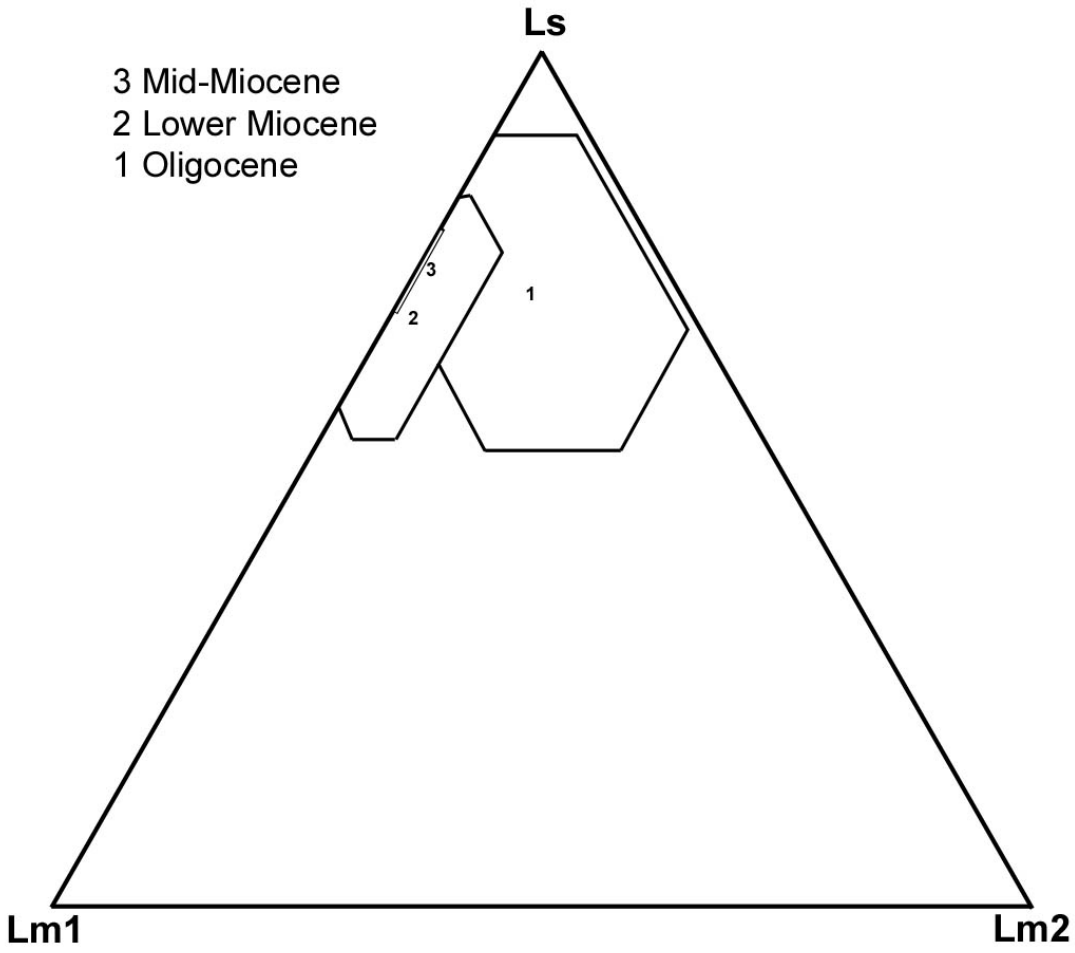

Figure 17. $LsLm_1Lm_2$ plot showing variation in the composition of lithic fragments in Bengal basin. Ls = sedimentary lithic fragments, Lm_1 = very low- to low-grade metamorphic rock fragments, and Lm_2 = low- to intermediate-grade metamorphic rock fragments.

4.2.1 Oligocene Barail Group

Twelve sandstones, mostly medium- to fine-grained, were examined from the Oligocene Barail Group. These samples are generally quartzolithic with low feldspar content. However, the abundance of feldspar increases towards the Oligocene-Miocene boundary. All the samples are dominated by mostly angular, monocrystalline quartz grains. A few detrital chert and polycrystalline quartz grains are present (Fig. 18A). Feldspars are rare in Oligocene rocks in Bengal Basin, and potassium feldspar dominates over plagioclase feldspar. Most of the plagioclase feldspars are altered and shows grain etching. Among the lithic rock fragments, volcanic rock fragments are rare to absent. Most of the samples contain abundant sedimentary lithic fragments, while some contain low- to medium-grade metamorphic rock fragments (Fig. 18B).

4.2.2 Lower Miocene Surma Group

Twenty-one samples of Lower Miocene Surma Group were analyzed for this study. Feldspar content in these Lower Miocene rocks is significantly higher than in the Oligocene Barail unit (Fig. 19 A, B). Surma Group sediments are mostly quartzolithic to quartzofeldspathic. They are fine- to medium-grained and grains range from subangular to subrounded. Quartz grains are mostly monocrystalline, highly undulose, and slightly strained in some samples. There are significant amount of feldspar in these samples and the abundance of plagioclase feldspar is approximately equal to that of potassium feldspar (Fig. 19 A, B). Most of the feldspars are unaltered and can be easily identifiable due to staining. These samples are also rich in lithic fragments. The most common types of lithic fragments are sedimentary and low- to medium-grade metamorphic types. A few samples show high-grade metamorphic rock fragments (e.g. schist and gneiss).

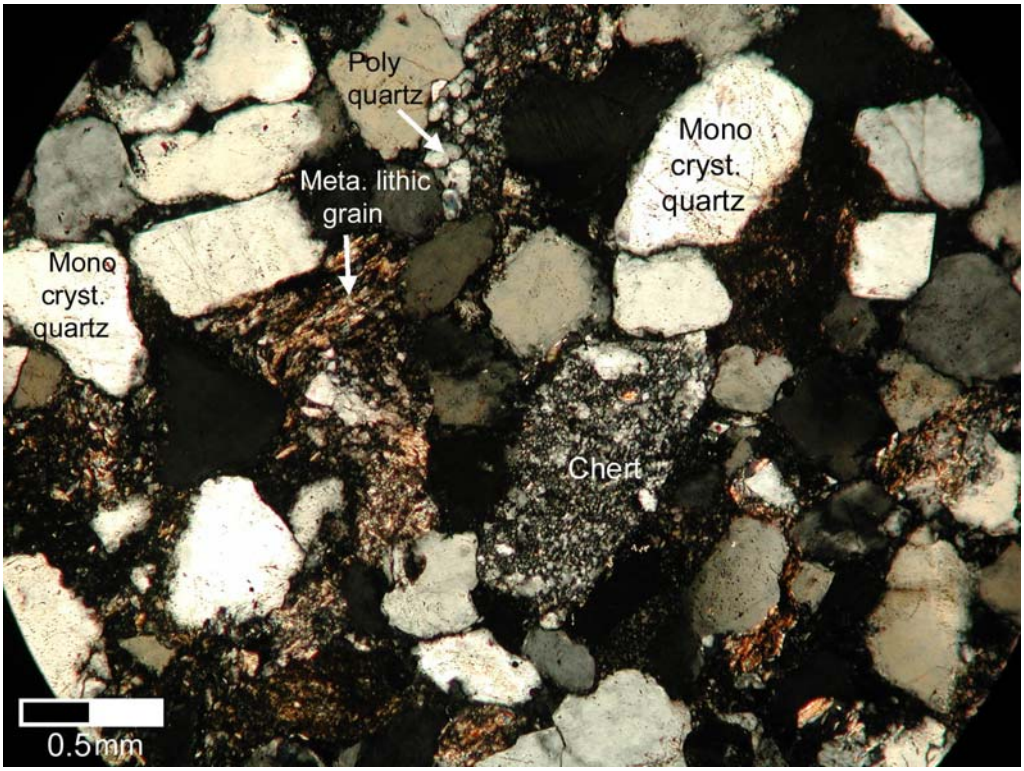

(A)

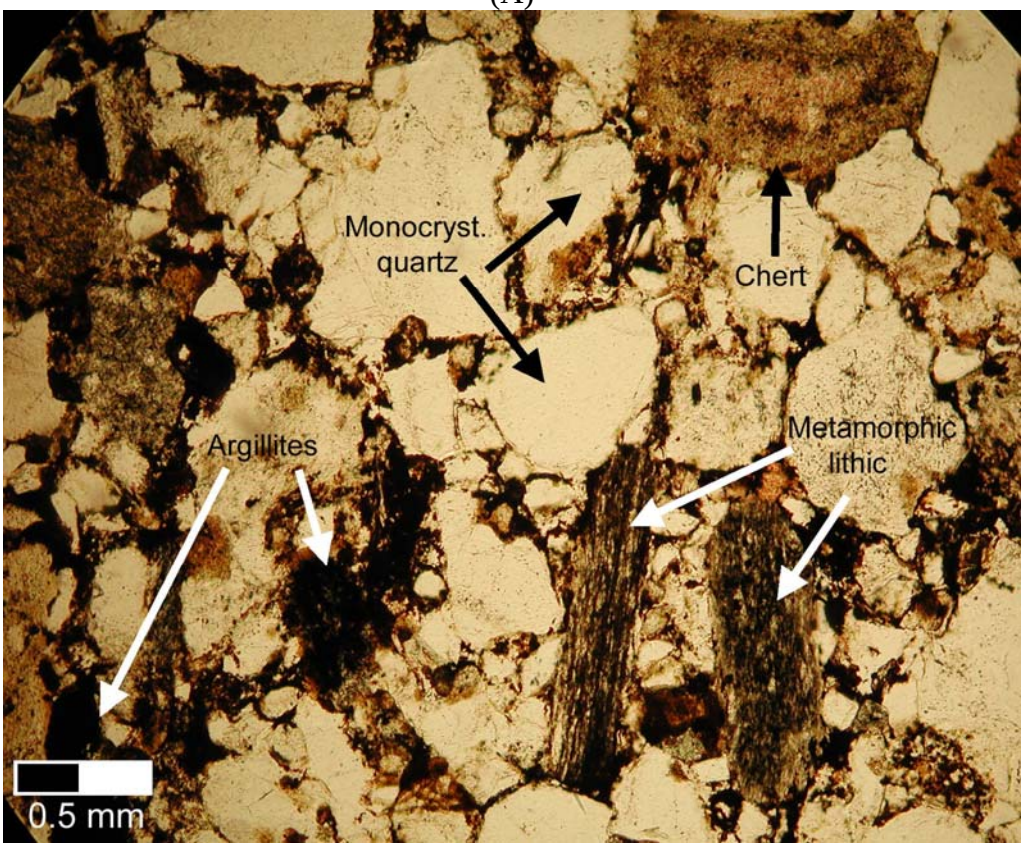

(B)

Figure 18. Representative photomicrographs of sandstone from Oligocene sediments from the Bengal basin showing (A) mono-and polycrystalline quartz, chert, and metamorphic lithic grains (sample# Bsr.22; crossed polar), (B) monocrystalline quartz, chert, sedimentary, and metamorphic lithics (sample# Bsr. 6.1; plane polar).

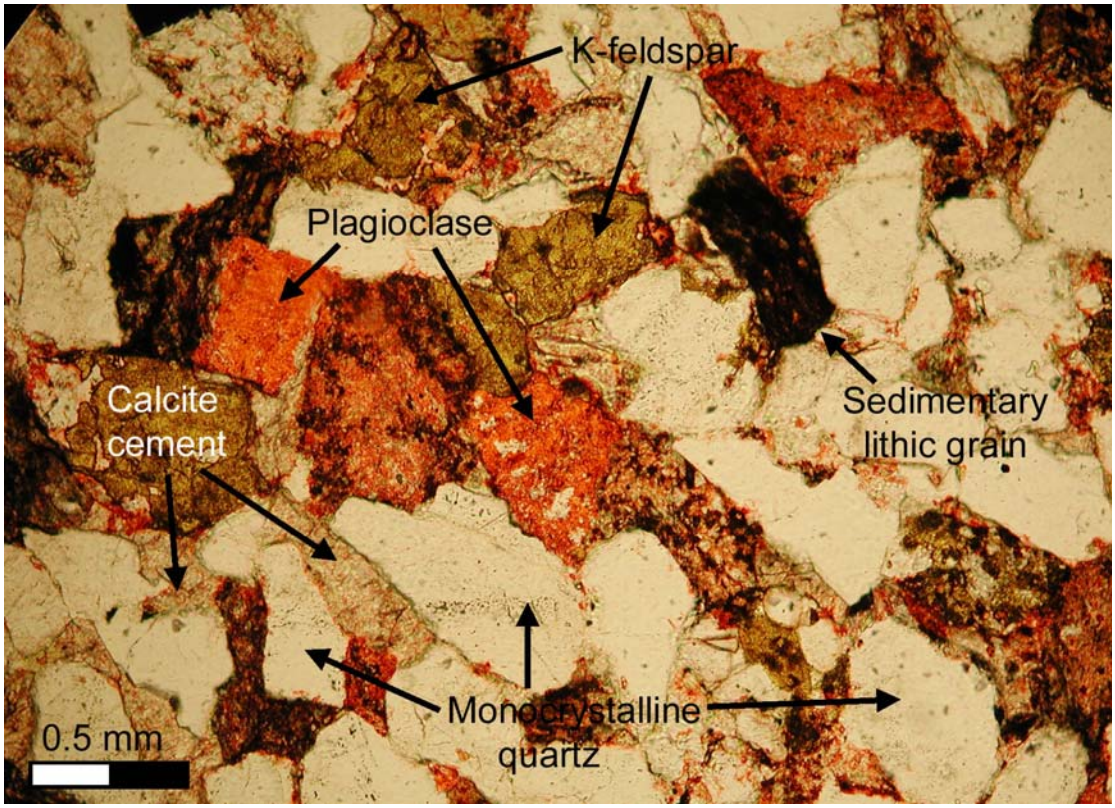

(A)

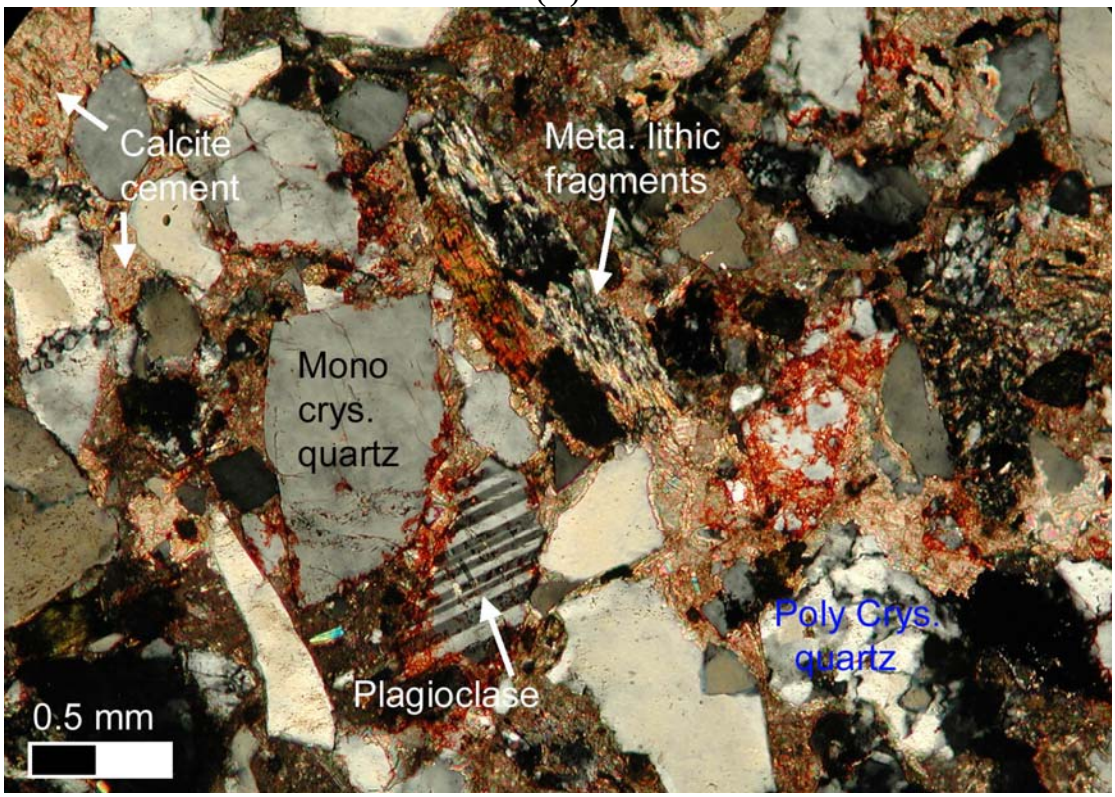

(B)

Figure 19. Representative photomicrographs of sandstones from Lower Miocene sediments from the Bengal basin showing (A) quartz, feldspars, sedimentary lithic grains, and calcite cement (sample# Sita 7; plane polar), (B) metamorphic lithic grains, plagioclase, and polycrystalline quartz (sample# Path5-2; crossed polar).

4.2.3 Middle Miocene Surma Group

Two samples were analyzed from the middle Miocene Surma Group. Sandstones from middle and upper Bhuban Formation are fine- to medium-grained, quartzolithic to quartzofeldspathic and contain mono- and polycrystalline quartz, abundant feldspar, and lithic grains. Monocrystalline grains are strongly undulose. Some chert and polycrystalline quartz are present in these rocks. These middle Miocene rocks are rich in feldspar, and potassium feldspar dominates over plagioclase feldspar. Lithic fragments are common in these samples. Sedimentary lithic fragments are most abundant, although some volcanics and low-grade metamorphic fragments also are observed.

4.3 SANDSTONE MODE AND PETROFACIES EVOLUTION

Ternary diagrams of the major components (monocrystalline grains and the phaneritic lithic fragments) show the variation in sand composition across the Paleogene-Neogene boundary. Plots of different lithic components (sedimentary lithic, Ls; very low- to low-grade metamorphic lithic, Lm1; and low- to medium-grade metamorphic lithic, Lm2) also reflect the unroofing trend in source area. The Oligocene Barail Group samples are highly quartz rich and plot in the ‘recycled orogen’ provenance field on QtFL and QmFLt diagrams (Fig. 13 and 14). The abundance of quartz and scarcity of feldspar grains with minor lithic fragments indicate erosion from a low-relief area under strong chemical weathering regimes. Oligocene sediments may have been derived from the Indian craton to the west and deposited on the passive continental margin. Paleogeographic position of the Bengal basin during Oligocene time was further south and distant from the Himalayas. The Himalayas was more then 1500 km north of the Bengal basin during Eocene and

Oligocene time (Le Fort, 1996). Orogenic detritus from early uplifts of the Himalayas were transported to the south somewhere further east of the Bengal basin. The Shillong Plateau, underlain by crystalline rocks, was not uplifted until the Pliocene time (Murthy et al., 1969; Johnson and Nur Alam, 1991). Hence, a Himalayan source seems unlikely for the Oligocene sediments in the basin. However, the Indo-Burman ranges, made up of Eocene to Oligocene turbidites underlain by Cretaceous to Eocene pelagic strata, could be a secondary source for these sediments.

In contrast to the Oligocene strata, the Lower and Middle Miocene sediments plot in the 'recycled orogenic' field on QtFL diagram and in the 'mixed' field on the QmFLt diagram. Monocrystalline (QmPK) components of sands show a relative abundance of potassium grains over plagioclase and trend of increasing potassium feldspar from Oligocene to Miocene. This sudden increase in feldspar grains and lithic fragments indicate the initial input from an orogenic source to the Bengal basin. This change may represent the initiation of uplift and erosion of Himalayas. However, radiometric dating (Hodges et al., 1994) suggests that orogenic activity began in the eastern Himalayas by Oligocene time. Large stream systems probably evolved during Miocene time and cut through the mountain belt to funnel voluminous detritus to the Bengal basin (Uddin and Lundberg, 1998a). Therefore, the sudden change in sandstone composition from Oligocene to Miocene time records the progressive unroofing of the Himalayas.

CHAPTER 5: HEAVY MINERAL ANALYSIS

5.0 INTRODUCTION

Heavy mineral analysis can play an important role in unraveling the extrabasinal (e.g., weathering of source area) and intrabasinal processes (e.g., hydraulic processes that influence the formation of clastic rocks). Heavy minerals have a specific gravity of 2.9 or more, and are generally present in sandstones in proportions of less than 1% (Tucker, 1988). There are over thirty common translucent detrital species of heavy minerals that can be used as provenance indicators (Morton, 1985; Mange and Maurer, 1992). Heavy mineral analysis is one of the most widely used techniques in provenance studies, because many heavy minerals are diagnostic of particular source rocks. Furthermore, the processes controlling the distribution of heavy minerals in sandstones are now reasonably well understood (Morton, 1985a; Uddin and Lundberg, 1998b; Morton and Hallsworth, 1999) and can be taken into account when reconstructing composition of the source rocks. Heavy mineral assemblages are affected not only by provenance, but also by a series of factors (weathering, transport, deposition and diagenesis) that operate during the sedimentation cycle (Basu, 1985; Morton, 1985; Morton and Hallsworth, 1999). Van Andel (1959) suggests that in an area where active erosion from the source area is followed by rapid deposition in a basin, all factors are of negligible importance and the heavy mineral assemblage directly reflects the source area. Heavy mineral analysis has already been an effective tool in provenance studies in different parts of

Himalayas. For example, previous heavy mineral studies have been performed for the Himalayan foreland basins to the east (Sinha and Sastri, 1973; Kumar, 2004) and the west (Chaudhri, 1972; Cerveny et al., 1989), and on deep-sea cores from the Bengal fan (Yokoyama et al., 1990; Amano and Taira, 1992). These studies have provided useful information in establishing relationships of source rocks to erosion from the Himalayas.

This study deals with semi-quantitative analysis of heavy mineral assemblages from Oligocene and Lower Miocene strata of the Bengal basin. Objectives of this study are to constrain the erosional history of the orogenic belts and assess changes in heavy mineral contents of sediments from Oligocene to Miocene transition. This study also attempts to recognize dominant varieties of mineral groups in Oligocene and Lower Miocene sequences, and identifies index minerals for those stratigraphic levels. Data from this study are compared to previously produced data from Bengal and Nicober fans, and proximal basins of eastern and western Himalayas.

5.1 METHODS

A number of heavy mineral species have an affinity to certain grain-size fractions because of the effect of hydraulic sorting. To remove the sorting effect, coherent samples were disintegrated first to liberate individual grains. Acid treatment (HCl and H_2O_2) was done to eliminate any carbonate or organic matter. Concentration of heavy minerals was then done by means of high-density liquids. There is a considerable difference in density between the framework grains and heavy accessory minerals. For this study, a gravity settling method was used with tetrabromoethane ($Br_2CHCHBr_2$, density 2.89 gm/cc). Dry and weighed samples were added to the

heavy liquid in a separating funnel. The mixture was stirred periodically to ensure that the grains were thoroughly wetted. Heavy minerals then gradually accumulated in the bottom of the funnel above the pinch clip. When sinking of heavy minerals stopped (after 10-15 hours), the stopcock was opened slowly, and heavy fractions were allowed to pour into filter paper in the lower funnel. The stopcock was then closed immediately to leave a layer of clear liquid below the lighter fraction. The light fraction was then drained into a new funnel. Both fractions were washed thoroughly with acetone and put into the oven for drying.

Resulting analysis showed that the 2-3 phi and 3-4 phi (250 to 63 micrometer) sediment fractions from the Bengal basin generally contain the highest concentration of heavy minerals. For heavy mineral point-count studies, 2-3 phi fractions were used because the grains were easier to identify under the petrographic microscope. Identification of heavy minerals was facilitated by grouping them into different fractions based on magnetic susceptibility. Using a magnetic separator, the 2-3 phi fractions were separated into low, medium, and high (0.4, 0.8, and 1.2 ampere) magnetic fractions based on mass magnetic susceptibility. The 0.4-ampere magnetic group at slide slope of 20º separates ilmenite, garnet, olivine, chromite, and chloritoid. The 0.8-ampere group at 20º slide slope isolates hornblende, hypersthene, augite, actinolite, staurolite, epidote, biotite, chlorite, and tourmaline (dark). The 1.2-ampere group at slide slope of 20º separates diopside, tremolite, enstatite, spinel, staurolite (light), muscovite, zoisite, clinozoisite, and tourmaline (light). At a slide slope of 5º, the magnetic fraction at 1.2-ampere includes sphene, leucoxene, apatite, andalusite, monazite, and xenotime. The non-magnetic fraction consists of zircon, rutile, anatase, brookite, pyrite, corundum, topaz, fluorite, kyanite, sillimanite, anhydrite, and beryl (Hess, 1966).

Slide mounts were then made of the magnetically defined heavy-mineral separates by sprinkling mineral grains (usually more then 300) onto a slide in a drop of oil with a refractive index of 1.550. All mineral identification was carried out with a petrographic microscope using a modification of the Fleet method (Fleet, 1926), in which nearly all grains on each microscope slide were counted. Grains identified from each magnetically separated fraction were then added together to calculate frequency percentage of heavy minerals present in the 2-3 phi size fractions of all the slides. For convenience, a chart was made listing important diagnostic properties of commonly found mineral species (Table 4). Thirteen different varieties of heavy minerals were identified, including opaque minerals as a single group.

5.2 RESULTS

Heavy mineral point-count data can be used to illustrate relationships among individual mineral species. Semi-quantitative point-counting results for heavy minerals from Oligocene and lower Miocene rocks of the Bengal basin are presented in Table 5. Total heavy mineral content is low in Oligocene sandstones compared to the lower Miocene. Total weight % of heavy minerals to framework grains is 0.35% for Oligocene samples and 0.63% for the lower Miocene samples. Heavy mineral assemblages did not show much variation between Oligocene to Miocene sediments.

Heavy mineral assemblages in Oligocene Barail sands are dominated by opaque and the stable minerals (zircon-rutile-tourmaline; Table 5). The ZTR (zircon-rutile-tourmaline) index (the fraction that includes these three stable heavy minerals) decreases from the Oligocene (39.44%) to the Lower Miocene (29.77%). Miocene sediments have lower amount of opaque minerals (28%) compared to Oligocene

Table 4. Diagnostic properties of commonly found heavy minerals in Bengal basin (after Deer et al., 1992; Mange and Maurer, 1992).

Name of Mineral	Color/ Relief	Pleochroism	Extinction	Cleavage	Birefringence	Interference	Distinguishing feature	Occurrence
Zircon	Colorless-Very high	Very week	Parallel	imperfect	Strong	Poor int. figure	Extreme relief, morphology, strong birefringence	Widespread in rocks of crustal origin, common in silicic and intermediate igneous rock.
Tourmaline	Dark brown, yellow, colorless-moderate	Present, marked	Parallel	none	Strong, color bands	Uniaxial	Moderate relief, variable morph and color, lack of cleavage	Granite, granite-pegmatite, pneumatolitic veins- in contact or regional metamorphic rocks.
Rutile	Shades of red-high	Distinct, deepening of red	Parallel	Good prismatic	Extreme but mostly red	Thin grains show uniaxial,	Very high relief, deep color, Pleochroism, birefringence	Widespread in metamorphic rocks, in schist, gneiss and amphibolites-high grade regional metamorphic terrains, less in igneous.
Garnet	Colorless- very high	None	Isotropic	poor	Isotropic	Uniaxial/biaxial neg. variable 2v	High relief, isotropic, colorless	In a variety of metamorphic rocks, also in plutonic igneous, pegmatites, in ultramafic, acid volcanics.
Epidote	Shades of green – high	Either week or distinct	Parallel, nearly parall.	Perfect in 1 direction	Moderate, increase with Fe^{3+}	Rare, straight isogyre	High relief, green color, Pleochroism and irregular morphology.	Index mineral of green-schist facies regional metamorphism. Also present in contact metamorphic rocks and in hornfels.
Biotite	Shades of brown for biotite.	Very weak to none	Parallel to nearly parallel	One directional basal	First order yellow	Centered acute bisectrix with small 2V	Flacky, foliated, very small 2V	Ubiquitous in igneous rocks, granite and granite pegmatite.
Kyanite	Colorless - moderate	None	Oblique, 27-32	Perfect 2 directional	Moderate to strong	well centered acute bisectrix big 2V	Habit, perfect cleavage and parting, large ext. angle, good interferenc	Gneissic, granulites and pelitic schists generated by regional metamorphism
Sillimanite	Colorless, fibrous are pale green	Rare	Parallel to prism & fibers	One but imperfect	Moderate to fairly strong	Well center acute bisec. Mod 2V	Long slender prismatic habit, nice interference sometimes fibrous,	High temp metamorphic rocks, in sillimanite – cordierite gneisses and biotite-sillimanite hornfels.
Andalusite	Colorless, rarely pinkish tinge. -mod relief	Some are, some not	Parallel to cleavage trace & crystal face	Irregular	Weak, but mostly 2nd order red coz of uneven thickness and irregular shape	Acute bisectrix with large 2V	Angular, irregular, large, high Pleochroism	Typically metamorphic appear in argillaceous rocks of contact aureoles around igneous intrusion.
Chlorite & Chloritoid	Chlorite-Shades of green. Chloritoid-grayish blue,	Not always except deep green,	Parallel to cleavage and fiber	One good direction	Basal plates are isotropic, blue.	Well centered biaxial with varying 2V	Mica habit, green color, low brief.	Widespread in low-grade metamorphic rocks and common in greenschist facies.
Apatite	colorless	Reddish variety has pleo..	Parallel, chloritoid -18	Imperfect basal	Weak to moderate	Anomalous biaxial	Mod-high relief, lack of color, morphology and weak birefringenc	All type of igneous rocks, found widespread in sedimentary rocks.

Table 5. Normalized abundances of heavy minerals, Bengal basin, Bangladesh. (ZTR – Zircon-Tourmaline-Rutile)

Minerals	**Oligocene**	**Percentage**	**Lower Miocene**	**Percentage**
Number of samples	**n = 8**		**n = 6**	
Non Opaque Minerals		ZTR% 39.44		ZTR% 29.77
Zircon	52	9.08	40	7.78
Tourmaline	77	13.44	78	15.18
Rutile	97	16.93	35	6.81
Amphibole	6	1.05	18	3.5
Chrome Spinel	18	3.14	0	0
Garnet	5	0.87	63	12.26
Chlorite & Chloritoid	6	1.05	43	8.37
Biotite & Muscovite	12	2.09	88	17.12
Monazite	6	1.05	2	0.39
Epidote	2	0.35	3	0.58
Anatase	3	0.52	0	0
Sillimanite	1	0.21	2	0.39
Opaque Minerals		**Opaque % 50.44**		**Opaque % 28**
Pyrite	3	0.52	8	1.56
Pyrrhotite	1	0.17	3	0.58
Ilmenite	16	2.79	29	5.64
Leucoxene	14	2.44	6	1.17
Magnetite	6	1.05	21	4.09
Unidentifiable	249	43.46	77	14.98
Total	**573**		**514**	

(50.44%). Of the ultra-stable minerals, rutile is more abundant than tourmaline and zircon (Table 5; Figs. 20 A, B; 21A, B). The majority of the opaque grains are unidentifiable under transmitted-light polar microscope. However, some opaque minerals, such as pyrite, pyrrhotite, ilmenite, leucoxene, and titanium-rich magnetite were identified using reflected light microscopy and an electron microprobe equipped with energy dispersion spectrometer (EDS) at the University of Georgia.

Garnets are rare to absent in Oligocene sediments (0.87% of total heavy mineral assemblage), but are abundant in lower Miocene strata (12.26%). Chemical analysis of mineral grains shows that most garnets are of the almandine-type (Fig. 22A). Chrome spinels are present in Oligocene sandstones, but are not seen in Lower Miocene strata. These chrome spinels are very dark to opaque and were not identifiable under the petrographic microscope. These spinels are mostly chromite-rich, with low-aluminum content. No compositional zoning can be observed in chrome spinels by EDS.

Aluminum silicate minerals (i.e., sillimanite, kyanite, and andalusite) were not observed in Oligocene samples, but sillimanite was found in minor abundance in Miocene sediments (Fig. 22B). Miocene heavy mineral assemblages are dominated by muscovite and biotite followed by chlorite and chloritoid (Table 5; Fig. 23A). Epidote is the only mineral that is found in both Oligocene and Lower Miocene units (Fig. 23B) in the epidote family (epidote, zoisite, and clinozoisite). Epidote is found in low quantities with no significant change in abundance from Oligocene to Miocene sandstones. Hornblende was not observed by petrographic microscopy although minor amounts (four grains) of hornblende were detected by microprobe analysis. Backscattered electron images of zircon and chrome spinel are shown in figures 24 A and B.

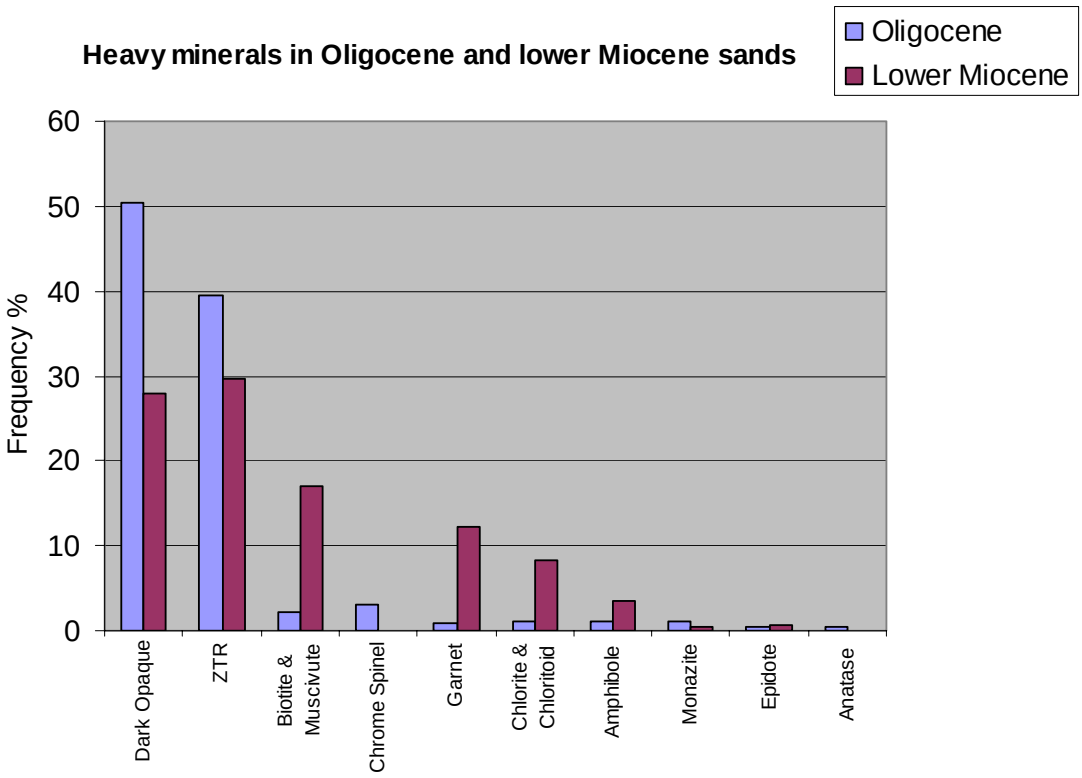

(A)

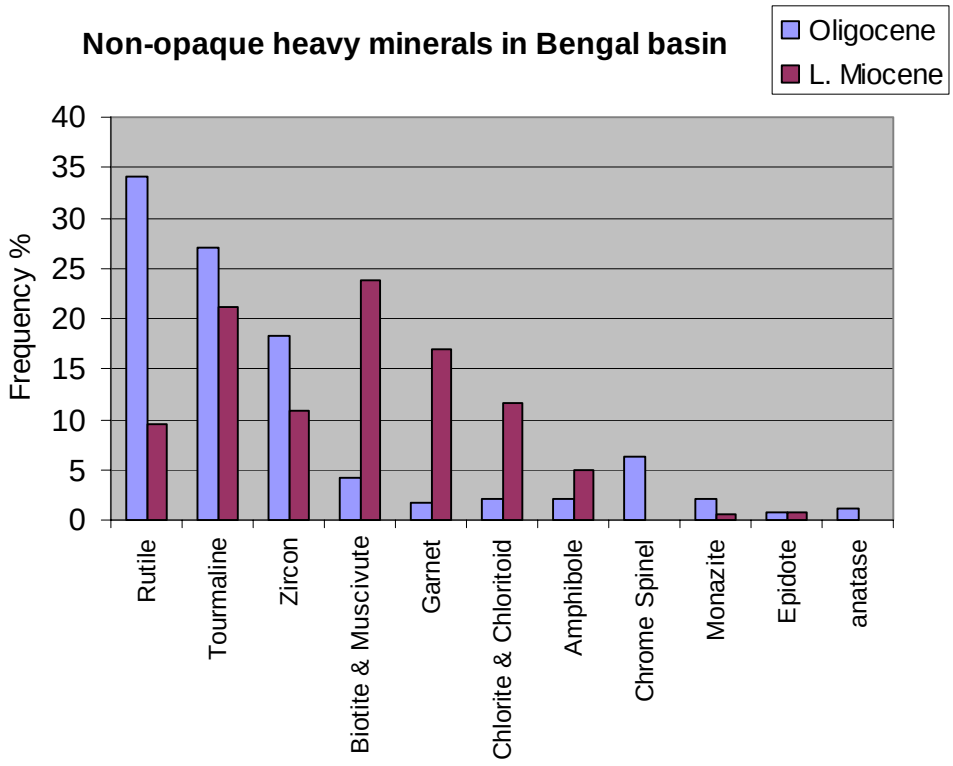

(B)

Figure 20. Heavy-mineral distribution in sandstones of Oligocene and lower Miocene sediments from Bengal basin showing (A) overall distribution of all observed heavy minerals including opaque grains, and (B) distribution of non-opaque heavy minerals including ultra-stable minerals. ZTR = zircon, rutile, and tourmaline.

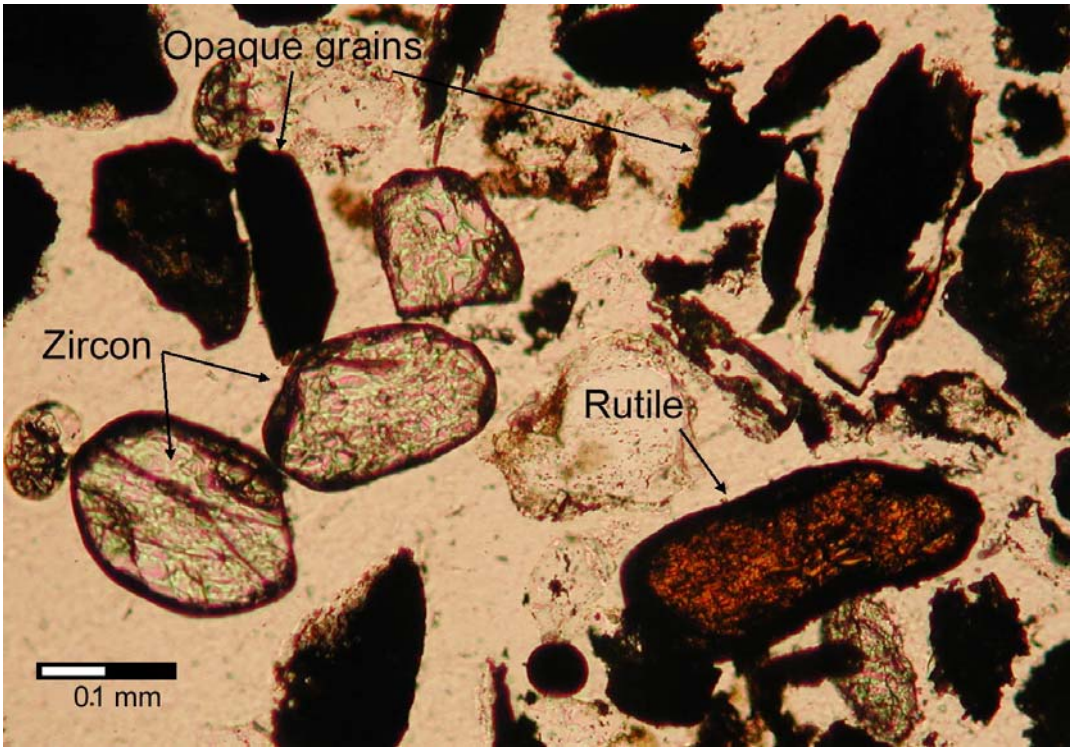

(A)

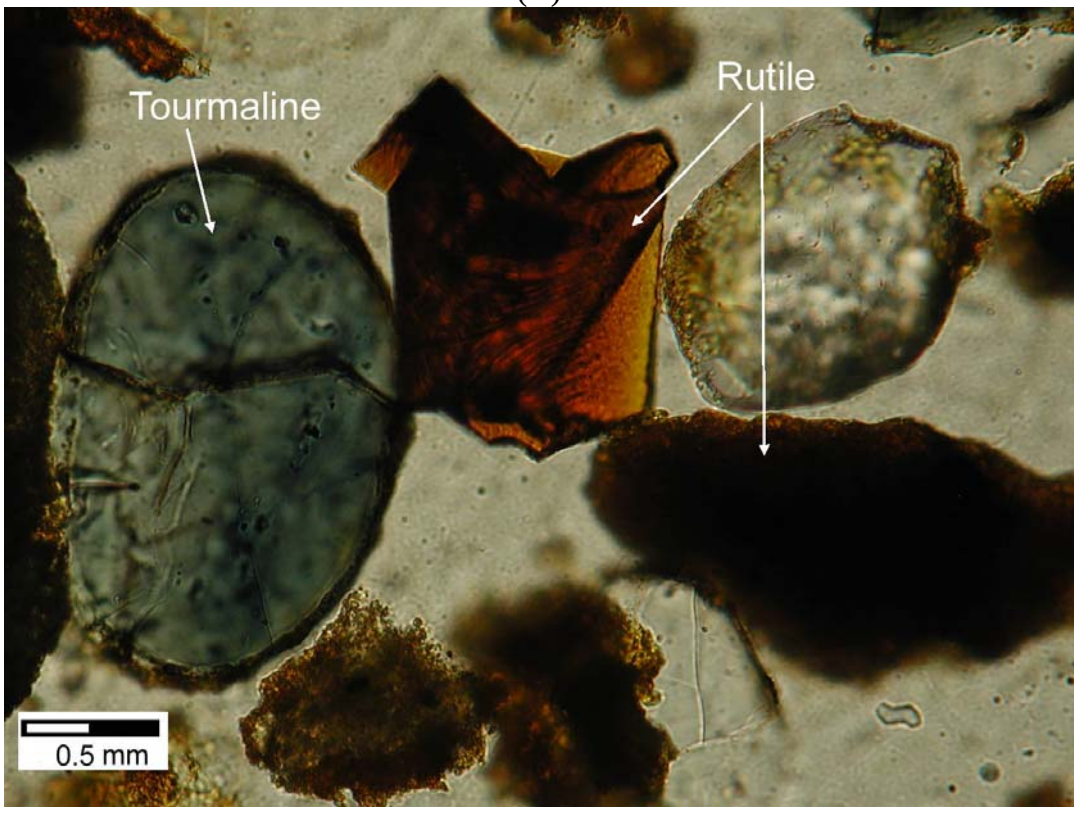

(B)

Figure 21. Photomicrographs of heavy minerals from Oligocene sediments of Bengal basin showing (A) zircon, rutile, and dark opaque minerals (sample # Bsr. 21.2), and (B) tourmaline and rutile (sample # Bsr 8.1).

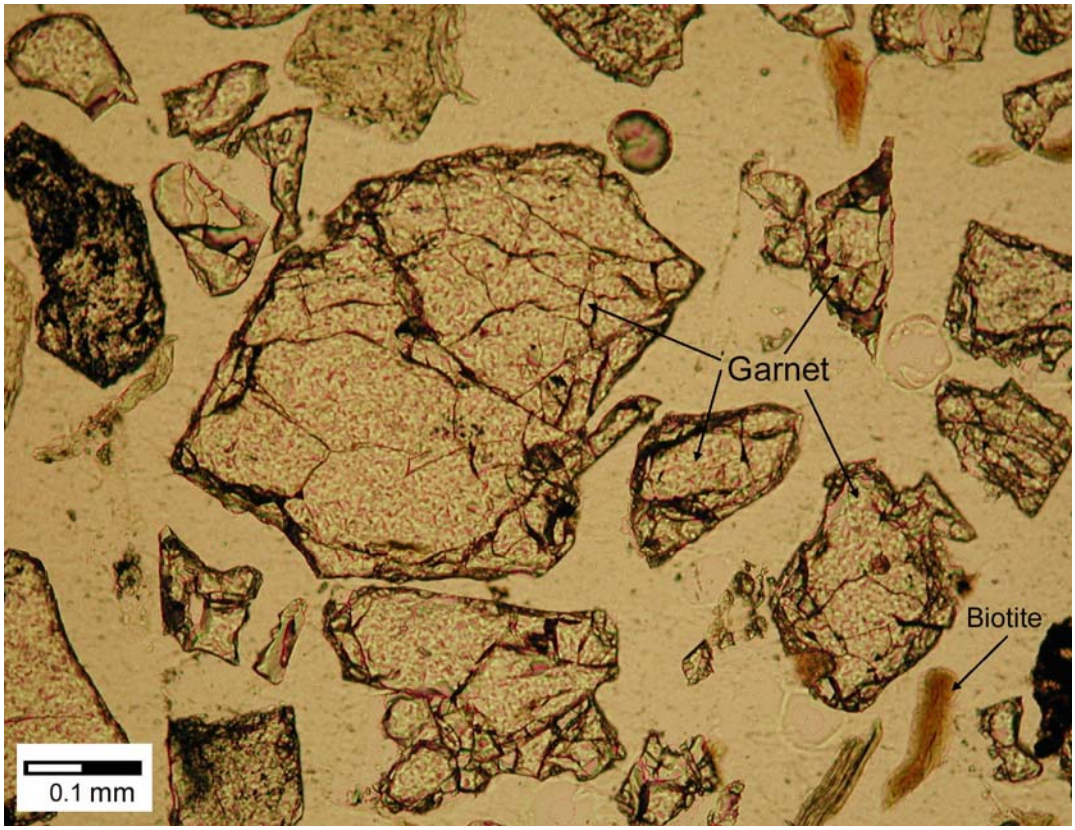

(A)

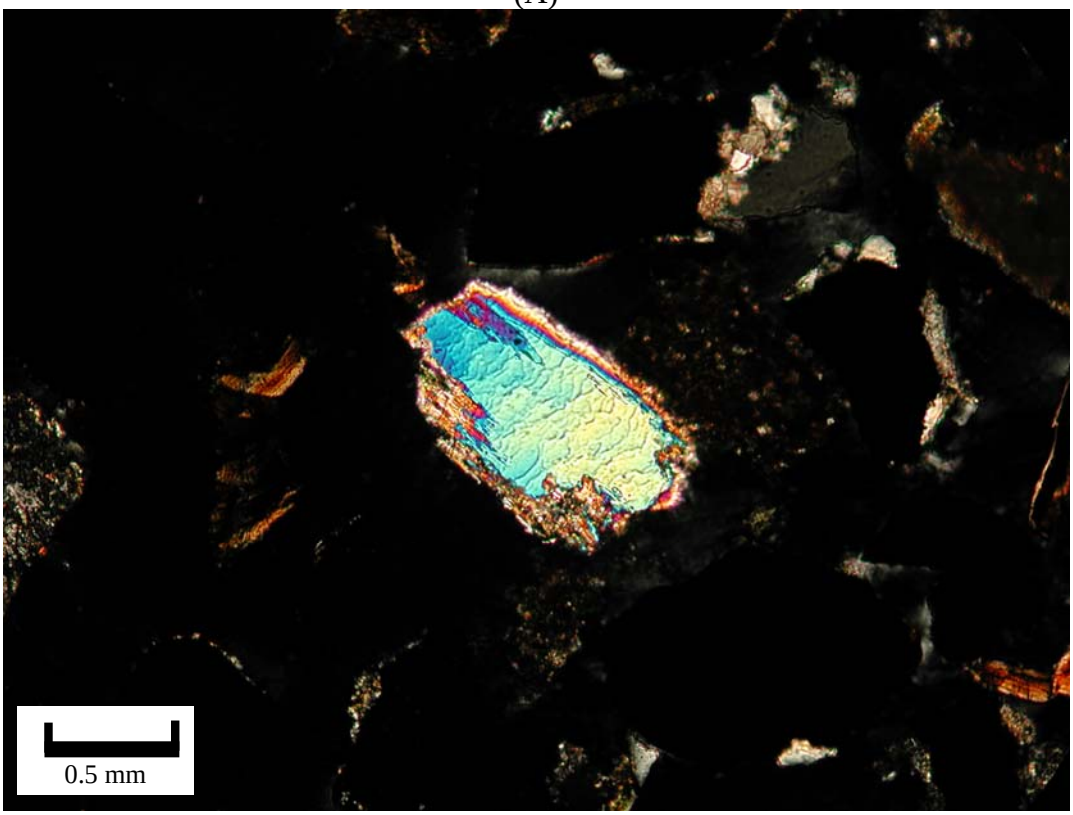

(B)

Figure 22. Photomicrographs of heavy minerals from Lower Miocene sediments of Bengal basin showing (A) garnets and biotite (sample - Fenchuganj), and (B) sillimanite (sample - Beani Bazar).

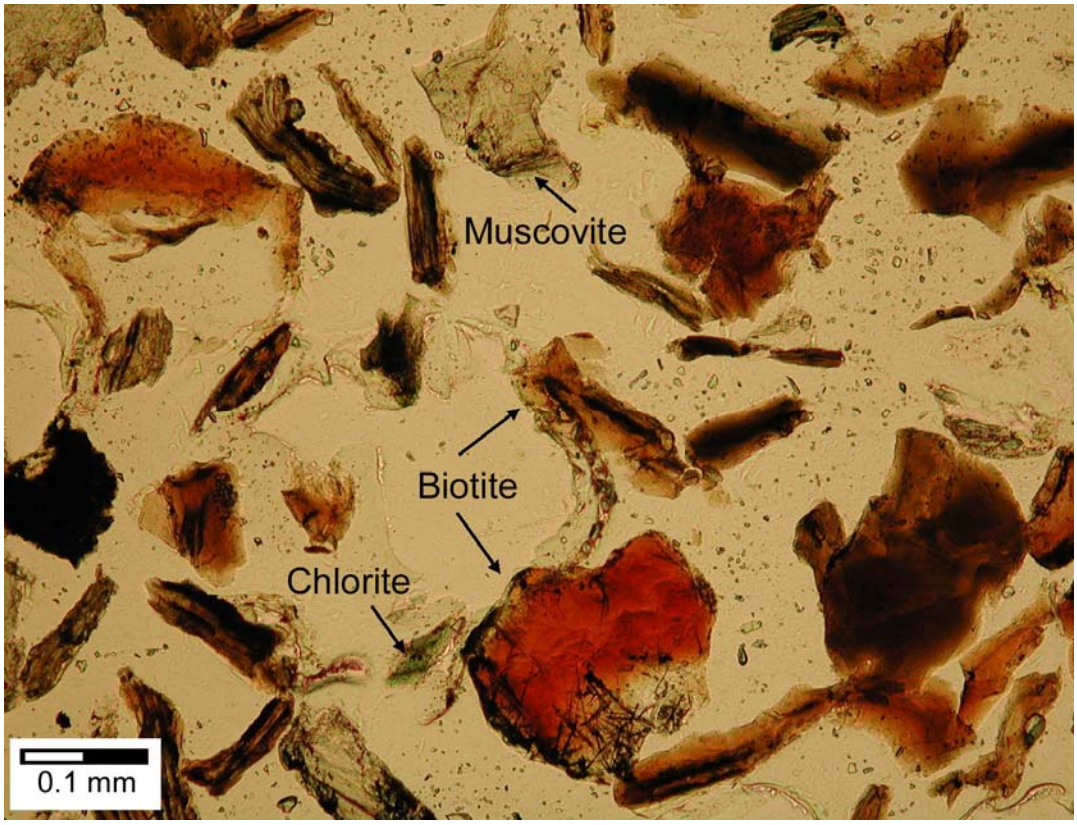

(A)

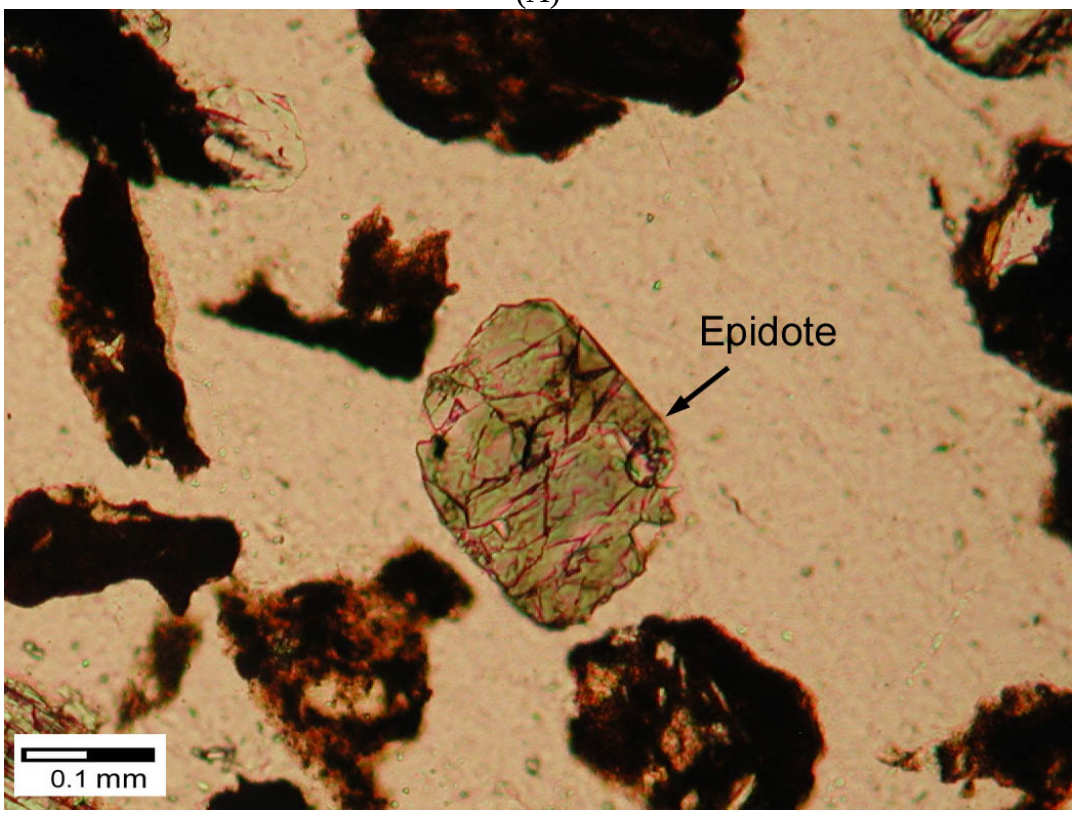

(B)

Figure 23. Photomicrographs of heavy minerals from sediments of Bengal basin showing (A) muscovite, biotite, and chlorite from Lower Miocene sands (sample # Feni 22), and (B) epidote from Oligocene strata (sample # Bsr. 11.1).

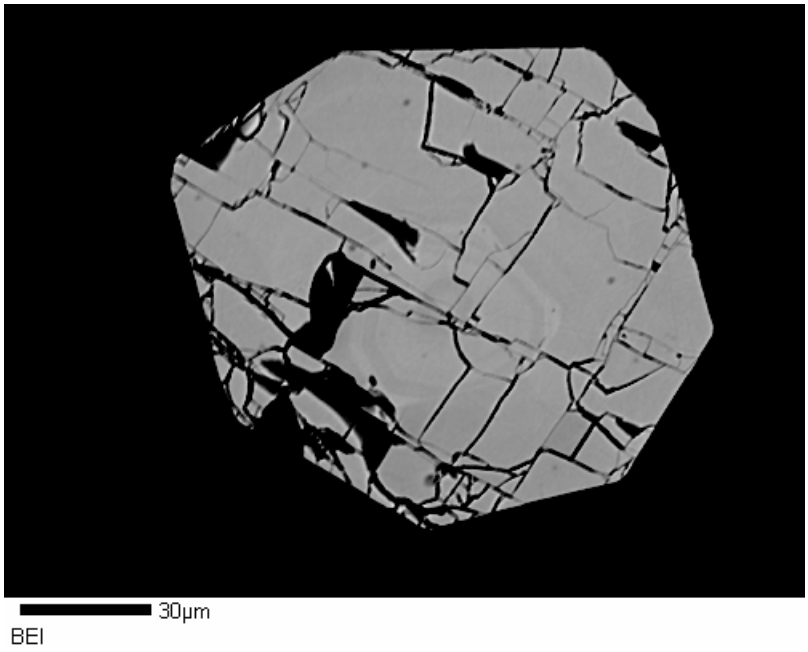

(A)

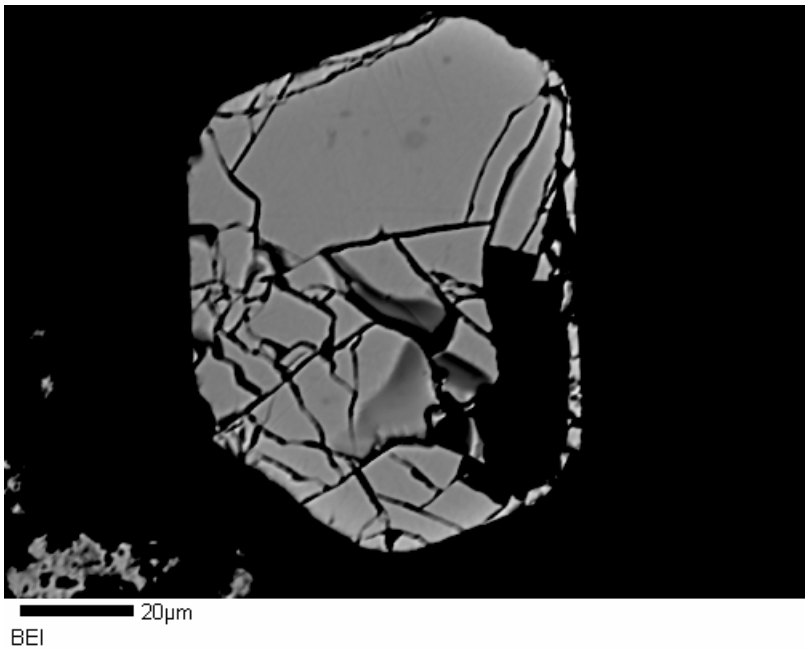

(B)

Figure 24. Backscattered electron image of (A) zircon (sample # Bsr. 21.2), and (B) chrome spinel (sample # Bsr. 8.1); showing crystal shape and surface morphology. Note that no compositional zoning can be observed at any of these grains.

5.3 PROVENANCE HISTORY

Heavy mineral studies have numerous advantages over light mineral studies, as they provide a much wider spectrum of silicates, sulfates, sulfides, oxides, and phosphates in the sand-size fraction (Milner, 1962; Mange and Maurer, 1992). Semi-quantitative point counts of heavy mineral assemblages in the Bengal basin sands and sandstones illustrate relationships that can be observed and inferred between individual mineral species and the assemblages in which they are found. It also indicates the source rocks from which they are derived.

Oligocene sediments from Bengal basin contain relatively small amounts of heavy minerals (0.35%), of which 50.44% are opaque varieties (Fig. 20). The few non-opaque heavy minerals in these sandstones are dominated by ultrastable species: tourmaline, zircon, and rutile (ZTR). The high ZTR index reflects relatively high maturity of these sediments (Hubert, 1962). Opaque minerals include pyrite, pyrrhotite, ilmenite, leucoxene, and magnetite. The non-opaque grains are subangular to subrounded and show little alteration. The suites include few tourmaline, zircon, rutile, garnet, and amphibole. The ZTR index for non-opaque minerals is 39.44% in the Barail Group (Table 5). The relative abundance of opaque minerals with high ZTR index indicates high mineralogical maturity of Oligocene Barail sediments. Complete absence of kyanite indicates either lack of kyanite-grade suites in the source area or subsequent dissolution of those grains after erosion. This composition also suggests intense chemical weathering due to the position of the Bengal basin near the paleoequator during the Oligocene -early Miocene time (Lindsey et al., 1991; Klootwijk et al., 1992).

The Lower Miocene sediments contain heavy mineral assemblages that are similar to the Oligocene sands. However, heavy minerals are more abundant in

Miocene and the assemblages are marked by the presence of chlorite, muscovite and biotite. The ZTR index is lower than that in Oligocene. Opaque minerals are also less abundant. The amount of garnet increases significantly during the Miocene, which may indicate a possible input from metamorphic sources. Presence of muscovite, biotite and chlorite also support this conclusion.

Textural and mineralogical composition of the heavy minerals from the Oligocene sediments from the Bengal basin suggests a relatively short transport distance and the source was somewhere close to the basin. The mineralogical maturation and mineral assemblage suggests the Indian craton to the west as a possible source area. The presence of abundant opaque minerals indicates a more basaltic source which could have been the Rajmahal trap located in the northwestern part of the basin (Fig. 4). However, the possibility of an orogenic source cannot be completely ruled out. Presence of epidote, garnet, and aluminosilicates (sillimanite) indicate erosion from medium- to high-grade metamorphic rocks. Indication of an orogenic source is more pronounced in the Lower Miocene than in the Oligocene sandstones.

CHAPTER 6: MICROPROBE ANALYSES

6.0 INTRODUCTION

Heavy mineral analyses have long been applied to provenance evaluation. A large number of detrital mineral species may be source diagnostic. An understanding of sandstone provenance is critical to the evaluation of any changes in sedimentation style, depositional environment, and sediment source. In addition, variations in provenance within a depositional system provide a basis for correlation between two comparable stratigraphic units. Thus, provenance studies are particularly important in nonmarine sequences like those of Bengal basin where biostratigraphic control is poor.

Major goals of this project are to place constraints on the provenance of Oligocene and Miocene sediments deposited in the Bengal basin of Bangladesh, and to shed light on the change of provenance through time. The Bengal basin lies near the junction of two major mountain system, the Himalayas to the north and northwest and the Indo-Burman Ranges to the east. It is important to establish the relative distribution of sediments from these two orogenic belts through time.

6.1 MINERAL CHEMISTRY

Four mineral groups – garnet, chrome spinel, tourmaline, and amphibole were chosen for mineral chemistry analysis for this study. Except for amphiboles, all are common in Oligocene and Miocene sediments. Each of these minerals can be

subdivided into compositional varieties that are indicative of the source rocks from which they derived. Several workers have studied provenance based on chemistry of these minerals (Henry and Guidotti, 1985; Morton, 1985; Henry and Dutrow, 1990; Morton and Taylor, 1991; Nanayama, 1997).

Garnet [$X_3Y_2(SiO_4)_3$], found commonly in metamorphic rocks and certain igneous rocks, provides an "index" of the source-rock bulk composition and, hence, potentially the pressure and temperature conditions of rock formation. Increasing metamorphic grade is reflected by an increase in the ratio (Fe^{2+} + Mg^{2+})/ (Ca^{2+} + Mn^{2+}) in the cubic-coordination (X) site, as noted by Sturt (1962) and Nandi (1967). In pelitic schists, as well as mafic protoliths, the Mg concentration increases with respect to Fe^{2+} with increase in metamorphism (Spear, 1993). Significant occupation of the octahedral site by cations other than Al^{3+} (i.e., Cr^{3+}, Fe^{3+}) also may be useful in constraining the chemical conditions of crystallization. Garnet chemistry has been used to evaluate provenance in a number of regions (Morton and Taylor, 1991), the most relevant to this study being in the offshore Bengal fan (Yokoyama et al., 1990).

Compositional analysis of chromian spinel is routinely applied in petrologic studies of spinel-bearing mafic and ultramafic rocks (Irvine, 1973, 1977; Dick and Bullen, 1984, Nixon et al., 1990), because chromian spinel composition is a sensitive indicator of parental melt condition. Chrome spinel [$A_8B_{16}O_{32}$], found most commonly in mafic igneous rocks, provides a particularly good index of the source rock. There are 32 oxygen ions and 24 cations in the unit cell; eight of the cations are in four-fold coordination (the A positions), and 16 are in six-fold coordination (the B positions) (Deer et al., 1992). Two structural types occur, differing in their distribution of cations among the A and B positions, and are known as normal and inverse spinels. $FeAl_2O_4$ (hercynite), $ZnAl_2O_4$ (gahnite), and $MnAl_2O_4$ (galaxite) are

normal spinels, while $MgFe_2^{3+}O_4$ (magnesioferrite) and $Fe^{2+}Fe_2^{3+}O_4$ (magnetite) have inverse structure. In nature, pure end-members are rare and occur mostly as solid-solution series; varieties are designated by the most dominant constituent cations (Deer et. al., 1992).

Tourmaline, with a general formula of $XY_3Z_6(BO_3)_3Si_6O_{18}(OH)_4$, is often overlooked in petrographic studies despite its widespread presence in sedimentary rocks. A very wide range of cation substitutions are possible in tourmaline. This mineral crystallizes under a wide variety of igneous and metamorphic conditions. Its ubiquitous nature probably accounts for its traditional neglect in provenance studies; the simple presence of tourmaline does not place many constraints on the source rock type. But if its chemistry is considered, tourmaline becomes a particularly valuable petrogenetic indicator. Tourmaline plots of AL-Fe(tot)-Mg and Ca-Fe(tot)-Mg have been shown to discriminate between tourmalines from a variety of rock types (Henry and Guidotti, 1985; Henry and Dutrow, 1990).

Amphiboles, found in minor quantities in the Oligocene samples, are a group of minerals with the generic formula $A_{0-1}B_2C_5T_8O_{22}(OH,F)_2$ (Leake, 1978). In metamorphic amphiboles, increasing grade results in an increase in $[Al]^{IV}$, $[Al]^{VI}$, Ti, Fe^{3+}, Na, and K relative to Si, Fe^{2+}, Mg, and Ca (Deer et al., 1992). Mineralogically, this corresponds to the actinolite-hornblende- pargasitic hornblende-pargasite progression. Prior study (Van Orman, unpublished data) related to this work indicates that there are systematic changes in abundance of calcic amphibole (identified optically) in the Sylhet trough samples that correspond closely in time with similar changes both in the Pakistan Himalayas (Cerveny et al., 1989) and in the offshore Bengal fan (Yokoyama et al., 1990). It has been suggested (Amano and Taira, 1992) that the appearance at ~11 Ma of calcic amphibole in the Bengal fan is related to the

unroofing of a large petrologic province of the Himalayas and that this unroofing event may signal a major pulse of uplift.

6.2 SAMPLE SEPARATION

All the samples were sieved into whole-phi fractions; the 2-3 and 3-4 phi fractions were used for the analysis. Highly magnetic fractions were removed from the heavy-mineral separates using hand held magnets and a Franz magnetic separator. The remaining "heavy" fraction was divided further into three to four groups using a Franz magnetic separator, with the aim of concentrating the mineral species that would be analyzed with electron microprobe. Slides were prepared by drilling 1/8" holes in 1.5" X 0.75" Plexiglas sheets, pouring grains from each magnetic subfraction into different holes (from low, medium to high magnetic susceptibility), and then setting them with epoxy. The Plexiglas sheets were then mounted on glass slides, ground to standard optical thickness of 30 micrometers, and polished for microprobe analysis. Before the samples were put into the microprobe sample chamber, electrically non-conductive samples were carbon-coated to ensure conduction. Standards and samples were coated to the same thickness. Carbon coating was carried out by carbon evaporation under vacuum. A polished brass block was used to monitor the thickness of the carbon coat. As the thickness of coat increases on the brass, it changes color from orange (150 Å) to indigo red (200 Å), then to blue (250 Å), and then to bluish green (300 Å).

6.3 THE ELECTRON MICROPROBE

The electron microprobe provides a complete micron-scale quantitative chemical analysis of inorganic solids. The method is nondestructive and utilizes

characteristic x-rays excited by an electron beam incident on a flat surface of the sample. In the electron microprobe, x-rays are emitted by the sample in response to a finely focused electron beam incident on the sample at a right angle. Some of the beam electrons are scattered backward. The backscattered electrons, as well as the characteristic x-rays of the elements, carry information about chemical composition. Backscattered electrons are a result of multiple elastic scattering and have energies between 0 and E_0 (the beam energy). Secondary electrons, which are specimen electrons, mobilized by the beam through inelastic scattering, have energies in the range 0-50 eV with a most probable energy of 3-5 eV. Because of energy differences between backscattered, characteristic X-rays, and secondary electrons, different detector setups are required for the detection of the three types of electron signal. The idea to use a focused electron beam to excite x-rays in a small area for the purpose of x-ray spectrometry was first patented by Marton and Hillier in the 1940s, and the first electron microprobes were built in the early 1950s.

The electron microprobe serves two purposes: (1) it provides a complete quantitative chemical analysis of microscopic volumes of solid materials through x-ray emission spectral analysis; and (2) it provides high-resolution scanning electron and scanning x-ray (concentration maps). There are two types of scanning electron images: backscattered electron (BSE) images, which show compositional contrast; and secondary electron (SE) images, which show enhanced surface and topographic features. Scanning-cathodoluminescence images form by light emission in response to the interaction between the scanning electron beam and the sample.

A JEOL JXA 8600 microprobe was used for mineral chemistry work for this study at the University of Georgia microprobe lab. The probe is automated by a Geller Micro analytical laboratory dQANT automation. The analysis was done using an

accelerating voltage of 15 K. V. and a beam current of 15 nanno amps. Both natural and synthetic standards were used to calibrate the data. A PRZ metric correction was used.

Standard intensity calibration: Standard x-ray intensities of the elements to be measured were obtained on appropriately chosen standards. Different standards were used for different elements. Secondary standards were analyzed as unknowns to check if their known compositions are reproduced. The analytical conditions (e.g., accelerating voltage, beam current, etc.) were maintained throughout the session.

Table 6 lists the standards that have been used for this analysis. Most of them come from the C. M. Taylor Corp. The USNM standards come from the National Museum of Natural History, a branch of the Smithsonian Institution. This study used two synthetic standards obtained from the University of Oregon microprobe lab, and an almandine standard obtained from the Harvard Mineral Museum. Calibration for each analysis session was checked using the Kakanui Hornblende (USNM) and Pryope #39 (C. M. Taylor) standards.

6.4 RESULTS

A total of 55 grains (12 garnets, 18 chrome spinel, 21 tourmalines, and 4 amphiboles) were analyzed for this study in the University of Georgia Microprobe Lab with assistance from Mr. Chris Fleisher. All the eleven slides were scanned thoroughly by the EDAX and only the grains of interest were analyzed for chemical composition. One spot analysis per grain was conducted. Results are provided in appendices A-D, and summarized below.

Table 6. Electron microprobe standards used in this study.

Electron Microprobe Standards			
Element	**Standard**	**Source**	**Comment**
Cr	Chromite #5	C M Taylor Corp	
Mn	Spessartine #4b	C M Taylor Corp	
TiO2	Rutile	C M Taylor Corp	
Ca	Sphene #1A	C M Taylor Corp	
Fe	Hematite #2	C M Taylor Corp	Used for oxide (spinel) analyses
Fe	Syn. Fayalite Ol-11	Univ. of Oregon	Used for silicate analyses
Ni	Ni metal	C M Taylor Corp	
Si	Diopside 5A	C M Taylor Corp	Si standard for all phases except garnet
Mg	Olivine #1	C M Taylor Corp	
Al	Syn. Spinel	C M Taylor Corp	
K	Orthoclase MAD-10	C M Taylor Corp	
Na	Ameila Albite	USNM	This is a ubiquitous Na standard
Si	Almandine	Harvard Mineral Museum	Si standard for garnet analyses
F	Syn. Fluoro-Phlogopite	oxygen standard #112140 University of Oregon M-6)	
Cl	Scapolite	USNM R 6600-1	

6.4.1 Garnet

Most of the garnets analyzed for this study are from the Lower Miocene sequences; only two are from Oligocene sediments. Garnets are scarce to none in Oligocene sequences. Most of the garnets found are colorless and occur as euhedral grains. Variations in different end components (pyrope, almandine, and grossular) in garnets are plotted in figures 25, 26, 27, 28, and 29. Detrital garnets analyzed from the Lower Miocene and Oligocene rocks of Bengal basin are almandine rich (average 70%, maximum 80%). Pyrope content is generally low (average 18%, maximum 35%) and grossular component is subordinate (average 9%). The spessartine component generally did not exceed 3% in any of the samples.

Data from chemical analysis of garnets from the Bengal basin have been plotted on the different ternary diagrams to evaluate the variations in elemental composition (Figs. 25-30). In the (Sp+Gro)- Py-Alm plot (Fig. 25), most of the garnet grains plot close to the almandine apex and indicate low pyrope content. However, on the (Py+Alm)-Sp-Gro plot (Fig. 26), all the grains plot close to Py+Alm apex and along the Py+Alm–Gr line. This reflects very low spessartine content. Similarly, when garnet compositions are plotted on the Sp-Alm-Py ternary diagram (Fig. 27), grains plot close to the almandine apex with a few in granulite facies field (GNF). In the Gro-And-Alm-Py plot, grains lie close to the almandine apex, but a few plot in metamorphic pegmatite and granulite facies (Fig. 28).

The grossular content (mol. %) of the garnet grains indicate that most are derived from low-pressure regimes (Fig. 30). These garnet grains are distributed into three fields based on pyrope contents to help understand the paragenesis and bulk composition of the source rocks (Morton, 1992). Some of the garnet grains of the Oligocene and Miocene sequences of the Bengal basin are high in pyrope but low in

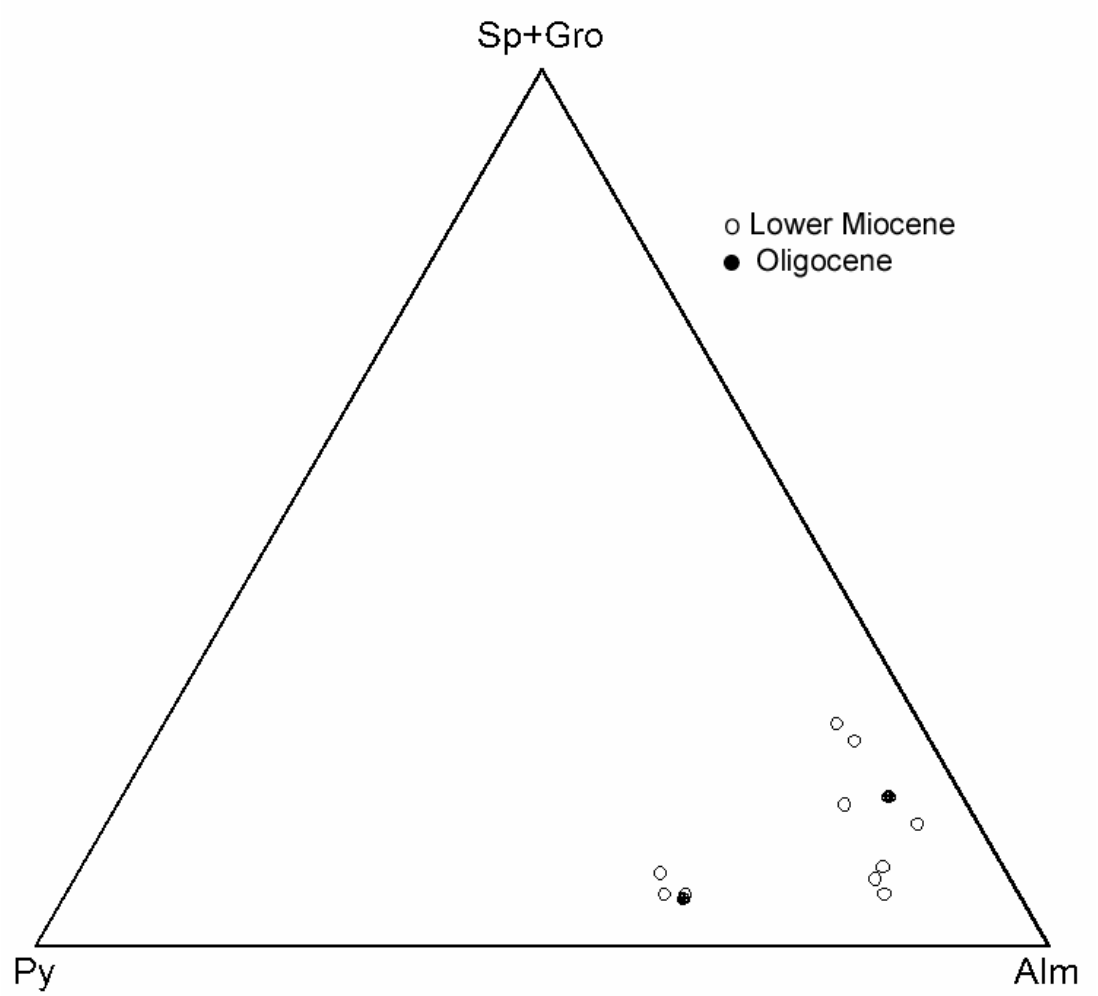

Figure 25. Chemical composition of garnets from the Bengal basin sediments plotted on (Sp + Gro) – Py- Alm. Sp = spessartine; Gro = grossular; Alm = almandine; Py = pyrope (adapted after Nanayama, 1997).

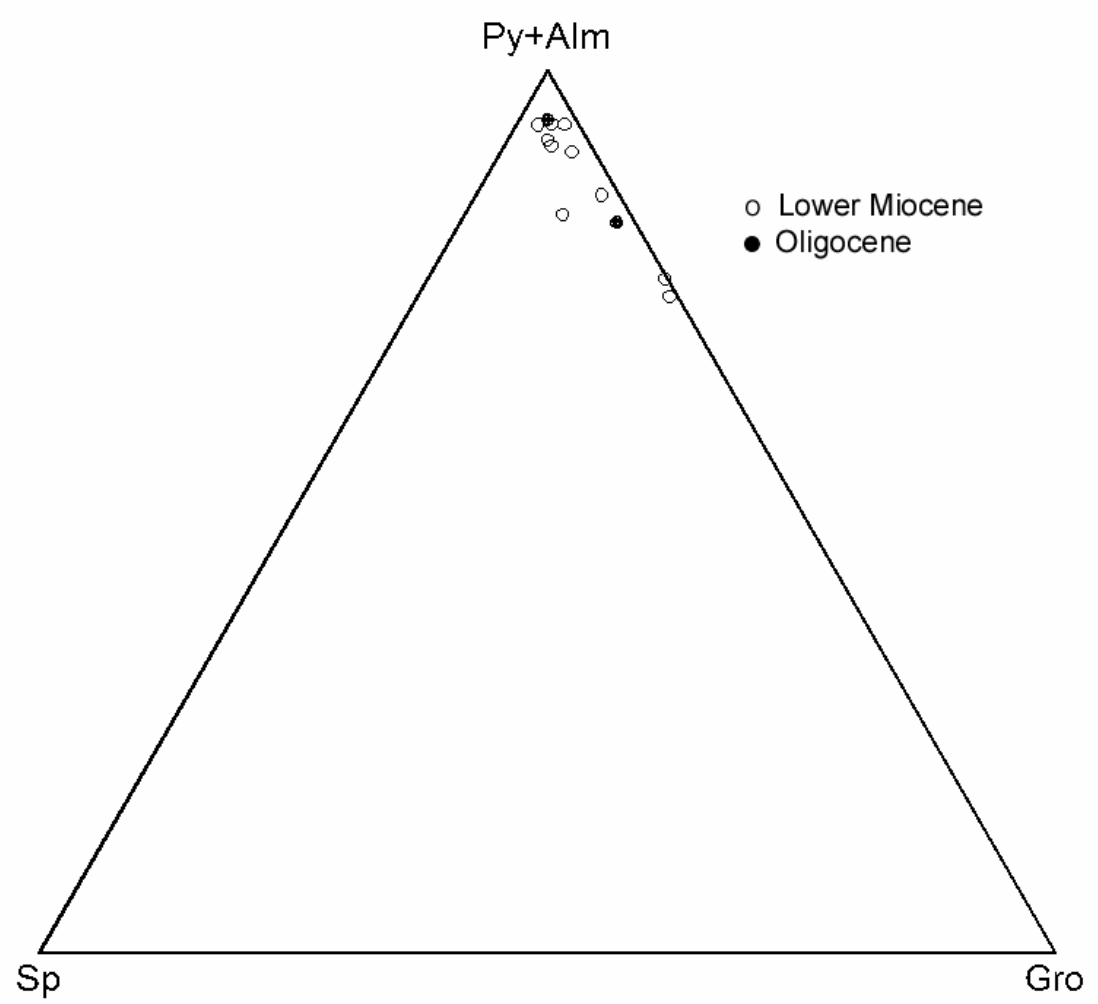

Figure 26. Chemical composition of garnet from the Bengal basin sediments, plotted on (Py + Alm)- Sp- Gro. Sp = spessartine; Gro = grossular; Alm = almandine; Py = pyrope (adapted after Nanayama, 1997).

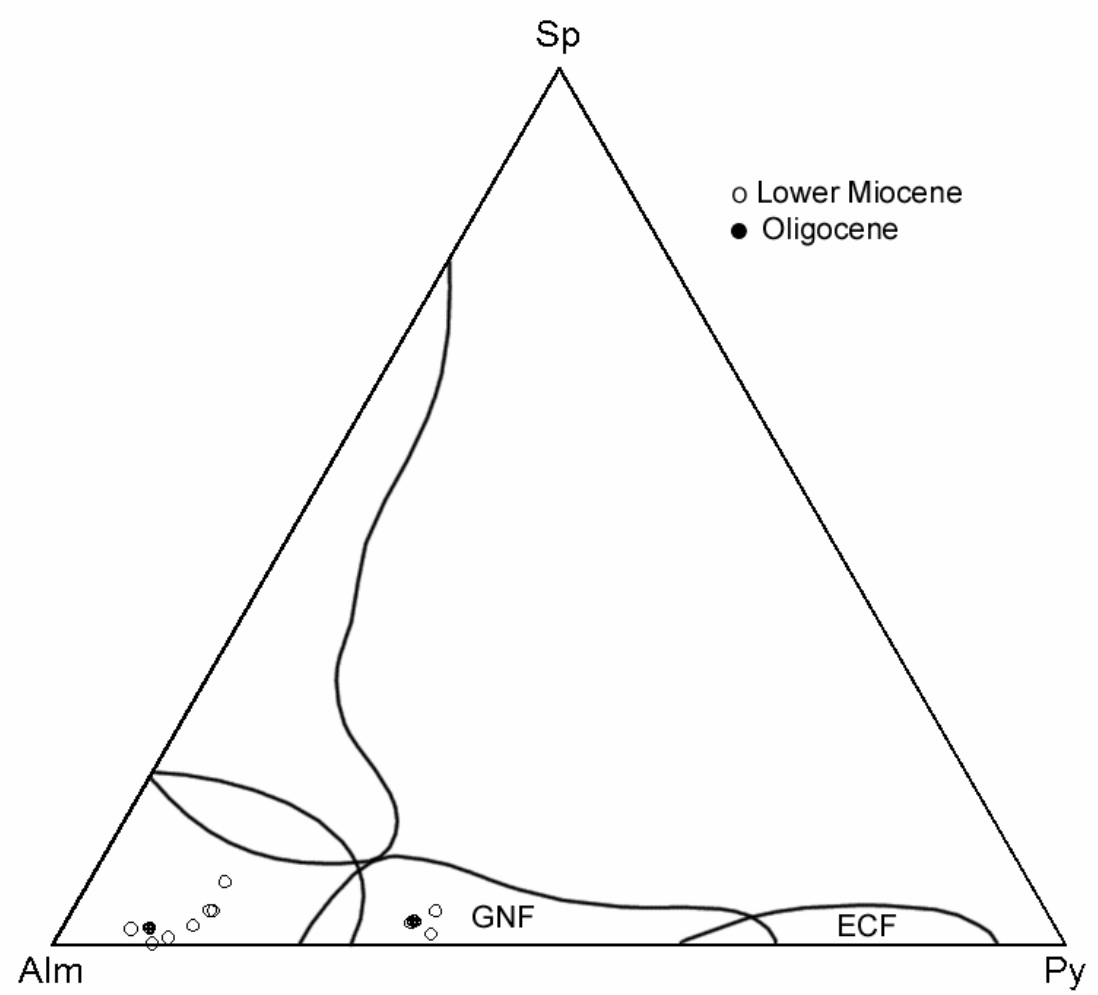

Figure 27. Chemical composition of garnet grains from the Bengal basin sediments. Sp = spessartine; Alm = almandine; Py = pyrope; GNF = granulite facies; ECF = eclogite facies (adapted after Nanayama, 1997).

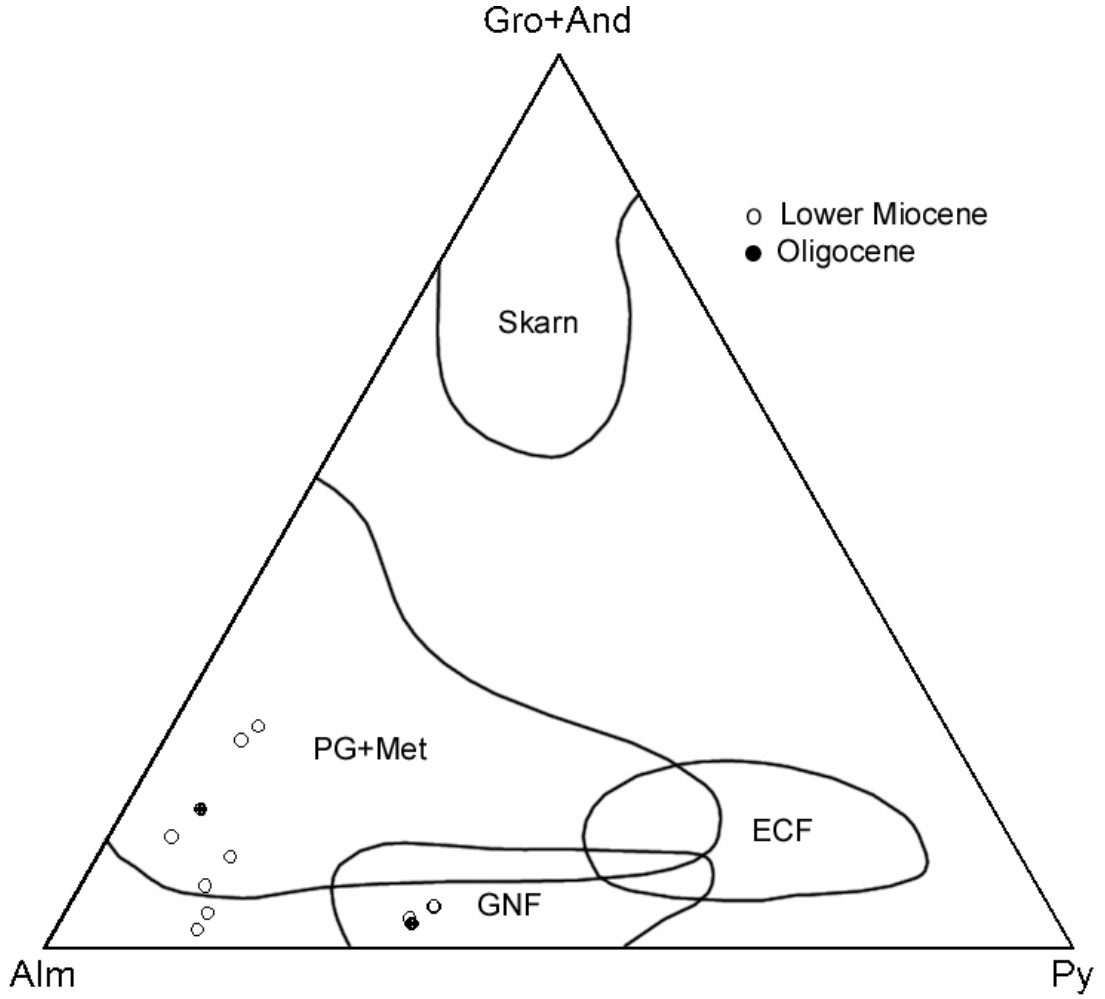

Figure 28. Chemical composition of garnets from the Bengal basin sediments in Alm-Py-(Gro + And) plot. Alm = almandine; Py = pyrope; Gro = Grossular; and And = Andradite. PG = pegmatite, Met = metamorphic; GNF = granulite facies; ECF = eclogite facies (after Nanayama, 1997).

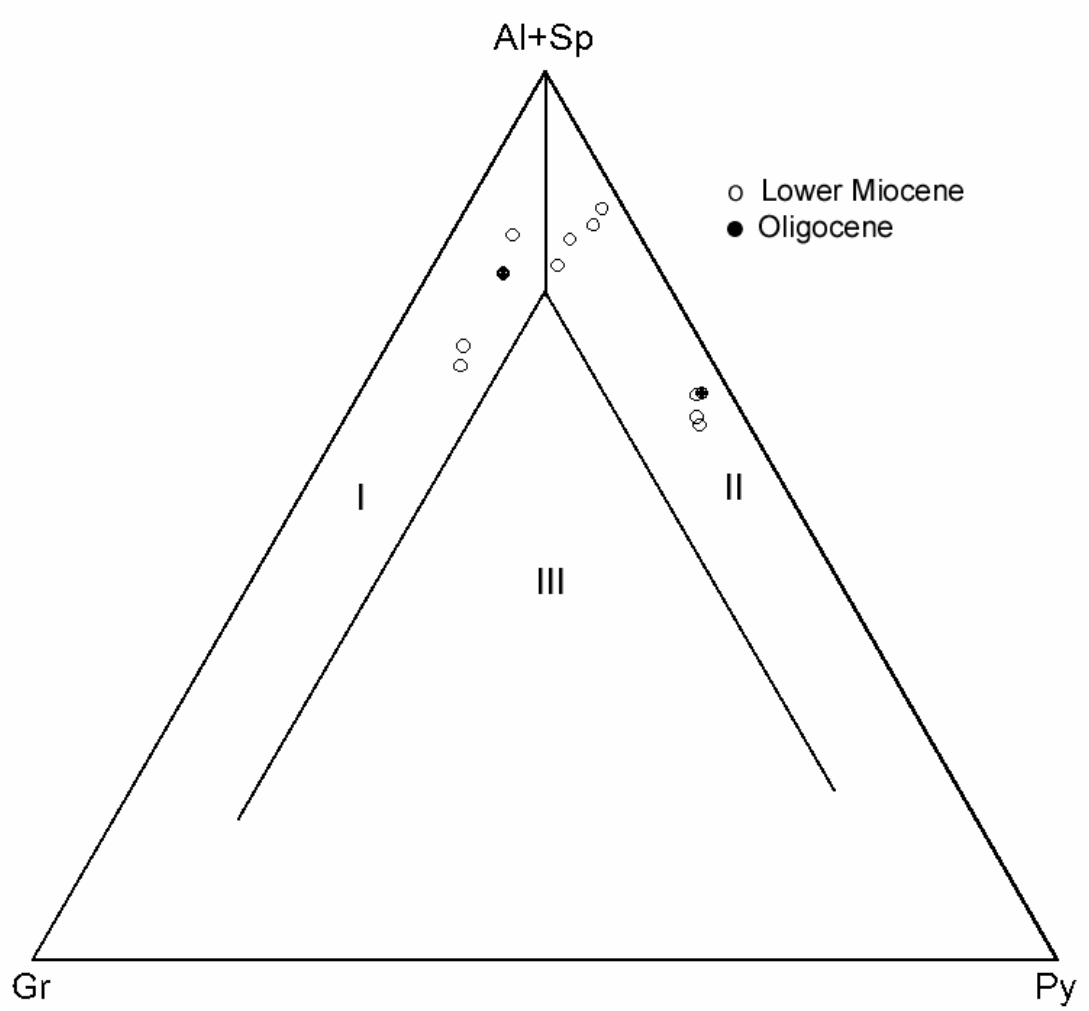

Figure 29. Chemical composition of garnets from Bengal basin sediments plot in 3 fields. I = garnets with almandine and grossular with < 10% pyrope; II = garnets with almandine and pyrope with < 10% grossular; and III = garnets with pyrope and grossular both with > 10% (Al-Almandine; Sp-Spessartine; Gr-Grossular; Py-Pyrope; adapted after Morton, 1992).

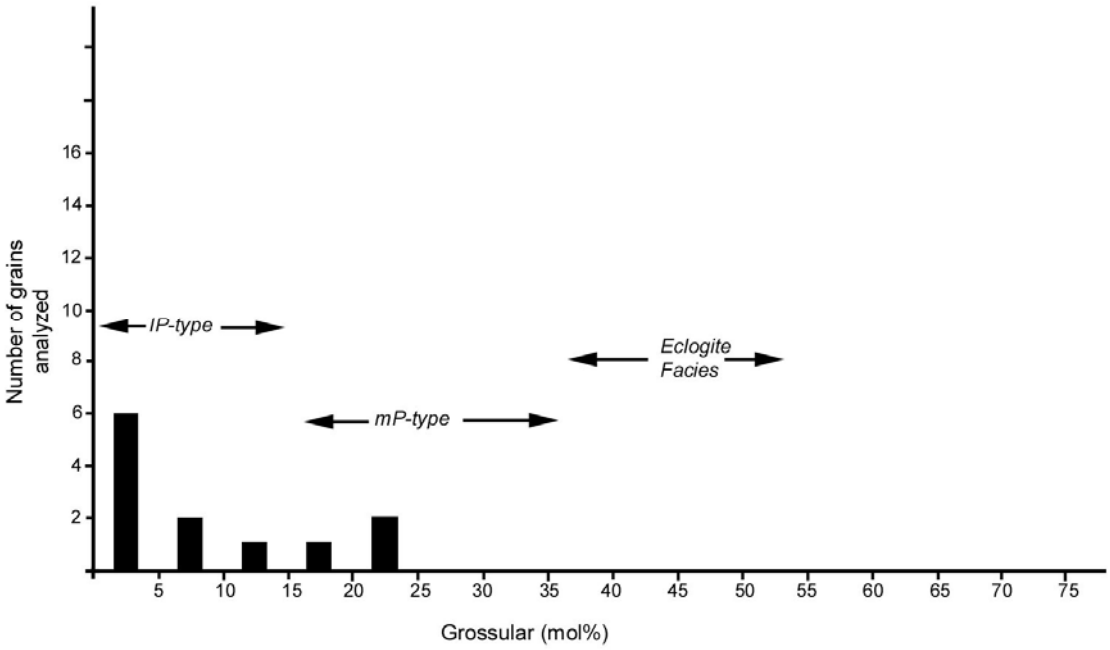

Figure 30. Grossular content (mol. %) from the Bengal basin in relation to lP-type (low pressure), mP –type (medium pressure), and eclogite facies (adapted after Nanayama, 1997).

grossular content, suggesting that they are derived from high-grade metamorphic facies. Others contain low pyrope which indicates low- to medium grade metamorphic source. So there are at least two different provenances for the garnets of the Bengal basin. One could be from a granulite facies rocks and the other could be from regionally metamorphosed garnet-mica schists (Le Fort, 1996; DeCelles, et al., 2001).

6.4.2 Chrome Spinel

Chrome spinel's unusual chemical stability favors preservation of compositional signature after burial in sedimentary strata. A total of 17 chrome spinel grains were found and analyzed for this study. The elemental percent of chromium in these spinels is high, ranging from 20% to 58% (average 42%). Other important trivalent cations common in these spinels are Al and Fe^{3+} and divalent Mg and Fe^{2+}.

Several plots have been made to evaluate the provenance signature of the chrome spinels (Figs. 31-33). A ternary plot of Fe^{3+} -Cr^{3+}-Al^{3+} (Fig. 31) discriminates Alpine-type peridotites from Alaskan-type and stratiform peridotite complexes (Dick and Bullen, 1984). Alpine-type peridotites consist of over 95% harzburgite and have origin as the depleted residues of partial melting. In this peridotites, Cr increases with increasing Fe^{3+}, but Fe^{3+} concentrations overall remain quite low. Both stratiform and Alaskan-type complexes generally exhibit much higher concentrations of Fe^{3+} than the Alpine-type peridotites, and greater scatter of Fe^{3+} concentrations relative to Cr concentrations. Spinels plots in this study partially overlap between Alpine-type and stratiform complexes although predominantly they be more of Alpine-type (Figs. 31, 32, and 33; Appendix B; Dick and Bullen, 1984).

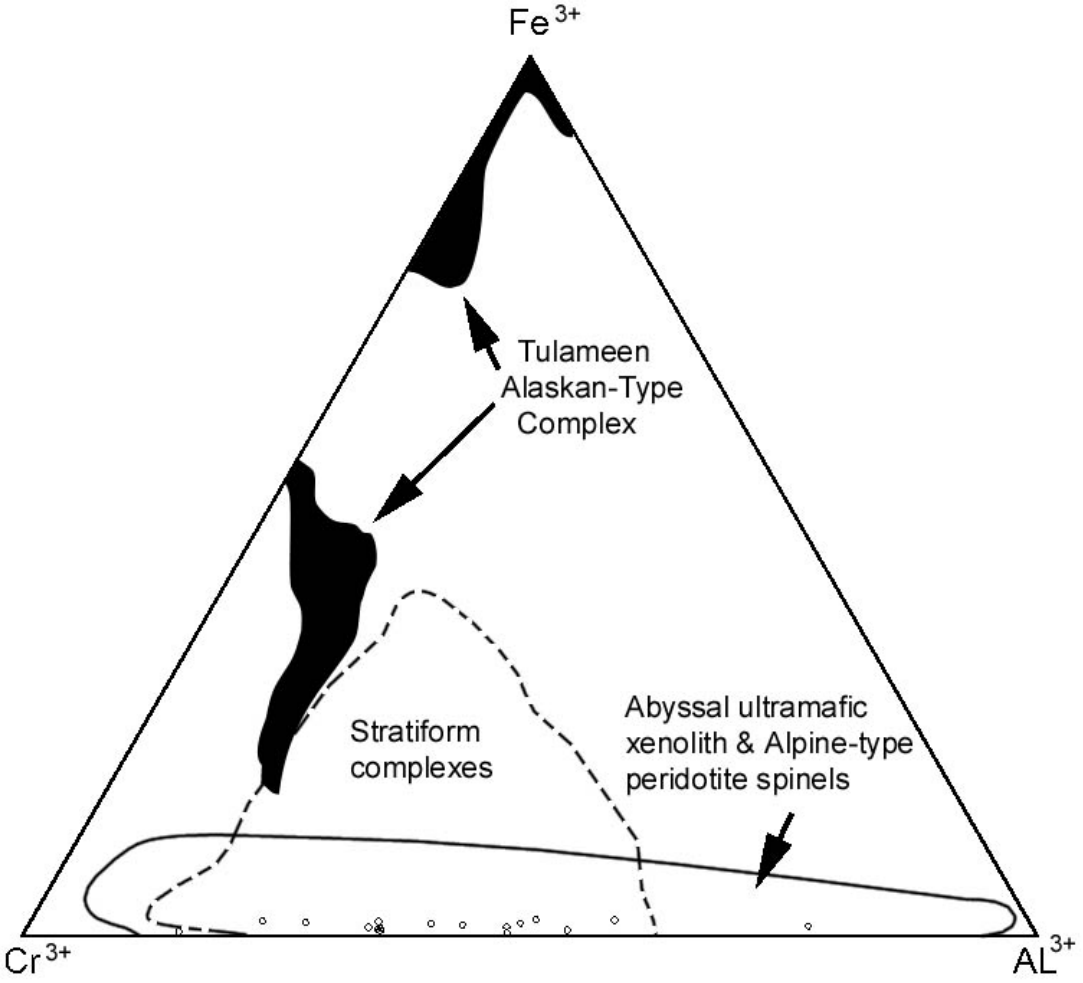

Figure 31. Ternary plot of major trivalent cations in chrome spinels. Three major provenance fields have been drawn to show the data distribution. Note that the abyssal ultramafic xenolith and Alpine-type peridotites overlap with stratiform complexes (after Nixon et al., 1990).

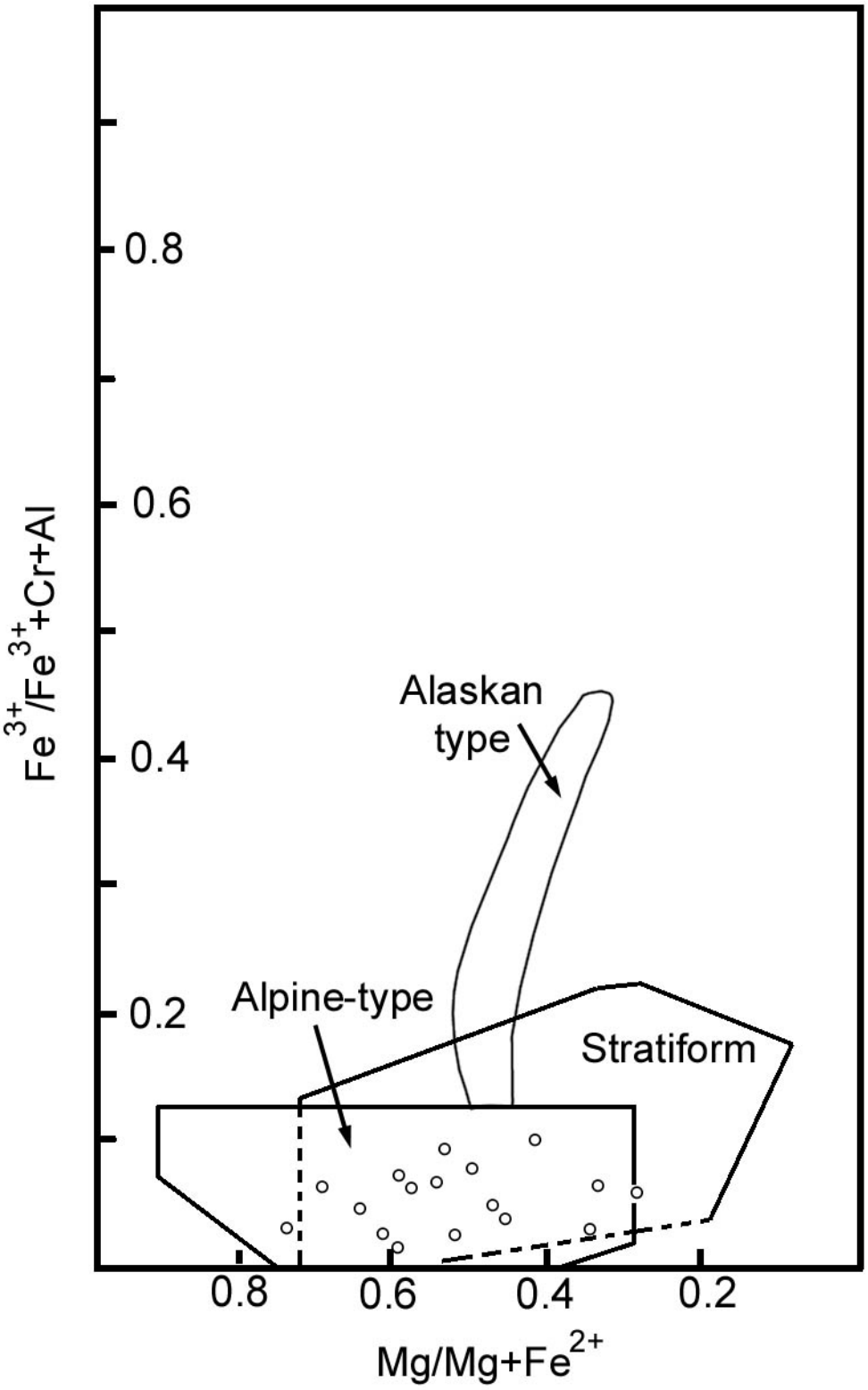

Figure 32. Plot of Mg/(Mg+Fe^{2+}) against the ratio of trivalent cations Fe3+/(Fe^{3+}+Al+Cr) for detrital spinels showing that Alpine and stratiform types overlap each other (Irving, 1974).

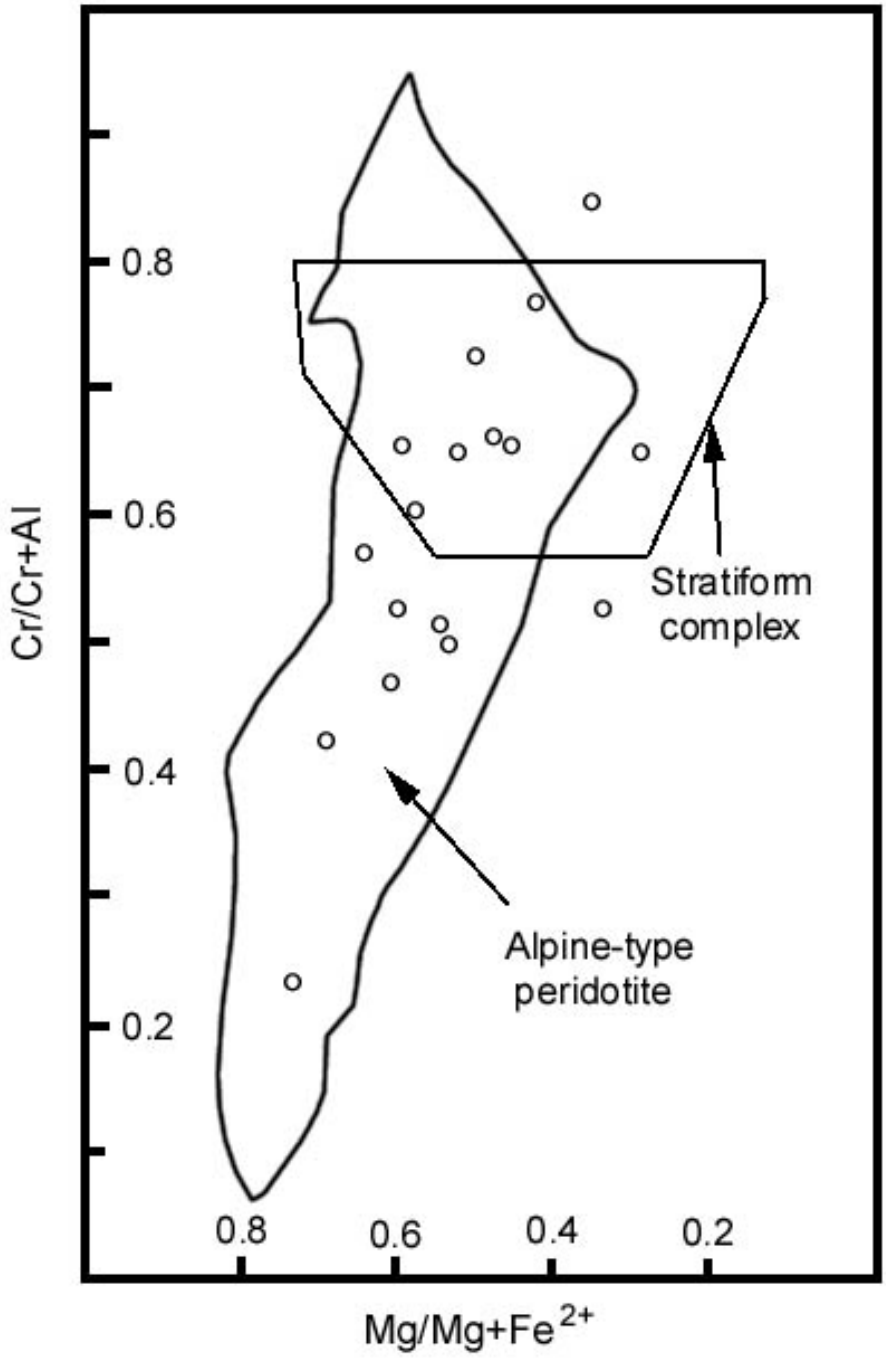

Figure 33. $Mg/(Mg+Fe^{2+})$ versus Cr/(Cr+Al) plot for detrital chrome spinels showing the distribution of samples relative to different provenance fields. Note that although some data points fall in the overlap between stratiform field complex (layers rich in chromite in a layered igneous complex) and Alpine-type peridotite (ophiolites), data on whole reflect a Alpine-type peridotites provenance (after Dick and Bullen, 1984).

A plot of $Mg/(Mg+Fe^{2+})$ against $Fe^{3+}/(Fe^{3+}+Al+Cr)$ shows the importance of Fe-rich spinel in ultramafic bodies formed by fractional crystallization in the crust (Alaskan-type peridotites and stratiform complexes, Fig. 32). The data for this study plot entirely within the field of Alpine-type peridotites (Irving, 1974). The field for Alaskan-type complexes plots entirely outside the range of sampled grains and can be excluded as a probable provenance. Likewise, the stratiform field partly overlaps the Alpine-type peridotites field (Fig. 33), but no grains show high Fe^{3+} composition that distinguishes at least some stratiform complex chrome spinels. Based on co-interpretation of the Mg# versus $Fe^{3+}/(Fe^{3+}+Al+Cr)$ and Cr-Al-Fe^{3+} plots, it can be concluded that detrital chrome spinels from Oligocene strata of the Bengal basin have close affinity to Alpine-type peridotites as a major source.

6.4.3 Tourmaline

Tourmaline is usually considered in terms of its common end-member components because of the large amount of potential substitution. In most cases, natural tourmalines belong to two completely miscible solid-solution series: schorl-dravite ($NaMg_3$ – $Na[Fe,Mn]_3$) and schorl-elbaite ($Na[Fe,Mn]_3$ – $Na[Li,Al]_3$). There is a miscibility gap that exits between dravite and elbaite (Deer et al., 1992). Therefore, tourmalines are typically described in terms of their position in the schorl-elbaite series or in the schorl-dravite series.

Al-Fe(tot)-Mg and Ca-Fe(tot)-Mg plots for Oligocene Barail tourmaline are shown in figures 34 and 35. According to the Al-Fe(tot)-Mg plot (Fig. 34), most of the tourmalines were sourced from metapelites and metapsammites. Only a few grains appear to have derived from Li-poor granitoid and associated pegmatites. The Ca-

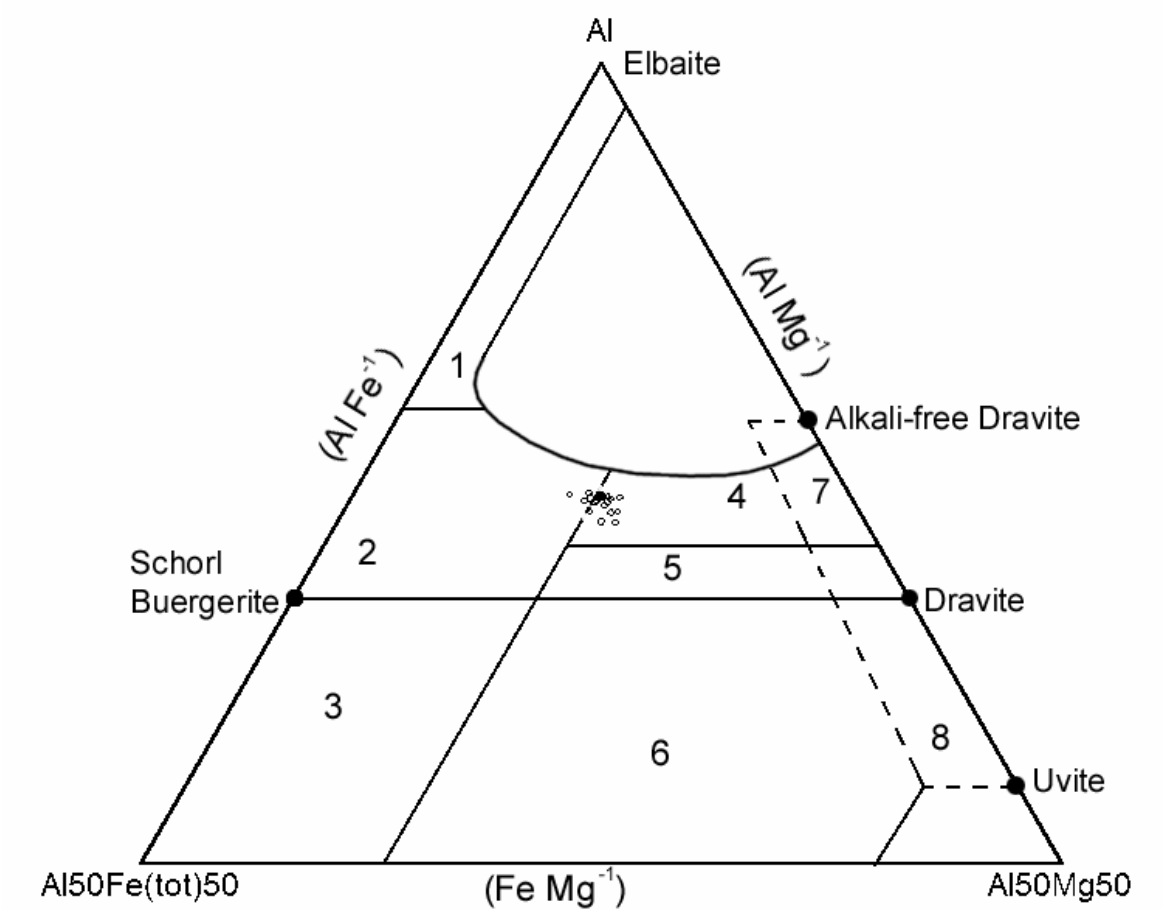

Figure 34. Al-Fe(tot)-Mg plot (in molecular proportion) for tourmalines from the Oligocene Barail Group of Bengal basin. Fe(tot) represents the total iron in the tourmaline. Several end members are plotted for reference. Different rocks types are: (1) Li-rich granitoid pegmatites and aplites, (2) Li-poor granitoids and their associated pegmatites and aplites, (3) Fe3+-rich quartz-tourmaline rocks, (4) metapelites and metapsammites (aluminous), (5) metapelites and metapsammites (Al-poor), (6) Fe3+-rich quartz-tourmaline rocks, calc-silicate rocks, and metapelites (7) low-Ca metaultramafics and Cr, V-rich metasediments, and (8) metacarbonate and meta-pyroxinites (after Henry and Guidotti, 1985).

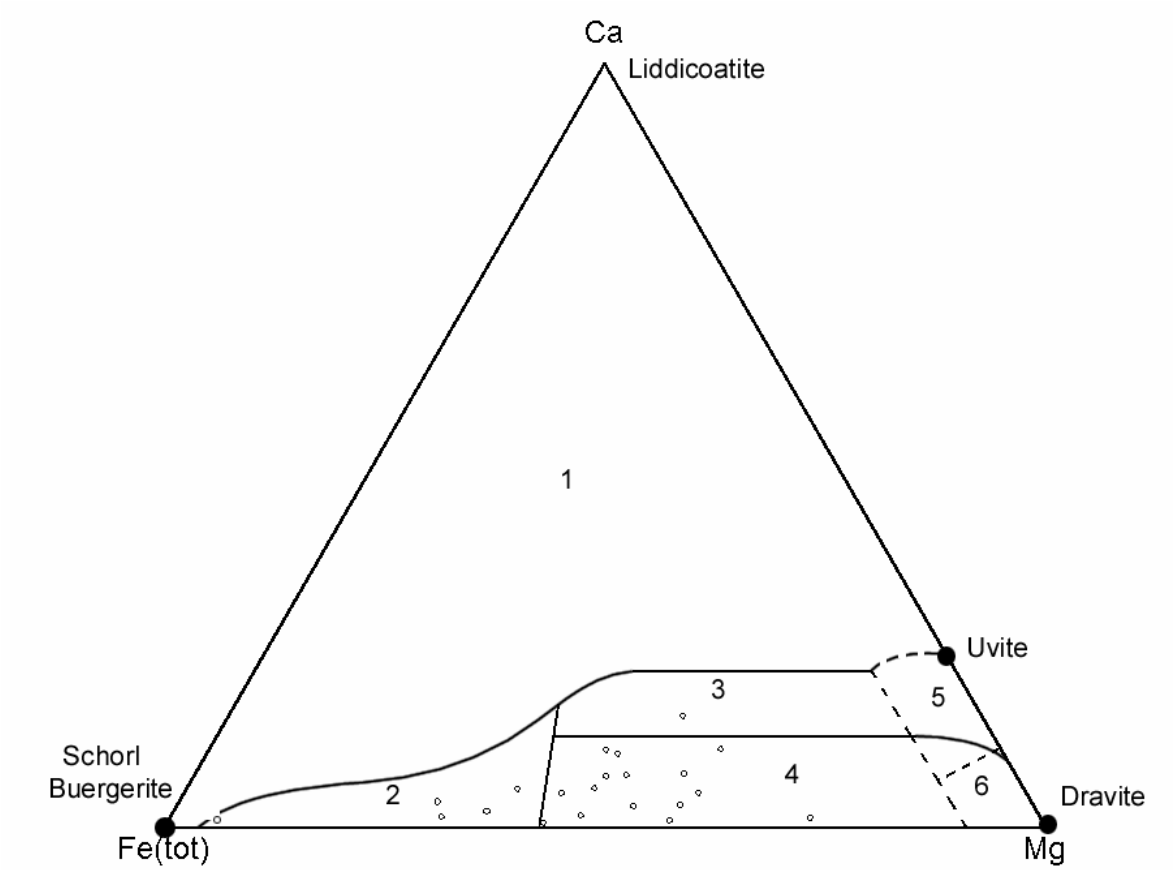

Figure 35. Ca-Fe(tot)-Mg plot (in molecular proportion) for tourmalines from the Oligocene Barail Group of Bengal basin. Several end members are plotted for reference. Different rocks types are: (1) Li-rich granitiod pegmatites and aplites, (2) Li-poor granitoid and associated pegmatites and aplites, (3) Ca-rich metapelites, metapsammites, and calc-silicate rocks, (4) Ca-poor metapelites, metapsammites, and quartz-tourmaline rocks, (5) metacarbonates, and (6) meta-ultramafics (after Henry and Guidotti, 1985)

Fe(tot)-Mg plot (Fig. 35) indicates Ca-poor metapelites, metapsammites, and quartz-tourmaline rocks as a source for the majority of the grains. Very few grains correspond to the Li-poor granitoid and associated pegmatites. Hence, there are at least two distinct sources for the tourmalines, one of which could be recycled metasedimentary rocks of the orogenic belt.

6.4.4 Amphibole

Amphiboles show a narrow range in chemical composition. This range in composition does not reflect paragenetic diversity. Only four blue-green amphibole grains were identified from the Oligocene sediments for this study. All of those grains are high in Na and K content. This is not sufficient to draw sound conclusions about any particular provenance. However microprobe data reveal that all of them are tschermakitic hornblende (Fig 36).

6.5 DISCUSSION

6.5.1 Garnet

Provenance characteristics have been constrained successfully using the compositions of detrital garnet populations. Since variations in garnet composition are dependent on paragenesis, they have proved very useful in identifying and characterizing different provenances (Morton, 1985). Garnet is particularly indicative of metamorphic origin but also can be found in some igneous rocks. Most garnet grains reflect solid-solution series between various end-members (pyrope, almandine, spessartine, grossular, andradite, and uvarovite).

Garnets from Bengal basin have been classified into three groups (after Morton et al., 1992): (1) type-I garnet reflects a solid solution between almandine and

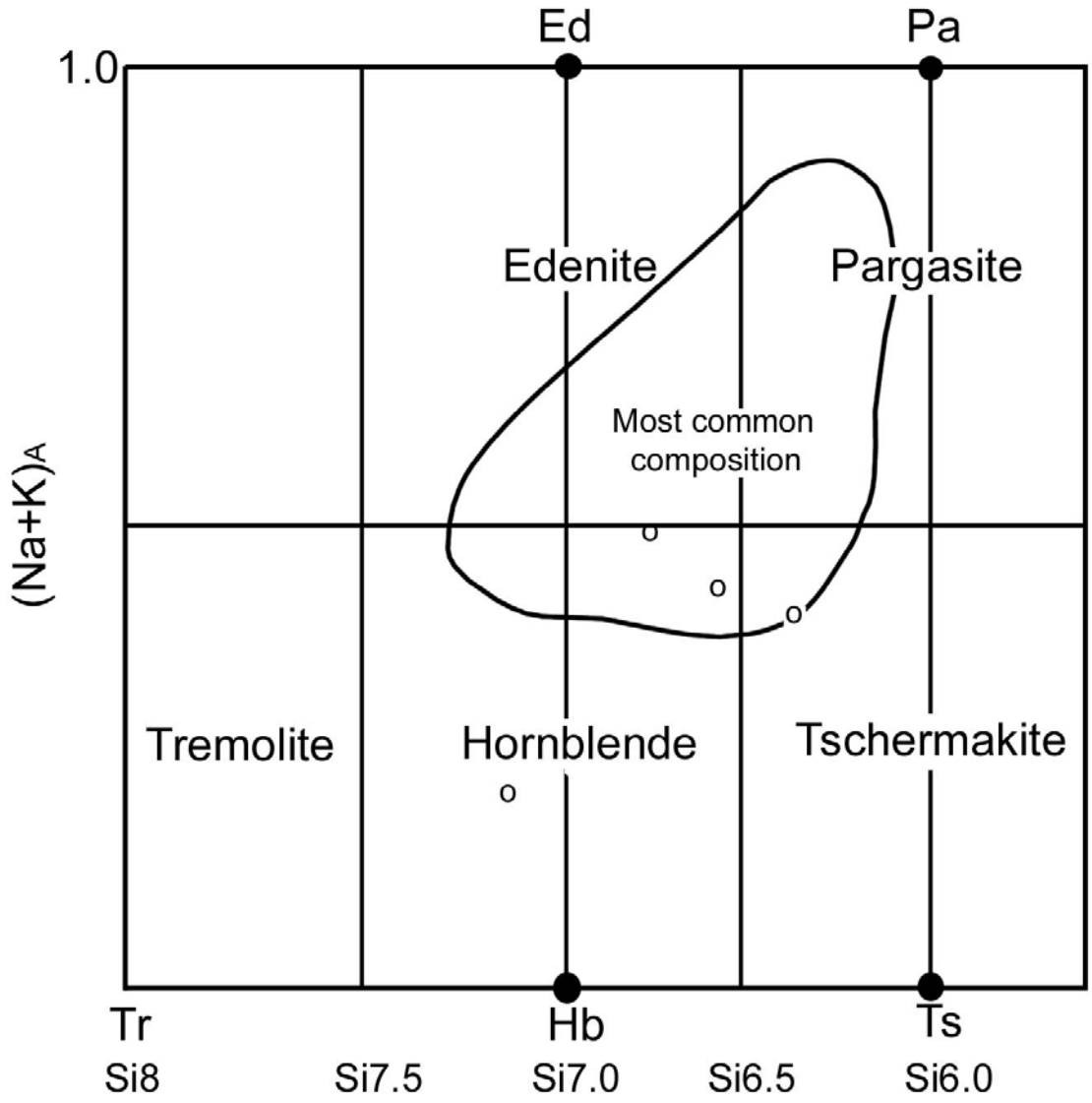

Figure 36. Na^{+}-K–Si plot for amphiboles from Oligocene sediments of Bengal basin which shows that the amphiboles are tschermakitic hornblende (modified from Deer et al., 1992).

grossular with <10% pyrope; (2) type-II garnets reflects a solid solution between almandine and pyrope with <10% grossular; and (3) type-III garnets are those wherein both pyrope and grossular are >10%. Most of the garnets of Bengal basin are type-II, with very few type-I grains. The majority of these garnets belong to low-grade metamorphic variety (Fig. 30). These garnets are rich in almandine, some rich in pyrope but all of them are low in spessartine content (Fig. 37). Almandine garnets could have derived from garnetiferous schists formed by regional metamorphism of argillaceous sediments. These rocks probably been derived from the Higher Himalayas to the north.

However, further downstream in the Bengal fan, garnets in the Bengal Fan sediments are mostly almandine-rich with very low pyrope content and have been suggested to have derived from the Himalayas to the north (Yokoyama et al., 1990). The higher pyrope content of the garnets from Bengal basin, however, does not necessarily indicate a Himalayan source. Garnets found in the coastal sediments of southern India show compositions similar to those of the Bengal basin. Those coastal sediment garnets were derived from the Archean basement of India, which is comprised of charnockites (garnet + orthopyroxene + clinopyroxene granulite facies rocks), khondalites (garnet + sillimanite + cordierite gneiss) and graphitic garnet-biotite gneisses (Harris et al., 1982; Sinha Roy et al., 1984; Chacko et al., 1987; Santosh, 1987). Therefore, the Indian craton also could be a possible source for the high pyrope garnets in the Oligocene and Lower Miocene sediments of the Bengal basin.

6.5.2 Chrome Spinel

Chrome spinels are unique among the heavy minerals for their occurrence and geotectonic implications. Spinel composition reflects the degree of melting in the

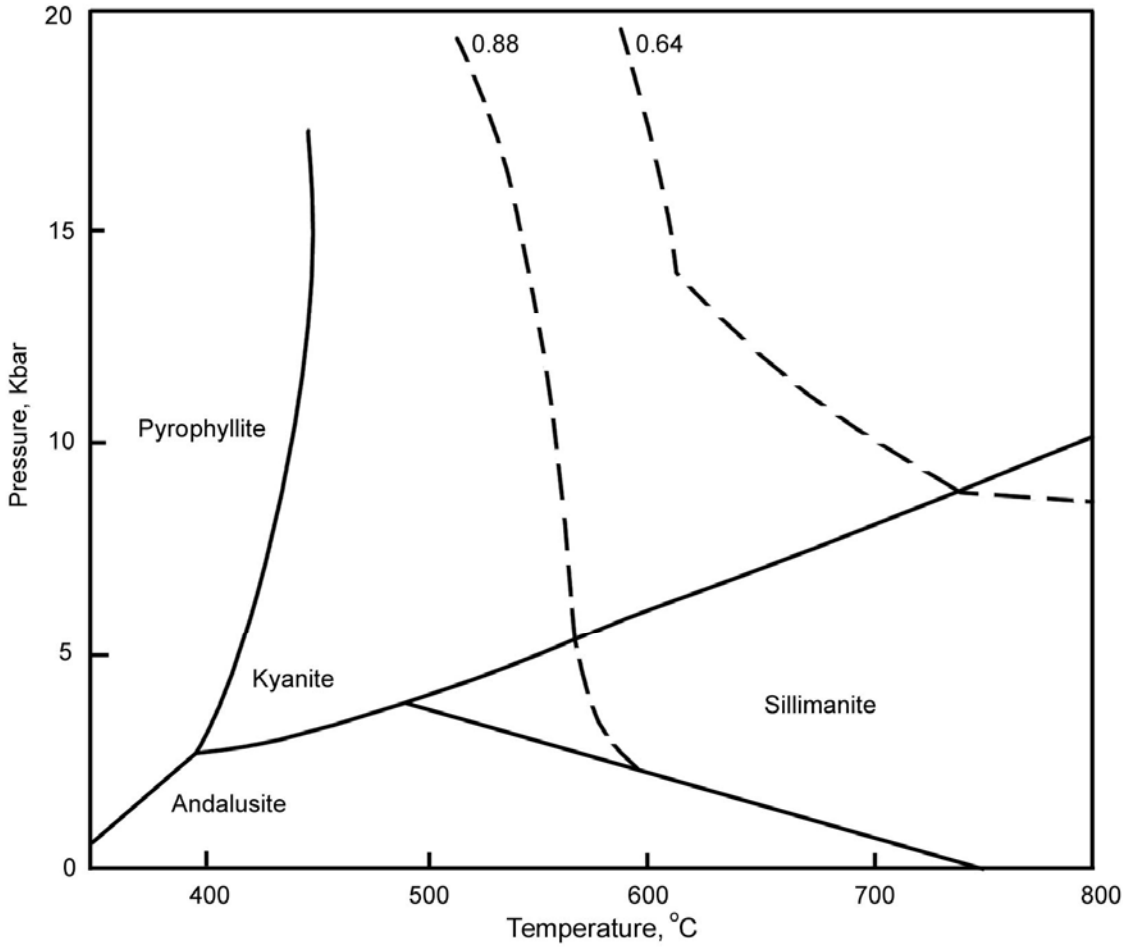

Figure 37. Pressure-temperature diagram for garnet data from the Bengal basin. Dashed lines are garnet Fe/(Fe+Mg) isopleths, constructed for the two garnet compositions observed in this study and assuming that garnet formed in equilibrium with biotite (Spear, 1993). About two thirds of the garnets observed (n=8) were of relatively low Fe/(Fe+Mg) content, and seem typical of regional metamorphism, whereas the remaining garnets (n=4) have higher pyrope content and seem consistent with high-grade metamorphism.

mantle source region (Dick and Bullen, 1984). The principal constituents of spinel behave very differently during fractional crystallization or partial melting, with Cr and Mg strongly partitioned into the solid and Al strongly partitioned into the melt. The Cr # (Cr/[Cr + Al]) of spinels reflects the degree of depletion of the mantle source, with increasing Cr # reflecting an increase in degree of partial melting. Spinels have used been widely as provenance indicators for mafic and ultramafic rocks, especially of Alpine type peridotites (Press, 1986; Cookenboo et al., 1997; Zhu et al., 2005). The origin of Alpine-type peridotites can be constrained by Cr# and Mg#. Chrome spinels from peridotites and basalts of mid-ocean ridges have Cr# less then 0.06, and typically have high Mg# (0.7 to 8.5; Dick and Bullen, 1984). In contrast, spinels in back-arc basin basalts usually have lower Mg# for a given Cr#, and associated island-arc spinels show Cr# in excess of 0.60 (Dick and Bullen, 1984). The detrital spinels of this study span a much greater range of Cr# compositions than abyssal spinels, and therefore abyssal rocks are excluded as a source (Fig. 38).

Peridotites from ophiolite complexes are classified as Type I if their spinel populations are similar in chemical characteristics with spinels from mid-oceanic ridge basalts. They are referred to as Type III if the spinel populations are largely similar in chemistry to the spinels from arc-settings and oceanic plateaus (Dick and Bullen, 1984). Ophiolites with spinels showing the range of composite compositions as found in Type I and Type III ophiolites are classified as transitional or Type II (Dick and Bullen, 1984).

The composition of spinels from the Bengal basin might be a mixture of mid-ocean ridge-derived basalts (type I) with more depleted marginal-basin and island-arc suites (type III; Fig. 37 and 38). Spinels with high Al (Cr # = 0.10-0.30) and high Mg

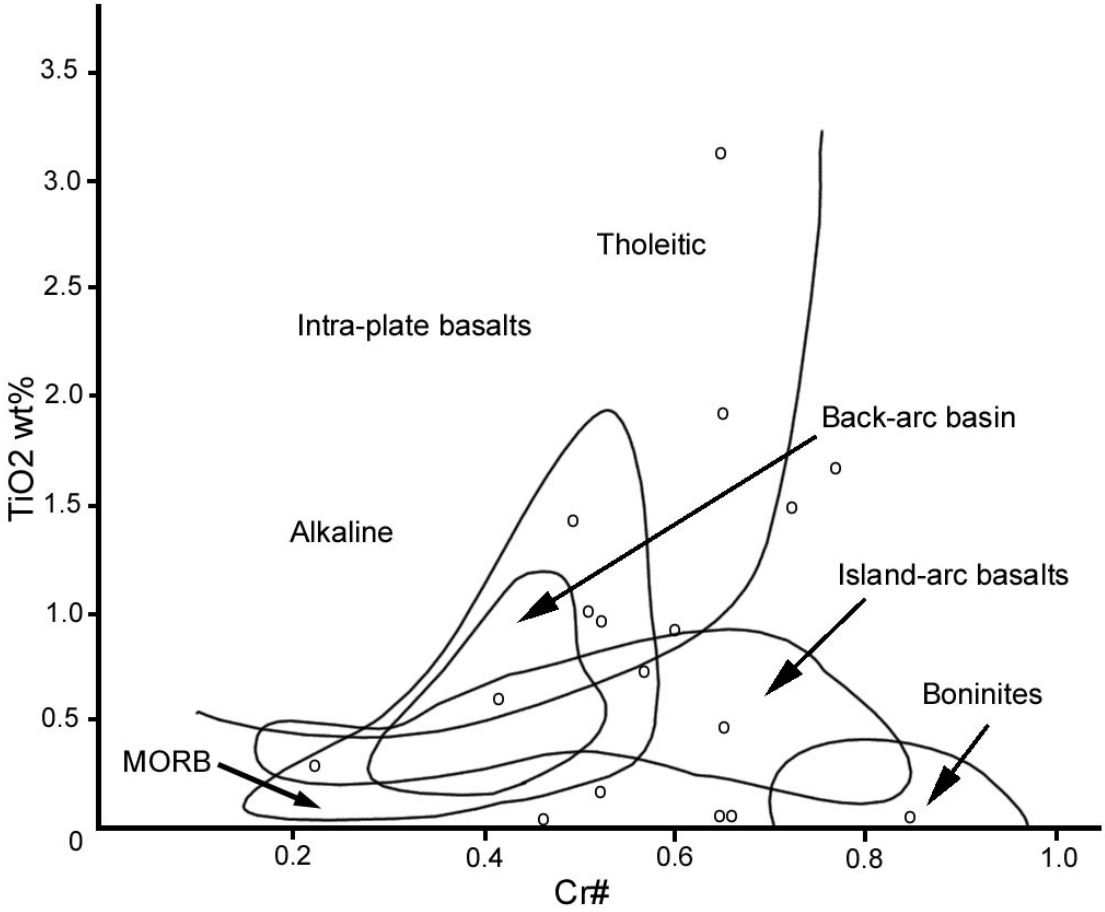

Figure 38. Plot of TiO_2 vs. Cr # of Bengal basin detrital spinel relative to spinels from various potential source rocks. MORB = Mid-oceanic ridge basalt (after Arai, 1992).

(Mg # 0.70-0.85) content are common constituents of abyssal peridotites, dunites, and basalt (Dick and Bullen, 1984). Bengal basin chrome spinels have low Al but high Cr content (Cr# 0.4 to 0.85). The lack of both high-Al and high-Mg spinels, which are indicative of mid-ocean-ridge origin, strongly suggests that the Bengal basin detrital chrome spinels did not originate from a mid-ocean-ridge source.

Spinels from the Bengal basin likely were derived either from the Himalayan arc material or ophiolites (Type III ophiolites or associated rocks with depleted mantle composition of Type II ophiolite), the continental flood basalt of the Deccan Traps, and/or the Indo-Burmese ophiolites (Type III or Type II setting). Although previous documentation of spinel compositions from continental flood basalts are sparse, available spinel data from the Deccan traps, including spinels from tholeiitic lavas (Sen, 1986), picritic lavas (Krishnamurthy and Cox, 1977), and lherzolite xenoliths (Mukherjee and Biswas, 1988), show that the Cr # of basic layered intrusion spinels is high. A Deccan trap source, therefore, cannot be ruled out. However, based on tectonic location of the Bengal basin, paleogeographic considerations, and provenance work on chrome spinels from the Tianba Formation of the northern zone of Tethyan Himalayas (Zhu et al., 2005), the Rajmahal trap (Fig. 2) is more logical source of those spinels. The microprobe results of detrital Cr-rich spinels from Tianba Formation (15–26 wt.% Al_2O_3, 36–45 wt.% Cr_2O_3, 10–12 wt.% MgO, 20–30 wt.% FeO_{tot}, and 1.5–2.0 wt.% TiO2) are similar to the composition of spinels from the Bengal basin, which are typical for spinels from Hawaiian basalts (Scowen et al., 1991; Kamenetsky et al., 2001; Zhu et al., 2005). Paleogene Subathu and Dagshai formations of Himalayan foreland basin in northern India have much lower Cr # (Najman and Garzanti, 2000). Compositions of spinels from the Subathu Formation compare well with those from the Chulung La Formation (Garzanti et al., 1987),

which is thought to have been derived from arc and ophiolitic sequences of the Indus suture zone (Najman and Garzanti, 2000). The composition of the spinels from the Bengal basin does not match those of the Himalayan foreland basins. The relatively narrow range of chemical compositions of Bengal basin spinels appears to exclude the possibility of a volcanic arc source. Spinels derived from arc and associated accretionary complexes normally show a wider range in the chemical composition (Barnes and Roeder, 2001). Therefore, a distant Himalayan source can be ruled out as a possible provenance for the Oligocene sediments of the Bengal basin.

Recent study of chrome spinels from the Assam basin suggests those spinels were derived from the ophiolites of the Indo-Burman Ranges to the east (Kumar, 2004). Tectonic settings of that area suggest that the thrust slices of the Schuppen belt have traveled ~ 300 km to the northwest during Oligocene-Pliocene time (Rangarao, 1983). The ophiolites in the Indo-Burman ranges consist of podiform chromite, cumulates, and harzburgite (Venkataraman et al., 1986). The Mg-Cr plot (Fig. 39) of spinels from the Bengal basin indicates strong chemical similarity to the Indo-Burman ophiolites. Based on low Al (Cr # 0.30 – 0.75) and low Mg (Mg # 0.40 to 0.71) contents, and a wide range in TiO_2 wt% (0.3 to 3%), the Bengal basin chrome spinels may have been derived from both Alpine-type ophiolites present in the Indo-Burman ranges and the Rajmahal Trap.

6.5.3 Tourmaline and Amphibole

Microprobe data show that tourmalines from the Bengal basin were derived from metapelites, metapsammites, and quartz-tourmaline rocks. Only a few grains correspond to the Li-poor granitoid and associated pegmatite occurrences (Fig 34 and 35). Although there are at least two different sources for the tourmalines, it can be

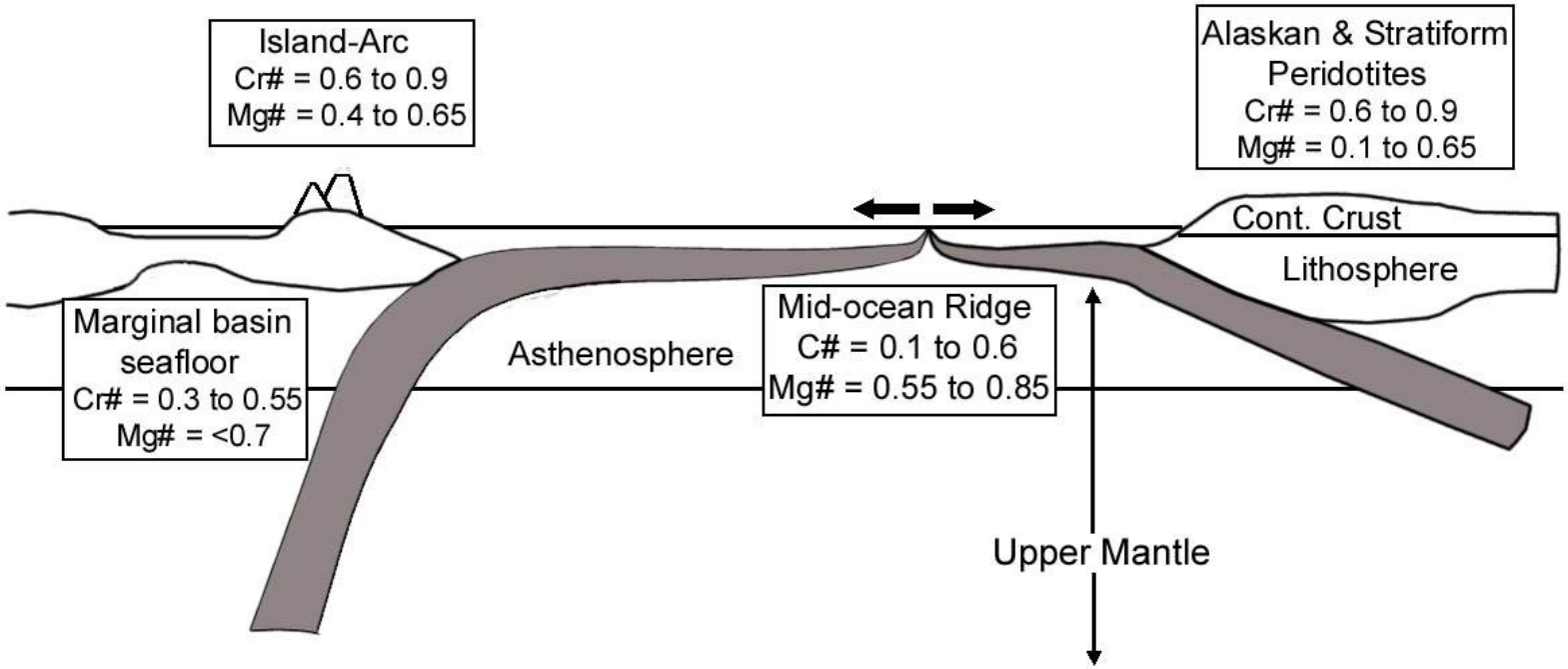

Figure 39. Schematic diagram (not to scale) showing spinel composition from different tectonic settings including those of sea-floor and continental crust origins (modified from Cookenboo et al., 1997).

argued that the Bengal basin sediments have a dominantly metasedimentary provenance, with minor contribution from granitoid and pegmatitic rocks.

Amphiboles from Bengal basin show narrow range in composition and therefore a narrow range of paragenesis. Microprobe data identify them as tschermakitic hornblende because of their high Na and K content. This also indicates derivation from low-grade regional metamorphic rocks (greenschist facies).

CHAPTER 7: OVERPRESSURE IN MIOCENE STRATA

7.0 INTRODUCTION

It has long been recognized that seismic wave characteristics measured at the Earth's surface can provide information not only about the attitude and distribution of lithologic interfaces but also the physical properties of subsurface rocks. In this study, interval transit time and acoustic velocities were calculated from sonic logs and compared with velocity information obtained during seismic exploration. This was done in order to predict factors that might be responsible for changes in velocity of subsurface units. Overpressures are observed in subsurface strata worldwide (Hunt, 1990; Powley, 1990; Osborne and Swarbrick, 1997) and overpressured zones have been frequently reported in Miocene formations in many exploratory wells drilled in eastern Bangladesh (Khan and Husain, 1980). Modal analysis of sandstone has been done and microfractures have been identified in Miocene sediments from the Sitakund anticline. An attempt was been made to understand the overpressure phenomenon and its relation to tectonics by comparing velocity data with temperature, depth, and lithologic information from four wells.

7.1 OVERPRESSURE IN BENGAL BASIN

The study area covers two important tectonic segments of the Bengal basin: the Sylhet trough in the northeast and the Chittagong hills in the east and southeast

(Fig. 1). This research deals with four different anticlinal structures: Rashidpur, Titas, Bakhrabad, and Sitakund, all of which encounters overpressure at different depths (Table 7).

The Titas structure (Titas-11 well) lies along the western margin of the eastern folded belt and exhibits showing a dome-like structure. Sonic and lithologic logs for depths between about 915 meters and 3080 meters from Titas-11well were available. This depth range encountered the Middle and Lower Miocene rocks (BAPEX Corelab, 1996; Table 8).

The Bakhrabad structure lies in the western continuation of the eastern folded belt (Fig. 1). It is symmetrical in shape and is about 64 km long and more than 6.5 km wide with a total area of 414 km^2 (Khan and Husain, 1980). The Bakhrabad-9 well was used for this study. Sonic and master logs were available for a depth range of about 915 meters to 3050 meters, which covers the entire Miocene sequences (Table 8).

The Rashidpur (Rashidpur-4 well) structure is situated in the eastern fold belt and is a narrow asymmetrical anticline (Khan and Husain, 1980). For the Rashidpur-4 well, sonic and master logs were available for the Miocene sequence from a depth range between 915 to 2866 meters.

The Sitakund anticline, situated at the southeastern part of the Bengal basin, is 70 km long and 12 km wide. This structure is a doubly-plunging and asymmetric anticline (Hossain, 1988). This anticline is flanked on the west by a major thrust fault that is parallel to the axis of this anticline. A total depth of about 1400 meters (2600 to about 4000 m) of sonic log was available for this study. The lithology log indicates that the Sitakund-1 core is mainly composed of shale with minor sandstones and siltstones.

Table 7. Depth to the top of overpressured zone in the four studied wells (from Ahmed, 1985 and BOGMC).

Tectonic Framework	Well	Top of overpressure zone (meter)
Sylhet trough	Rashidpur- 4	3680
Eastern fold belt	Titas- 11	4140
	Bakhrabad- 9	3100
	Sitakund- 1	1100

Table 8. Stratigraphic table showing velocity and formational depth ranges of the strata drilled at the four wells (BAPEX Corelab Report, 1996)

Wells	Formation	Depth range (meter)	Average Velocity (m/sec)	Velocity range (m/sec)
Titas 11	Tipam (Upper Miocene to Pliocene)	+539 to 842	Data not available	---
	Boka Bil (Mid to Upper Miocene)	842 to 1445	2630	2117 to 3278
	Bhuban (Lower to Mid Miocene)	1445 to 3189+	3480	2722 to 4355
Bakhrabad 9	Tipam (Upper Miocene to Pliocene)	Near surface to 800	Data not available	---
	Boka Bil (Mid to Upper Miocene)	800 to 1890	2820	2292 to 3350
	Bhuban (Lower to Mid Miocene)	1890 to 3038+	3750	3143 to 4690
Rashidpur 4	Tipam (Upper Miocene to Pliocene)	From surface to 1127	2630	2400 to 3049
	Boka Bil (Mid to Upper Miocene)	1127 to 1968(?)	3430	1993 to 5081
	Bhuban (Lower to Mid Miocene)	1986(?) to 2868+	3843	3111 to 4550

7.2 METHODS

In this research, sonic and lithologic logs were used to interpret subsurface velocity profiles. Well-completion reports have been compared with data obtained from the sonic and lithologic logs. Selection of the four particular wells of this study was based on availability of and permission to use data from the data centre of the Bangladesh Oil, Gas and Mineral Corporation (BOGMC). Sonic logs available for the northern 3 wells (Rashidpur, Titas, and Bakhrabad) include data from depths of 915 meters to 3050 meters. Sonic log values are given in microseconds (μs) per foot. For interpretative purposes, root mean square velocity (V_{RMS}) was determined for each formation at each well using the transit times and sequence thicknesses. These V_{RMS} values have been used to compare velocity across different wells for every individual formation as well as formations within a well. The gradual change of velocity with progressively deeper formations also has been considered. Comparisons were made with available formation temperature, pressure data and maps from the repositories of BOGMC. Twelve samples from the Sitakund structure were point counted (Table 3) and special attention was given to overpressure-related hydrofracturing.

7.3 RESULTS

Sonic logs available for this study encounter three formations in the Rashidpur structure, two formations in Titas and Bakhrabad structures, and one formation in the Sitakund structure (Table 8). The amount of variation in velocity ranges from 32% in Miocene to Pliocene stratigraphic units in Titas and Bakhrabad structures and 21% in Rashidpur structure. Average velocities of Miocene Boka Bil and Bhuban formations are 2630 m/sec and 3480 m/sec, respectively, at the Titas structure; 2820 m/sec and 3750 m/sec, respectively, at Bakhrabad; and 3430 m/sec and 3843 m/sec,

respectively, at the Rashidpur structure (Table 8). According to velocity-depth distributions, the Titas-11, Bakhrabad-9, and Rashidpur-4 wells show a gradual increase of velocity with depth, reflecting a normal trend related to increasing compaction (Fig. 40). However, from the velocity data of the four wells used in this study, no sharp velocity contrast at the formation boundaries can be observed in all the four wells. Presence of hydrocarbons in an interval has a significant effect on velocity distribution. Gas-bearing zones in the Boka Bil and Bhuban formations in three wells show lower velocity (as much as 3 to 7%), as expected, relative to the average formation. In the Sitakund structure, however, the velocity-depth distribution shows a short interval of initial increase followed by a decrease in velocity with increasing depth, indicating the probable presence of overpressured and undercompacted shale in the depth range of about 3000 to 4000 meters.

Modal analyses of sandstones of the Miocene Surma Group from the Sitakund structure suggest that these sands are orogenic (Fig. 13 and 14). Petrographic studies also reveal the presence of poikilotopic calcite cement and microfractures in sandstones from the overpressure zone. These microfractures are occupied by gray, argillaceous material and typically follow grain boundaries, producing a tortuous fracture path. Mode of formation of these microfractures is likely related to release of fluids from compacted formations generated by overpressure. When pore-fluid pressure approaches lithostatic pressure, the fluid pressure is released by rock failure. These released fluids lead to precipitation of calcite cement and subsequent diagenesis. Poikilotopic calcite cement has been observed in thin sections in the over-pressured zone sediments from the Sitakund structure (Fig. 41). The fractures in Sitakund sandstones were produced almost parallel to bedding planes. Compaction-

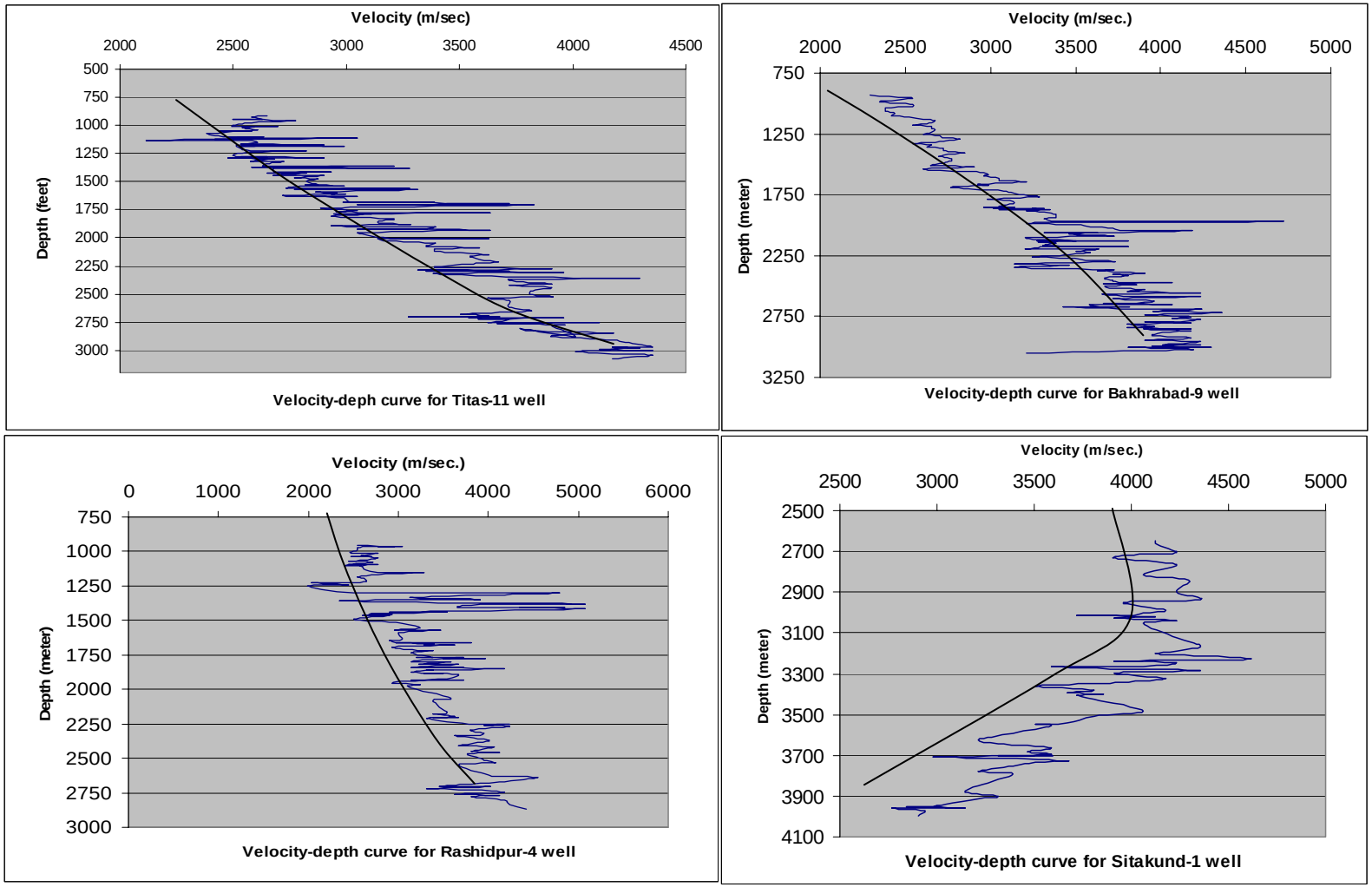

Fig. 40. Velocity-depth curves in four studied wells. Note that, unlike the other three wells, a decrease in sonic velocity with depth is observed in Sitakund-1 well.

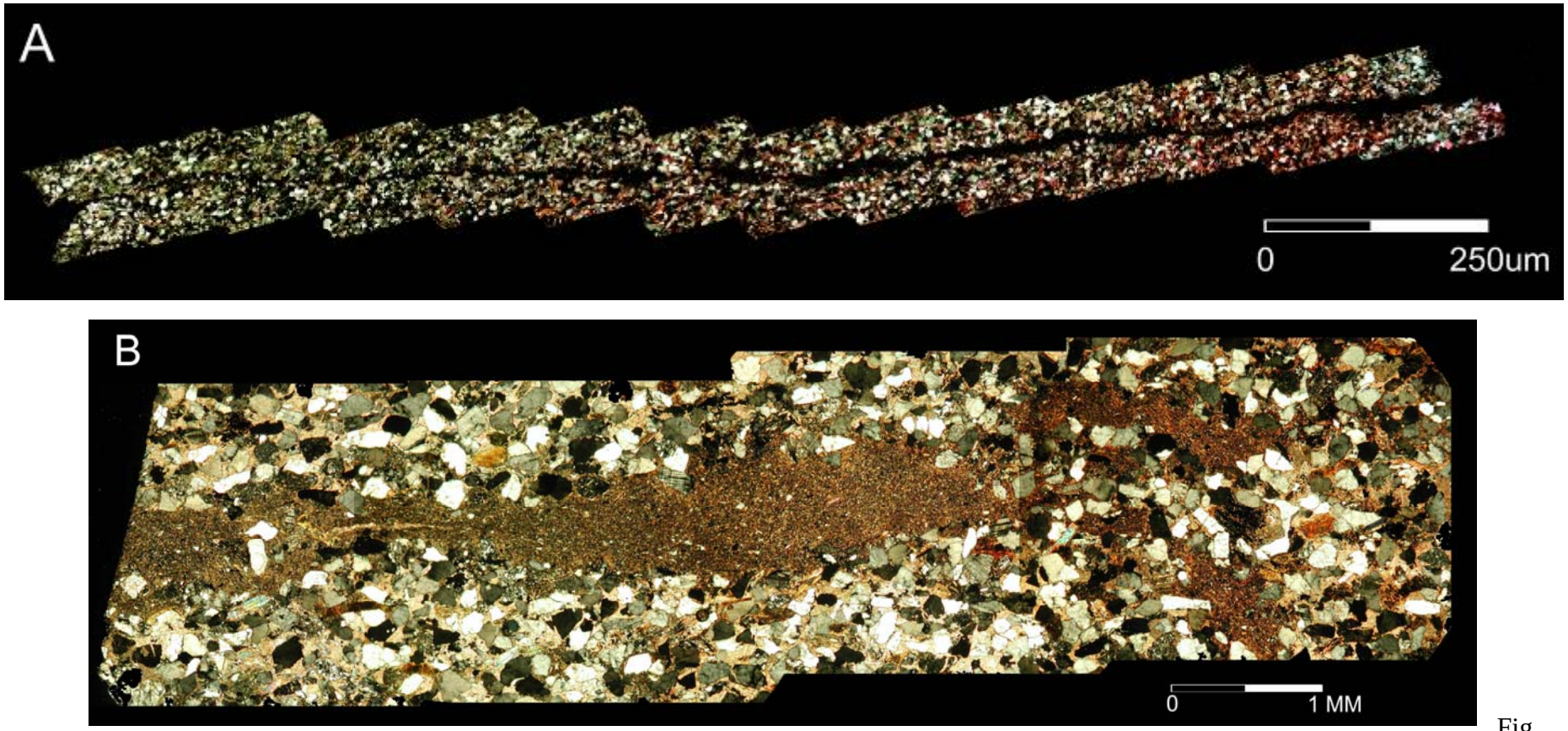

Fig. 41 (A) Compaction induced hydrofracturing in a sand layer from Sitakund anticline at a depth of 1550 m. The depth to this fracture in the core was just below the first occurrence of overpressure in the anticline; (B) Injection of shale in a sand body induced by overpressure at a depth of 1100 m. This shale injection is approximately at an angle of 40^0 to bedding.

induced hydrofracturing commonly occurs in mud-rich sequences, as found in the Sitakund structure at a depth where overpressure has initiated.

7.4 GEOLOGICAL CONTROLS OF OVERPRESSURE

Many sedimentary basins throughout the world exhibit some degree of non-hydrostatic fluid pressure, particularly overpressure (Hunt, 1990; Fertl et al., 1994; Neuzil, 1995; McPherson and Garven, 1999; Xie et al., 2001). Formation of high pressure in the Sitakund structure at shallow depth (Table. 7) may be controlled by two factors (Ahmed, 1985; Uddin, 1987): (1) overall structural regimes wherein overpressures are present within the folded flank areas; and (2) lithology, whereby overpressures are preferentially developed in an over-thickened shale with alternating sandstone.

Consideration of the above two points and the overall geological setting of the Bengal basin suggest three possible explanations for the development of overpressures in Miocene sequences in the Bengal basin: (1) rapid burial and incomplete dewatering of fine-grained sediments; (2) diagenesis of clay minerals; and (3) tectonic compression associated with the Indo-Burman Ranges to the east. (Colton-Bradly, 1987; McPherson and Garven, 1999). Overpressured-strata at Sitakund-1 were first detected at a shallow depth of around 1100 m (Table 8). A possible explanation is that the Sitakund anticline developed more proximal to an orogenic belt compared to the other three anticlines (Fig. 2), similar to the situation in the California Coast Range, where tectonism plays a major role in developing overpressure (Berry, 1973). This may have exacerbated high fluid pressures produced by probable rapid deposition of the strata that have been folded into the Sitakund anticline (Khan et al., 2002), similar to the situation in the U.S. Gulf Coast where

rapid subsidence and sedimentation play a major role in developing overpressure (Dickinson, 1953; Bethke, 1986). Thus, sharp uplift and concomitant erosional unroofing might bring the overpressured strata at a much shallower depth at Sitakund.

Miocene Strata of the Sitakund anticline contain abundant shaly intervals, and intense folding may have added to development of high fluid pressures. The Sitakund anticline is a large-amplitude, complex and faulted structure in which Miocene core rocks have experienced significant uplift along an east-dipping thrust fault developed at the western flank of the anticline. The anticline is marked by a relative gravity high flanked by gravity minima (Fig. 42). A gravity maximum (greater than10 mgal) in the axial region of the Sitakund anticline may be attributed to the anomalously shallow occurrence of deeper, well-compacted strata (the Bhuban Formation) compared to younger sediments in the adjacent rim synclines. Relative gravity lows are observed in the Patiya and Jaldi anticlines (-30 to –20 mgal), suggesting that these anticlines have lower amplitude and are less deformed than the Sitakund structure. The anticlines of this region of the eastern fold belt developed as buckle folds over a regional detachment during the initial stage of shortening (Sikder and Alam, 2003).

Fluid overpressure in strata of the California Coast Ranges has been attributed principally to tectonic compression (Berry, 1973). This phenomenon corresponds closely to the situation observed in the Sitakund structure of southeastern Bengal basin. The Sacramento basin of northern California is located in a transpressional tectonic setting similar to that of the eastern Bengal basin (Uddin et al., 2002). Overpressure in the Sacramento basin is observed on a regional scale in an area where sedimentary compaction, geochemical diagenesis, and aquathermal pressuring are considered subordinant to tectonic compression (McPherson and Garven, 1999). We infer that tectonic compression has been the dominant factor for overpressure

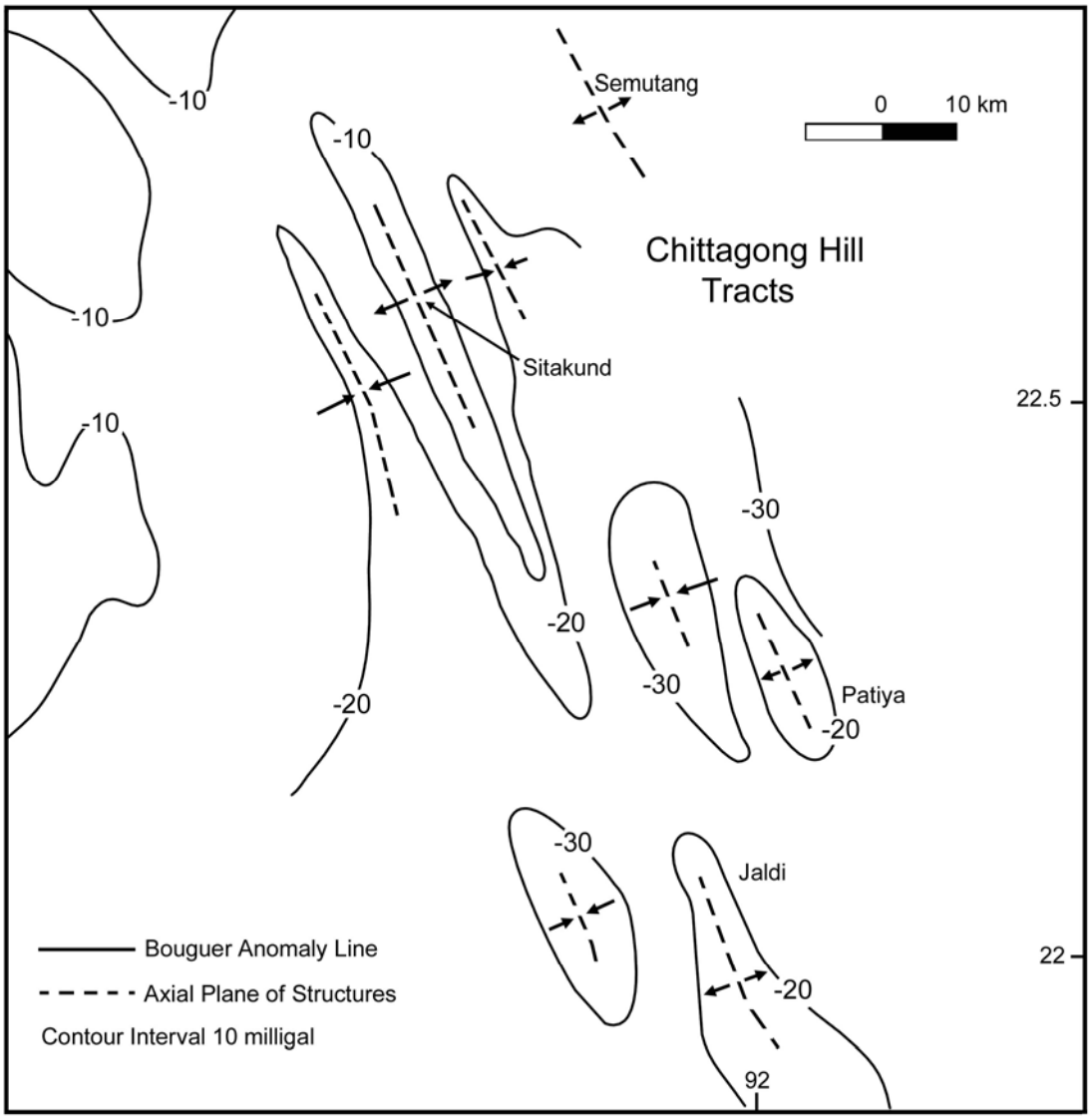

Figure 42. Bouguer anomaly pattern at Sitakund anticline and adjacent structures. Note that the Sitakund anticline shows a relatively higher gravity value than other anticlines (after Ali and Raghava, 1985).

generation of the Sitakund structure (Fig. 43). Factors that favor generation of overpressure by burial processes over tectonic compaction include high sedimentation rates, extremely low permeability of confining units, and very high compressibility distribution. An inverse illitization trend has been reported at Sitakund, which suggests that clay diagenesis is not responsible for development of overpressure at Sitakund (Sikder and Alam, 2003). In contrast, for the other three structures in this study, sedimentary compaction with subsequent clay diagenesis is the most plausible cause for the high fluid overpressures developed farther west of the advancing orogenic front of the Indo-Burman Ranges (Fig. 2).

7.5 DISCUSSION

Formation velocity data of the four wells analyzed in this study reveal that the velocity-depth distributions at the Titas-11, Bakhrabad-9, and Rashidpur-4 wells show a gradual increase of velocity with depth in Miocene sediments, reflecting normal trends. However, velocity-depth distribution at the Sitakund structure shows a short interval of initial increase of velocity followed by a constant decrease with depth, indicating the presence of overpressured and undercompacted shale. Hydrofracturing due to release of formation water has been observed at the microscopic level along these overpressured zones. There are no previous reports of overpressure in Oligocene sediments in the Bengal basin. Overpressure in the Miocene sequence in the Sitakund structure may have been caused by a combination of factors, including strong horizontal deviatoric regional stresses and uplift produced by fault propagation folding and concomitant shale diapirism. Compressive stresses associated with the Indo-Burmese plate convergence to the east are inferred to be the main cause of

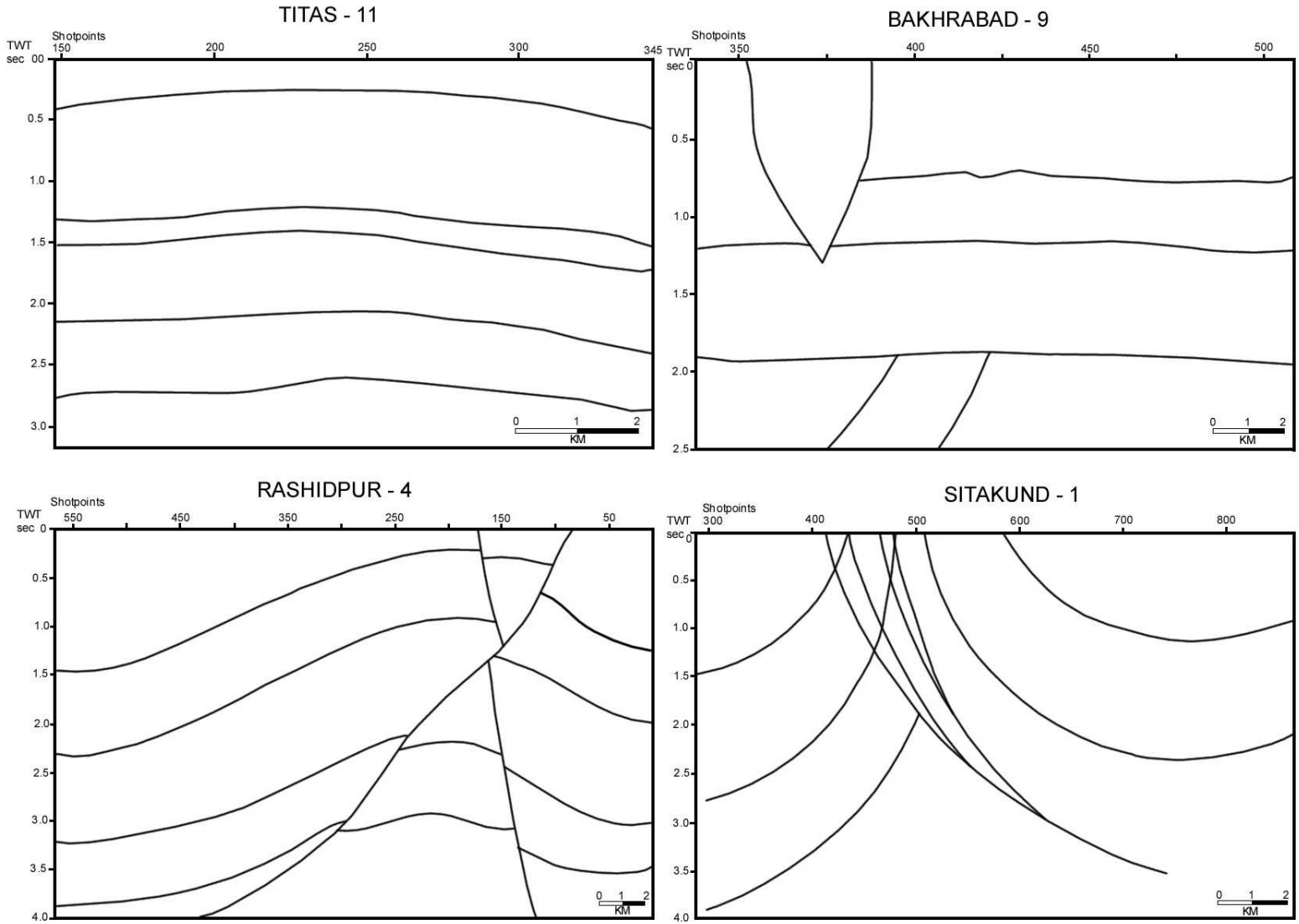

Figure 43. Seismic profile showing major seismic reflectors in the four studied wells. Note that the Sitakund structure is folded intensely due to advancing orogenic front from the east of Indo-Burman Ranges (data from BAPEX).

overpressure. The tectonics of Indo-Burman Ranges is controlled by the interaction between the north-south plate convergence along the Himalayas and east-west plate convergence along the Indo-Burman Ranges (Fig. 1; Brunschweiler, 1966; Sengupta et al., 1990; Johnson and Alam, 1991). Tectonic evolution involving folding and westward-directed overthrusting with a probable component of dextral movement in the western part of the Indo-Burman Ranges can be explained by obduction of the Indian Plate beneath the Asian Plate (Curray et al., 1978; Mitchell, 1981). The thrusting was presumably accompanied by an initial uplift of the Indo-Burman Ranges, and corresponds to Eocene-Oligocene unconformity in the western trough of the central Tertiary basins (Mitchell 1981, 1993). Absence of overpressure in the Bengal basin in Oligocene time indicates the lack of significant orogeny in the east.

CHAPTER 8: DISCUSSION

8.0 SYNTHESIS

The Bengal Basin is a complex foreland basin of the southeastern Himalayas that experienced a varied tectonic history. The earliest phase of sedimentation in the basin started when India began separating from Antarctica during the Late Cretaceous. Thick Tertiary deposits started filling up the basin at the beginning of Late Eocene, with deposition increasing rapidly with the eventual uplift of the Himalayas to the north and the Indo-Burman Ranges to the east. Syn- to post-tectonic sediments of the Bengal basin preserve a record of orogenesis in these two mountain belts. Modal analyses of sandstone and heavy mineral assemblages reveal variations in sediment composition that reflect the unroofing history of the source area.

8.1 OLIGOCENE PROVENANCE

8.1.1 Bengal Basin

Sandstones from Oligocene Barail Group are medium- to fine-grained and quartzolithic with low feldspar content (Figs. 13, 14, 15, 16, 17). All samples are dominated by mostly monocrystalline quartz grains. A few detrital chert and polycrystalline quartz are present. Feldspars are rare in Oligocene sediments in the Bengal basin and potassium feldspar dominates over plagioclase feldspar. Most of the plagioclase feldspars are altered and show grain etching. Among the lithic constituents, volcanic rock fragments are rare to absent. Most of the samples contain

abundant sedimentary lithic fragments, while some contain low- to medium-grade metamorphic rock fragments. The abundance of quartz and scarcity of feldspar grains and lithic fragments indicate erosion from a low-relief area under strong chemical weathering. This dominance of monocrystalline quartz and paucity of metamorphic lithic fragments and feldspar suggest erosion from a craton rather than a collisional orogen.

Heavy mineral assemblages in Oligocene sediments are dominated by opaque and ultra-stable minerals. Of the ultra-stable minerals, rutile is more abundant than tourmaline and zircon. Garnets are rare in Oligocene sands. Chrome spinels, rich in Cr and depleted in Al, are present in substantial amounts. Identified opaque minerals include pyrite, pyrrhotite, ilmenite, leucoxene, and titanium-rich magnetite. Low maturity index of the heavy mineral assemblages from the Oligocene sediments from the Bengal basin suggests a relatively short transport distance and proximal source. The presence of abundant opaque minerals indicates a more basaltic source, which could have been the Rajmahal Trap located adjacent to the northwestern part of the basin. However, presence of epidote, garnet, and aluminosilicate (sillimanite) indicate the possibility of input from an orogenic source from the eastern Himalayas (Kumar, 2004) and Indo-Burman Ranges.

8.1.2 Assam Basin

The Paleogene sandstones from the Assam basin (Disang and Barail groups) are quartzolithic in composition (Fig. 44). The sandstones are mostly fine grained. Feldspars are rare except in the Baragolai Formation of the Barail Group, which shows moderately high feldspar content (Kumar, 2004). The Disang sediments were

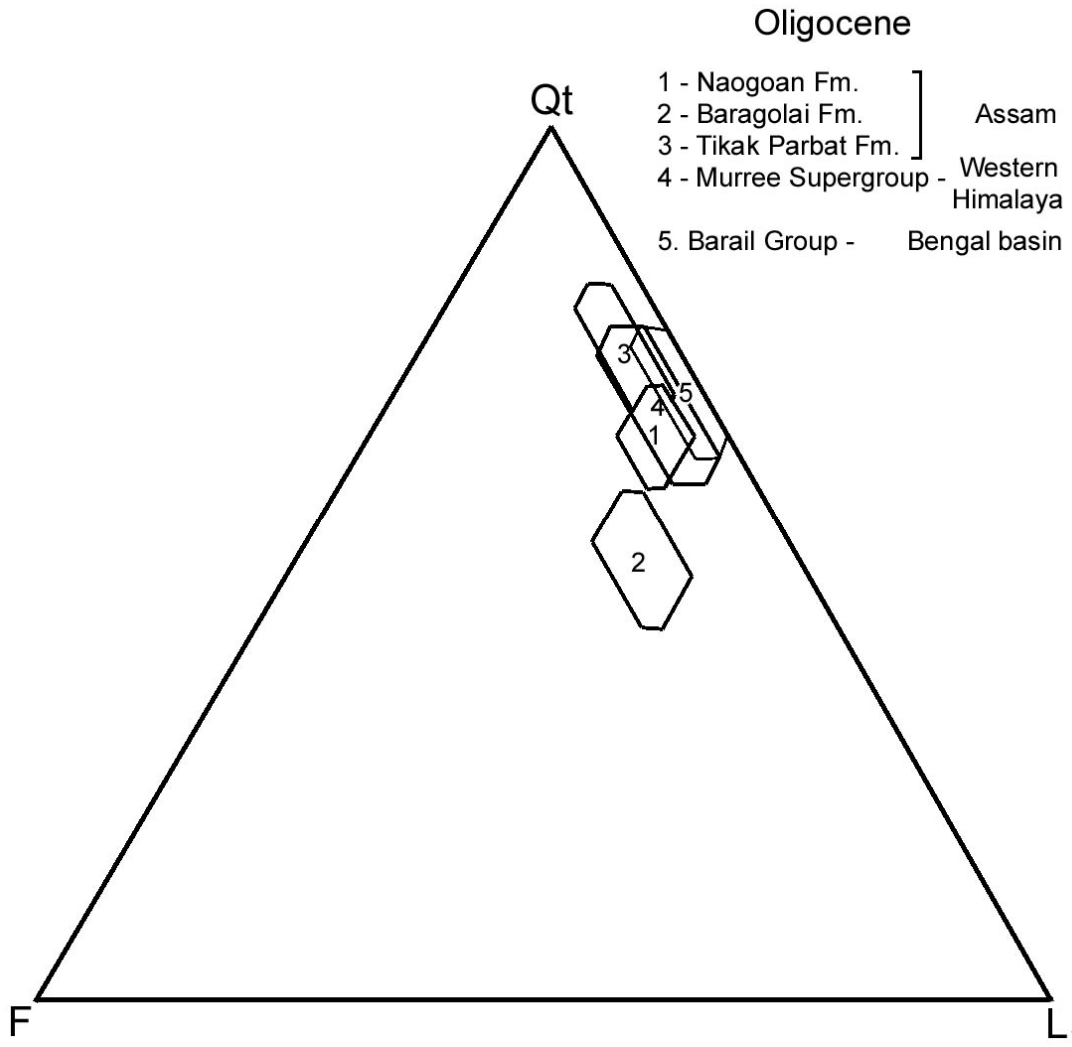

Figure 44. QtFL Diagram showing Oligocene sandstone composition from Assam, Western Himalayas and the Bengal Basin (Critelli and Garzanti, 1994; Critelli and Ingersoll, 1994; Kumar, 2004). Note that other then unit 2 of Kumar (2004), all data plots overlap.

deposited in deep-marine environments close to an arc-trench system during the Eocene. At the end of the Eocene, depositional facies changed from deep marine to deltaic environments during which sediments of the Barail Group were deposited. There is a general increase in the number of coal beds in the upper part of the Barail (Tikak Parbat Formation) Group in the northeastern part of Schuppen belt, indicating progradation of a delta from northeast to southwest (Rangarao, 1983). With delta progradation, delta plains were enlarged and forming environments became widespread (Rangarao, 1983). Presence of radiolarian chert fragments in basal conglomerates may indicate a contribution from the eastern Ophiolite belt of the Indo-Burman Ranges. The heavy-mineral assemblage in the Oligocene Barail Group shows mostly ultrastable grains such as zircon, tourmaline, and rutile (ZTR) with few other grains such as staurolite, pyroxene, garnet, and micas (Kumar, 2004).

8.1.3 Western Himalayas

In the western Himalayas, the Oligocene Murree Supergroup has a quartzolithic composition ($Qt_{68}F_5L_{27}$; Critelli and Garzanti, 1994) indicating a collisional orogen provenance. This unit was deposited in the western Himalayas in tidal-flat to fluviatile environments along evolving foreland basins. These sediments were derived from a suture belt that included thrust sheets consisting of metasedimentary and sedimentary rocks, volcanic and volcaniclastic rocks, and ophiolites. Detrital mode of sandstones and a southeastward-prograding clastic wedge indicate provenance from the proto-Himalayas in the north. The mean composition (QtFL) of the Murree Supergroup is very close to that of Oligocene sediments from Assam (Kumar, 2004). This may suggest that the early convergence of India with

Asia at the two syntaxes may have been that relatively isochronous (Dewey et al., 1989; Uddin and Lundberg, 1998a).

8.2 LOWER MIOCENE PROVENANCE

8.2.1 Bengal Basin

The Lower Miocene sediments of the Bengal basin have much higher feldspar content than those of the Oligocene Barail unit. Increase in both feldspars and lithic fragments indicate the initial input from an orogenic source to the Bengal basin. The Surma Group sediments are mostly quartzolithic to quartzo-feldspathic (Fig. 45). Quartz grains are mostly monocrystalline, undulose, and slightly strained in some samples. Feldspars are abundant, and plagioclase feldspar and potassium feldspar are roughly equal in abundance. Lithic fragments, most commonly sedimentary and low- to medium-grade metamorphic lithic fragments, are common. Some samples contain rare high-grade metamorphic rock fragments. The change in sandstone modes in the Oligocene-Miocene transition may represent the initiation of the uplift and erosion of Himalayas. Radiometric dating of alkali feldspars (Hodges et al., 1994) suggests initiation of orogenic activity in the eastern Himalayas by Oligocene time. The change in sandstone composition from the Oligocene to early Miocene time records input from an orogenic source likely associated with the unroofing of the Himalayas.

8.2.2 Assam Basin

The Miocene Surma Group in its type location in the Surma Valley is more than 4000 m thick. A major unconformity formed near the end of the Oligocene in the Assam basin (Evans, 1964). The Surma Group sandstones are quartzolithic ($Qt_{65}F_5L_{29}$; Kumar, 2004). The sandstones are rich in lithic fragments that include

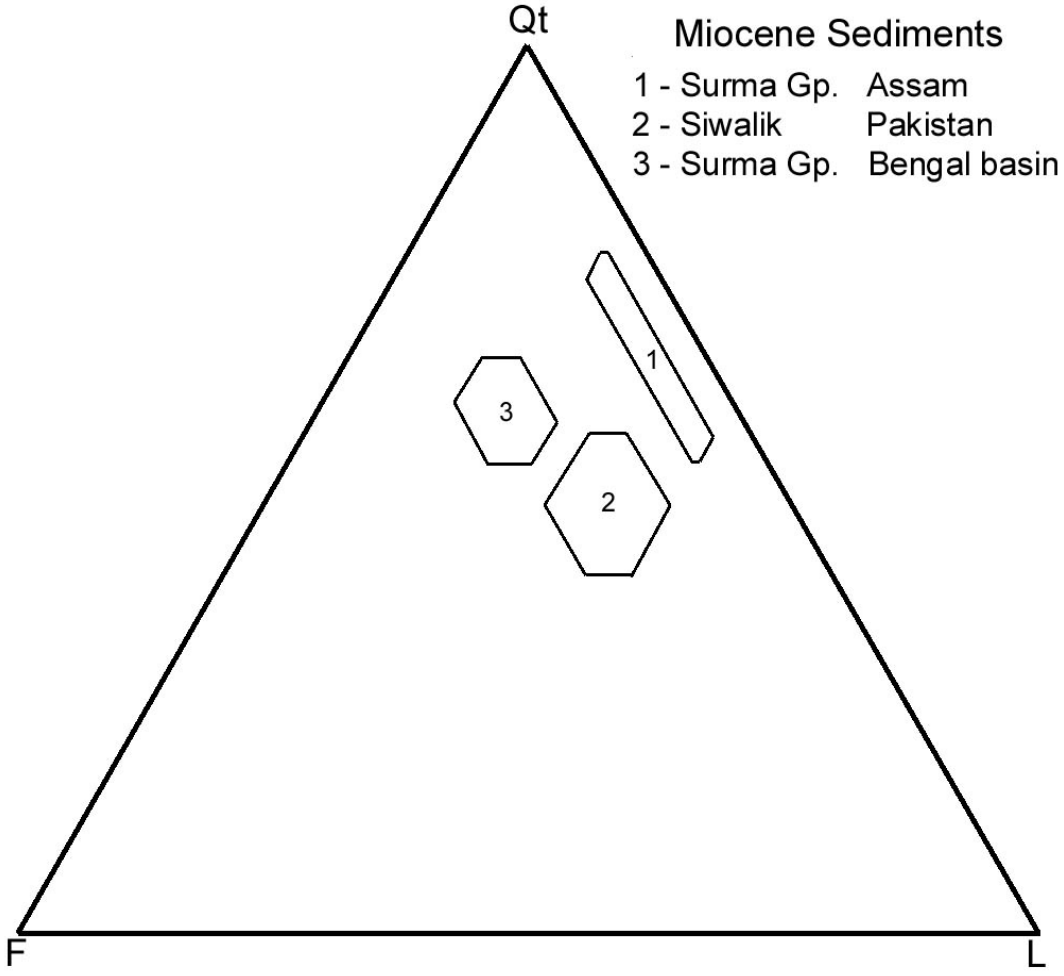

Figure 45. QtFL Diagram showing composition of Miocene sandstone from Assam, Siwalik Pakistan, and Bengal basin (Suczek and Ingersoll, 1985; Critelli and Ingersoll, 1994; Kumar, 2004).

schist, quartzite, slate, chert and argillites. Miocene Surma sequences most likely were derived from the Himalayas and the Indo-Burman ranges.

Heavy-mineral assemblages in the Surma Group contain abundant chlorite and chloritoid group minerals. They also are characterized by abundant garnet and high ZTR indices compared to the underlying Barail Group. The heavy minerals are more diverse in the Neogene compared to Paleogene sandstone in the Assam basin. The presence of high-grade metamorphic minerals, as well as garnets, suggests that they were derived from low- to intermediate-grade metamorphic rocks (probably from contact metamorphic rocks).

8.2.3 Western Himalayas

The Miocene-Pliocene Siwalik sandstones of Pakistan are quartzolithic but rich in feldspar ($Qt_{48}F_{28}L_{34}$; Critelli and Ingersoll., 1994). Lithofacies are composed of low- to medium-grade metamorphic and sedimentary fragments with few volcanic and ophiolite fragments. The metamorphic fragments consist of fine-grained schists, phyllite, and gneiss derived from the Higher and/or Lesser Himalayas. Sedimentary fragments were derived from the Tethyan Himalayas, and ophiolitic, volcanic fragments were derived from the Indus suture and Trans-Himalayan belt (Critelli and Ingersoll, 1994).

8.2.4 Indo-Burman Ranges

Miocene clastic deposits of the Indo-Burman Ranges (Laung, Yezaw, and Mayu formations) suggest derivation from the Himalayas (Khin, 2000). The Lower Miocene Laung Formation ($Qt_{50}F_{10\text{-}23}L_{12}$), which has abundant feldspars and lithic fragments, includes low- to intermediate-grade metamorphic lithic fragments,

suggesting onset of uplift and erosional unroofing in the eastern Himalayas around 21.5 Ma. The Lower to Middle Miocene Yezaw Formation ($Qt_{58}F_{22}L_{20}$) is rich in subangular monocrystalline quartz grains, chert, and argillite with less common feldspar and metamorphic fragments (Khin, 2000). Sandstones of the Upper Miocene Mayu Formation ($Qt_{60}F_{20}L_{20}$) sandstones are rich in potassium feldspar compared to the plagioclase-rich lower to middle Miocene sandstones, suggesting a granitic source in the High Himalayan Crystalline belt.

8.3 MICROPROBE ANALYSIS

8.3.1 Garnet

Garnets are rare in Oligocene Barail Formation, but are relatively common in Lower Miocene sediments. Most of the garnets found in both formations are colorless and occur as euhedral grains. Detrital garnets analyzed from the Lower Miocene unit of the Bengal basin are mostly almandine-rich. Pyrope content is generally low and the grossular component is minor. The spessartine content generally did not exceed more then 3% of the four components. Presence of these garnets suggests a derivation from regionally metamorphosed garnet-mica schist rather than a high-grade metamorphic facies. Garnets from sediments of the Bengal fan, further downstream from the Bengal basin, were thought to be derived from greenschist to granulite facies metamorphic rocks on the Indian continent, including some from the Deccan Traps (Amano and Taira, 1992). The garnets found in coastal sediments from southern India are compositionally similar to those of the Bengal basin (Harris et al., 1982; Sinha Roy et al., 1984; Santosh, 1987). Therefore, the Indian craton also could be a possible source for the garnets from the Oligocene and Lower Miocene sediments of the Bengal basin.

8.3.2 Chrome Spinel

Chrome spinels are present in the Oligocene sequence of the Bengal basin. The elemental abundance of chromium in these chrome spinels is high. Other important abundant cations include trivalent Al and Fe^{3+} and divalent Mg and Fe^{2+}. Spinel compositions may reflects a mixture of mid-ocean ridge-derived basalts and more depleted marginal-basin and island-arc suites. However, lack of both high-Al and high-Mg spinels strongly suggests that the detrital chrome spinels of the Bengal basin did not originate from a mid-ocean-ridge source. These spinels may have been derived either from Himalayan arc material or ophiolites, continental flood basalts of the Deccan Traps and/or the Indo-Burmese ophiolites. The presence of detrital Cr-rich spinels in basinal sediments and/or adjacent to an orogenic belt is generally interpreted as an indicator of derivation from peridotites/ophiolite sequences. Hence, the presence of Cr-rich spinels in the Oligocene Barail Formation could be derived from an ophiolite obducted on the northern Indian continental margin during the cretaceous. However, in this scenario, wide variation in spinel compositions would be expected because Cr-spinel from obducted ophiolite and associated subduction/ accretionary materials of arc complexes has diverse origin (Cookenboo et al., 1997). In contrast, the detrital spinels in the Barail Formation have a limited range of chemical compositions and have wide range in TiO_2 contents (0.3-3). Since the TiO2 contents in arc spinels are generally <1%, sole contribution of spinels from an arc-trench system is not likely. Tectonic location of the Bengal basin and paleogeographic considerations suggest the Rajmahal Trap as one of the possible sources of these spinels.

Chrome spinel studies from the Assam basin suggest derivation from ophiolites of the Indo-Burman Ranges (Kumar, 2004). The Mg-Cr plot (Fig. 33) of

spinels from the Bengal basin suggests strong chemical similarity with the ophiolites of the Indo-Burman Ranges. Low Al and Mg contents, together with the wide range in TiO_2 wt. % of the Bengal basin chrome spinels, also suggest a possible derivation from Alpine-type ophiolites present in the Indo-Burman Ranges.

8.3.3 Tourmaline and Amphibole

Tourmalines are ubiquitous in both Oligocene and Miocene formations in the Bengal basin. Al-Fe(tot)-Mg and Ca-Fe(tot)-Mg plots of tourmaline show that most of the grains were sourced from metapelites and metapsammites. Some were derived from Ca-poor metapelites, metapsammites, and quartz-tourmaline rocks. Others were derived from Li-poor granitoids and associated pegmatites. Hence, there are at least two distinct sources for the tourmalines, one of which likely was recycled sedimentary rocks in an orogenic belt. Sediments from the Bengal basin apparently had a dominantly metasedimentary provenance, with minor contribution from granitoid and pegmatitic rocks.

Amphibole data from the Bengal basin is insufficient to draw any meaningful conclusions. However, wide variations in composition indicate a wide range of paragenesis. All amphiboles from the Bengal basin analyzed in this study are calcic in nature and have high magnesium contents. This suggests derivation from low-grade regional metamorphic rocks (greenschist facies).

8.4 OVERPRESSURE AND TECTONICS

Overpressured zones frequently have been reported in exploratory wells in Bangladesh. Four studied wells in the Bengal basin show an overpressured zone in Miocene strata at different depths. Titas, Bakhrabad, and Rashidpur structures show

overpressure at depth more then 3100 m. In contrast, the overpressured zone is relatively shallow in the Sitakund structure (1100 m). Miocene Strata of the Sitakund anticline contain abundant shaly intervals. These thick shale units, along with intense folding due to tectonism, contributed to development of high fluid pressures. Generation of overpressure in the other three wells was relatively more to burial processes rather than tectonic compaction. This study suggests that high sedimentation rates, extremely low permeability of confining units, and very high compressibility distribution are the main reasons for overpressure in the three structures. In contrast, overpressure in the Sitakund structure may have been caused by additional factors, including strong horizontal deviatoric regional stresses and uplift produced by fault propagation folding and concomitant shale diapirism. Compressive stresses associated with the Indo-Burmese plate convergence to the east likely contributed to the formation of overpressure in Miocene strata.

8.5 PALEOTECTONIC SETTING

Modal composition analyses of Oligocene and Miocene sandstones from the Bengal basin show variations in provenance history. Oligocene sands of the Barail Group are mostly quartzose and contain lithic fragments with rare to no feldspar. The abundance of quartz and paucity of lithic fragments and feldspars suggest that the nearby Indian Craton was the principal source of sediments. High ZTR indices and dominance of opaque minerals also support this source. During Oligocene time, the Bengal basin was located further south at the continental margin of the Indian plate. Although the eastern Himalayas was in its early uplift stage, the distal geographic position of Bengal basin did not allow Himalayan sediments to reach the basin

(Fig. 46A). However, the possibility of minor input of sediment from the Indo-Burman ranges cannot be ruled out based on the mineral chemistry data.

Early Miocene sandstones record a significant change in detrital composition and mark the unroofing of the Indo-Burman Ranges and eastern Himalayas. The influx of clastic sediments into the basin from the north and the east increased markedly at this time (Fig. 46B). Rocks in source areas were dominated by supracrustal rocks that produced monocrystalline quartz, feldspar and low- to intermediate-grade metamorphic lithic fragments. Although there are no known granitic terranes in the Indo-Burman Ranges, it is possible that such terranes existed during the Miocene time and contributed sediments to the basin. Bengal basin moved proximal to the Himalayan orogeny and started receiving sediments from the northeast and the east.

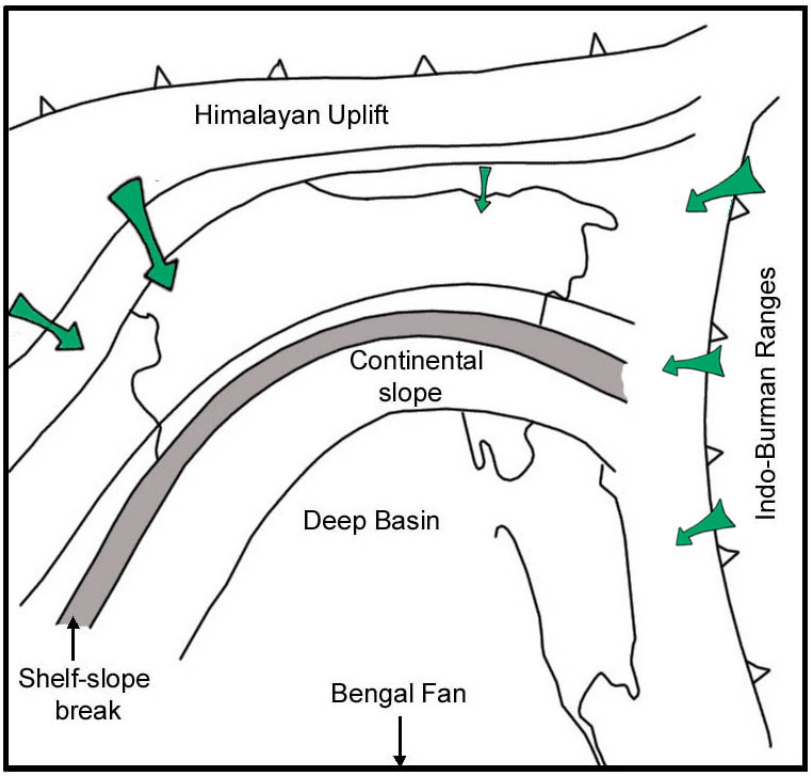

(A)

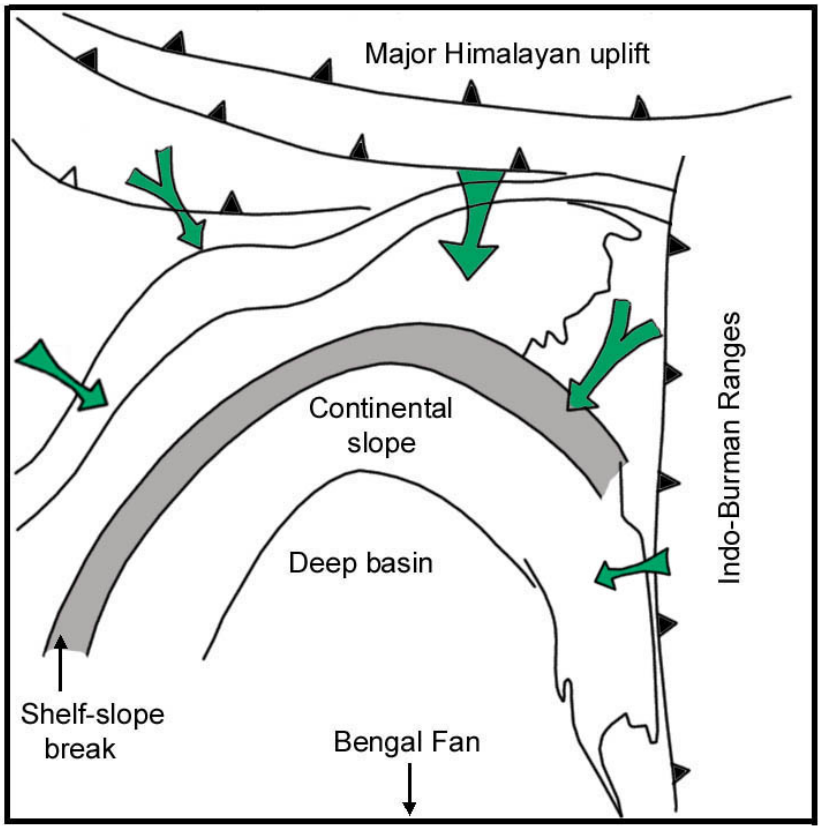

(B)

Figure 46. Paleotectonic setting of Bengal basin during (A) Oligocene, and (B) Early Miocene time (after Lindsay et al., 1991; Uddin and Lundberg, 1998a).

8.6 CONCLUSIONS

Based on sandstone modal analysis, heavy-mineral assemblages, and mineral chemistry data, the following conclusions can be drawn:

1. Oligocene sediments from the Bengal basin are quartzolithic, and are similar to those deposited in the western Himalayan and the Assam basin. Oligocene sandstones from the Bengal basin may have been derived from the Indian craton to the west.
2. Lower Miocene sediments have much higher feldspar contents compared to Oligocene sediments, indicating input from evolving orogenic sources.
3. Heavy mineral assemblages of Oligocene sediments have high ZTR indices and are dominated by opaque grains. In contrast, Miocene sediments are characterized by low ZTR indices and fewer opaque grains.
4. Garnets are absent in Oligocene sands but are abundant in Lower Miocene sediments. These garnets are rich in almandine, some rich in pyrope, but all are poor in grossular.
5. Garnet composition indicates derivation mostly from low- to medium-grade regional metamorphic source including some from high-grade granulite facies rocks.
6. High Cr, low Mg and Fe, and varied TiO_2 contents of chrome spinels may indicate derivation from the Rajmahal trap, the northeastern continuation of the Deccan trap and the ophiolites from the Indo-Burman ranges.
7. Occurrence of overpressure in Miocene rocks in the Bengal basin likely reflects the combined effects of sedimentary compaction, subsequent clay diagenesis, and subsequent tectonic events. No overpressured zones have been observed in the Oligocene sediments.

8. Very shallow occurrence of overpressure in the Sitakund structure can be attributed to the westward advancing tectonic compression from the Indo-Burman Ranges. Proximity of this structure to the orogenic belt compared to other sites indicates that tectonism here had a greater impact than diagenetic alteration on the development of overpressure.

REFERENCES

Acharyya, S.K., 1986, Tectono-stratigraphic history of Naga Hills ophiolite in geology of Nagaland Ophiolite: Geological Survey of India, Memoir, v. 119, p. 94-103.

Ahmed, A., 1983, Oligocene stratigraphy and sedimentation in the Surma Basin, Bangladesh: [unpublished M.Sc. thesis], University of Dhaka, 96 p.

Ahmed, I., 1985, Overpressure phenomenon - Its geological controls in Bangladesh gas fields with particular reference to the Sitakund test drilling: [unpublished M.S. thesis], University of Dhaka, 72 p.

Alam, M., 1989, Geology and depositional history of Cenozoic sediments of the Bengal Basin of Bangladesh: Palaeogeography, Palaeoclimetology, Palaeoecology, v. 69, p. 125- 139.

Alam, M., Alam, M.M., Curray, J.R., Chowdhury, M.L.R., and Gani, M.R., 2003, An overview of the sedimentary geology of the Bengal Basin in relation to the regional tectonic framework and basin-fill history: Sedimentary Geology, v. 155, p. 179-208.

Alam, M.M., 1991, Paleoenvironmental study of the Barail successionexposed in northeastern Sylhet, Bangladesh: Bangladesh Journal of Scientific Research, v. 9, p. 25– 32.

Ali, S.M.M., and Raghava, M.S.V., 1985, The Bouguer gravity map of Bangladesh and its tectono-geologic implications: Bangladesh Journal of Geology, v. 4, p. 43-56.

Allan, J.F., Sack, R.O., and Batiza, R., 1988, Cr-rich spinels as petrogenetic indicators: MORB-type lavas from the Lamont seamount chain, eastern Pacific, American Minerals, v. 73, p. 741–753.

Amano, K., and Taira, A., 1992, Two-phase uplift of Higher Himalayas since 17 Ma: Geology, v. 20, p. 391-394.

Arai, S., 1992, Chemistry of chromian spinel in volcanic rocks as a potential guide to magma chemistry: Mineralogical Magazine, v. 56, p. 173-184.

Bakhtine, M.I., 1966, Major tectonic features of Pakistan, Part II, The eastern province: Science and Industry, v. 4, p. 89-100.

Baksi, S.K., 1965, Stratigraphy of Barail series in southern part of Shillong Plateau, Assam, India: Geological Notes, v. 49, p. 2282-2288.

Banerji, R.K., 1981, Cretaceous–Eocene sedimentation, tectonism and biofacies in the Bengal basin, India: Palaeogeography Palaeoclimatology Palaeoecology, v. 34, p. 57-85.

Barnes, S.J., and Roeder, P., 2001, The range of spinel compositions in terrestrial mafic and ultramafic rocks, Journal of Petrology, v. 42, p. 2279– 2302.

Basu, A., 1976, Petrology of Holocene alluvial sand derived from plutonic source rocks; Implication to paleoclimate interpretation: Journal of Sedimentary Petrology, v. 4, p. 694-709.

Basu, A., and McKay, D.S., 1985, Chemical variability and origin of agglutinitic glass: Journal of Geophysical Research Supplementary., v. 90, p. D87-D94.

Berry, F.A.F., 1973, High fluid potentials in California Coast Ranges and their tectonic significance: American Association of Petroleum Geologists Bulletin, v. 57, p. 1219-1249.

Bethke, C.M., 1986, Inverse hydrologic analysis of the distribution and origin of Gulf Coast-type geopressured zones: Journal of Geophysical Research Supplementary, v. 91, p. 6536-6545.

Bhattacharji, V., and Bhattacharji, T.K., 2002, An Early Cretaceous age for the Rajmahal traps, Panagarh area, West Bengal: Palynological evidence: Cretaceous Research, v. 23, p. 789-805.

Bradley, J.S., 1975, Abnormal formation pressure: American Association of Petroleum Geologists Bulletin, v. 59, p. 957-973.

Brunnschweiler, R.O., 1966, On the geology of the Indo-Burman ranges (Arakan coast and Yoma, Chin Hills, Naga Hills): Geological Society of Australia Bulletin, v. 13.

—, 1974, Indo-Burman ranges, in Spencer, M.A., ed., Mesozoic-Cenozoic orogenic belts: Geological Society of London, Edinburgh: Scottish Academy Press, p. 279-299.

—, 1980, Lithostratigraphic monsters in modern oil exploration: Offshore Southwast Asia Conference, SEAPEX Session, p. 7 p.

Burst, J.F., 1969, Diagenesis of Gulf Coast clayey sediments and its possible relation to petroleum migration: American Association of Petroleum Geologists Bulletin, v. 53, p. 73-93.

Cerveny, P.P., Johnson, N.M., Tahirkheli, R.A.K., and Bonis, N.R., 1989, Tectonic and geomorphic implications of Siwalik Group heavy minerals: in Malinconico, L.L. Jr., and Lillie, R.J., eds., Tectonics of the western Himalayas: Geological Society of America, Special Paper 232, p. 129-136.

Chacko, T., Ravindrakumar, G.R., and Newton, R.C., 1987, Metamorphic P-T conditions of the Kerala (South India) khondalite belt, a granulite facies supracrustal terrain: Journal of Geology, v. 95, p. 343- 358.

Chaudhri, R.S., 1972, Heavy minerals from Siwalik formations of the northwestern Himalayas: Sedimentary Geology, v. 8, p. 77-82.

Chowdhury, K.R., Haque, M., Nasreen, N., and Hasan, R., 2003, Distribution of planktonic foraminifera in the northern Bay of Bengal: Sedimentary Geology, v. 155, p. 393-405.

Chowdhury, S.Q., 1982, Palynostratigraphy of the Neogene sediments of the Sitapahar anticline (western flank), Chittagong Hill Tracts: Bangladesh Journal of Geology, v. 1, p. 35-49.

Colton-Bradly, V.A.C., 1987, Role of pressure in smectite dehydration-effects on geopressure and smectite-to-illite transition: American Association of Petroleum Geologists Bulletin, v. 71, p. 1414-1427.

Cookenboo, H.O., Bustin, R.M., and Wilks, K.R., 1997, Detrital chromian spinel compositions used to reconstruct the tectonic setting of provenance; Implications for orogeny in the Canadian Cordillera: Journal of Sedimentary Research, v. 67, p. 116-123.

Corelab, B., 1996, The Petroleum Geology and Hydrocarbon Potential of Bangladesh: [unpublished report]: Bangladesh Oil, Gas and Mineral Corporation, p. v. I (139 p.) and II (129 p.).

Curray, J.R., Emmel, F.J., Moore, D.G., and Raitt, R.W., 1982, Structure, tectonics and geological history of the northeastern Indian Ocean, in Nairn, A.E.M., and Stehli, F.G., eds.: The Ocean Basin and Margins, v. 6, The Indian Ocean: New York, Plenum, p. 399-450.

Curray, J.R., and Moore, D.G., 1974, Sedimentary and tectonic processes of the Bengal deep-sea fan and geosyncline: in Burk, C.A., and Drake, C.L., eds., The Geology of Continental Margins: New York, Springer-Verlag, p. 617-628.

Curray, J.R., Moore, D.G., Lawver, L.A., Emmel, F.J., Raitt, R.W., Henry, M., and Kieckhefer, R., 1978, Tectonics of Andaman Sea and Burma: American Association of Petroleum Geologists Memoir, v. 29, p. 189-198.

Dasgupta, A.B., 1977, Geology of Assam Arakan region: Mining and Metallurgy Society of India Quarterly Journal, v. 49, p. 1-54.

Dasgupta, S., and Nandy, D.R., 1995, Geological framework of the Indo-Burmese convergent margin with special reference to ophiolitic emplacement: Indian Journal of Geology, v. 67 (2), p. 110– 125.

DeCelles, P.G., Robinson, D.M., Quade, J., Ojha, T.P., Garzione, C.N., Copeland, P., and Upreti, B.N., 2001, Stratigraphy, structure, and tectonic evolution of the Himalayan fold-thrust belt in western Nepal: Tectonics, v. 20, p. 487-509.

Deer, W.A., Howie, R.A., and Zussman, J., 1992, An introduction to the rock-forming minerals: Longman Scientific Technical, Harlow, United Kingdom, 696 p.

Dick, H.J.B., and Bullen, T., 1984, Chromian spinel as a petrogenetic indicator in abyssal and alpine-type peridotites and spatially associated lavas: Contributions to Mineralogy and Petrology, v. 86, p. 54-76.

Dickinson, G., 1953, Geological aspects of abnormal reservoir pressures in Gulf Coast, Louisiana: American Association of Petroleum Geologists Bulletin, v. 37, p. 410-432.

Dickinson, W.R., 1970a, Interpreting detrital modes of graywacke and arkose: Journal of Sedimentary Petrology, v. 40, p. 695-707.

—, 1970b, Tectonic setting and sedimentary petrology of the Great Valley sequence: Geological Society of America Abstracts with Programs, v. 2, p. 86-87.

—, 1982, Composition of sandstones in circum-Pacific subduction complexes and fore-arc basins: American Association of Petroleum Geologists Bulletin, v. 66, p. 121-137.

—, 1985, Interpreting provenance relations from detrital modes of sandstones: G. G. Zuffa (ed.), Provenance of Arenites, D. Reidel Publishing, Boston, p. 333-361.

Dickinson, W.R., and Suczek, C., 1979, Plate tectonics and sandstone compositions: American Association of Petroleum Geologists Bulletin, v. 63, p. 2164-2182.

Dorsey, R.J., 1988, Provenance evolution and unroofing history of a modern arc-continent collision: Evidence from petrography of Plio-Pleistocene sandstones, eastern Taiwan: Journal of Sedimentary Petrology, v. 58, p. 208-218.

Evans, P., 1964, The tectonic framework of Assam: Journal of Geological Society of India, v. 5, p. 80-96.

Fertl, W.H., Chapman, R.E., and Hotz, R.F., 1994, Studies in abnormal pressures: Developments in Petroleum Science, v. 38, 454 p.

Fleet, W.F., 1926, Petrological notes on the Old Red Sandstones of the West Midlands: Geological Magazine, v. 65, p. 6-8.

Freed, R.L., and Peacor, D.R., 1989, Geopressured shale and sealing effect of smectite to illite transition: American Association of Petroleum Geologists Bulletin, v. 73, p. 1223-1232.

Gansser, A., 1964, Geology of the Himalayas: Interscience, London, p. 289 p.

Garzanti, E., Angiolini, L., Sciunnach, D., 1996, The Mid-Carboniferous to lowermost Permian succession of Spiti (Po Group and Ganmachidam Formation; Tethys Himalaya, northern India); Gondwana glaciation and rifting of Neo-Tethys: Geodinamica Acta, v. 9, p. 78-100.

Garzanti, E., Baud, A., and Mascle, G., 1987, Sedimentary record of the northward flight of India and its collision with Eurasia (Ladakh Himalaya, India): Geodinamica Acta, v. 1, p. 297-312.

Graham, S.A., Dickinson, W.R., and Ingersoll, R.V., 1975, Himalayan-Bengal model for flysch dispersal in the Appalachian-Ouachita system: Geological Society of America Bulletin, v. 86, p. 273-286.

Graham, S.A., Ingersoll, R.V., and Dickinson, W.R., 1976, Common provenance for lithic grains in Carboniferous sandstones from Ouachita Mountains and Black Warrior Basin: Journal of Sedimentary Petrology, v. 46, p. 620-632.

Harris, N.B.W., Holt, R.W., and Drury, S.A., 1982, Geobarometry, geothermometry, and late Archaean geotherms from the granulite facies terrain of south India: Journal of Geology, v. 90, p. 509- 527.

Henry, D.J., and Dutrow, B.L., 1992, Tourmaline as a low grade clastic metasedimentary rock: an example of the petrogenetic potential of tourmaline: Contributions to Mineralogy and Petrology, v. 112, p. 203-218.

Henry, D.J., and Guidotti, C.V., 1985, Tourmaline as a petrogenetic indicator mineral: an example from the staurolite grade metapelites of NW Maine: American Mineralogists, v. 70, p. 1-15.

Hess, H.H., 1966, Notes on operation of Frantz isodynamic magnetic separator: Princeton University, User manual guide, p. 1-6.

Hiller, K., and Elahi, M., 1984, Structural development and hydrocarbon entrapment in the Surma Basin, Bangladesh (northwest Indo–Burman Fold belt): Proceedings of 4th Offshore Southeast Asia Conference, Singapore, p. 6-50 – 6-63.

—, 1988, Structural growth and hydrocarbon entrapment in the Surma basin, Bangladesh. In Wagner, H.C., Wagner, L.C., Wang, F.F.H., Wong, F.L. (Eds.): Petroleum Resources of China and Related Subjects, Houston, Texas. Circum-Pacific Council for Energy and Mineral Resources Earth Science Series, v. 10, p. 657-669.

Hodges, K.V., Hames, W.E., Olszewski, W., Burchfiel, B.C., Royden, L.H., and Chen, Z., 1994, Thermobarometric and 40Ar/39Ar geochronologic constraints on Eohimalayan metamorphism in the Dinggye area, Southern Tibet: Contributions to Mineralogy and Petrology, v. 117, p. 151-163.

Holtrop, J.F., and Keizer, J., 1970, Some aspects of stratigraphy and correlation of the Surma Basin wells, East Pakistan: New York, United Nations, ECAFE Mineral Resources Development Series no. 36, p. 143-155.

Hoque, M., 1982, Tectonic set-up of Bangladesh and its relation to hydrocarbon accumulation: Center for Policy Research, Dhaka, Bangladesh, 177 p.

Hossain, K.M., 1988, Plate tectonic theory and the development of the folds of Chittagong and Chittagong Hill Tracts: Bangladesh Journal of Geology, v. 4, p. 57-68.

Hottman, C.E., and Johnson, R.K., 1965, Estimation of formation pressures from log derived properties: Journal of Petroleum Technology, v. 17, p. 717-722.

Hubbert, M.K., and Rubey, W.W., 1959, Mechanics of fluid-filled porous solids and its application to over thrust faulting: Geological Society of America Bulletin, v. 70, p. 115-166.

Hubert, J.F., 1962, A zircon-tourmaline-rutile maturity index and the interdependence of the composition of heavy mineral assemblages with the gross composition and texture of sandstones: Journal of Sedimentary Petrology, v. 32, p. 440-450.

Hunt, J.M., 1990, Generation and migration of petroleum from abnormally pressured fluid compartments: American Association of Petroleum Geologists Bulletin, v. 74, p. 1-12.

Hutchison, C.S., 1989, Geological evolution of south-east Asia: Oxford, Clarendon Press, 368 p.

Ingersoll, R.V., 1978, Petrofacies and petrologic evolution of the Late Cretaceous fore-arc basin, northern and central California: Journal of Geology, v. 86, p. 335-352.

—, 1984, Felsic sand/sandstone within mafic volcanic provinces; rift sand sandstone shows no basaltic provenance: Geological Society of America, Abstracts with Programs, v. 16, p. 548.

Ingersoll, R.V., Graham, S.A., and Dickinson, W.R., 1995, Remnant ocean basins: Tectonics of sedimentary basin: Cambridge, Massachusetts: Blackwell Science, p. 363-391.

Irvine, T.N., 1974, Petrology of the Duke Island ultramafic complex, southern Alaska: Geological Society of America Bulletin, v. 138, p. 240.

—, 1977, Origin of chromitite layers in the Muskox Intrusion and other stratiform intrusions; a new interpretation: Geology, v. 5, p. 273-277.

Ismail, M., 1978, Stratigraphic position of the Bogra Limestone of the platform area of Bangladesh: Bangladesh Geological Society, Proceedings of the 4th Annual Conference, v. 78, no. 31, p. 19-25.

Johnson, S.Y., and Nur Alam, A.M., 1991, Sedimentation and tectonics of the Sylhet trough, Bangladesh: Geological Society of America Bulletin, v. 103, p. 1513-1527.

Jones, P.H., 1969, Hydrology of Neogene deposits in the Northern Gulf of Mexico basin: Louisiana Water Resource Research Institute Bulletin, v. GT-2, 105 p.

Johnson, N.M., Stix, J., Tauxe, L., Cerveny, P.P., and Tahirkheli, R.A.K., 1985, Paleomagnetic chronology, fluvial processes, and tectonic implications of the Siwalik deposits near Chinji Village, Pakistan: Journal of Geology, v. 93, p. 27-40.

Kamenetsky, V.S., Crawford, A.J., and Meffre, S., 2001, Factors controlling chemistry of magmatic spinel: an empirical study of associated olivine, Cr-spinel and melt inclusions from primitive rocks: Journal of Petrology, v. 41, p. 655-671.

Kent, R.W., Pringle, M.S., Muller, R.D., Saunders, A.D., and Ghose, N.C., 2002, Ar/Ar geochemistry of the Rajmahal Basalts, India, and their relationship to the Kerguelen Plateau, Journal of Petrology, v. 43, no. 7, p. 1141-1153.

Khan, A.A., Hoque, M.A., Shaharier, K.M., Akhter, S.H., and Hoque, M., 2002, Convergent tectonics and sedimentation in the eastern margin of the Indian plate with emphasis on the Bengal basin: Bangladesh Journal of Geology, v. 21, p. 9-21.

Khan, M.A.M., 1978, Geology of the eastern and the northeastern part of sadar subdivision, Sylhet district, Bangladesh: Geological Survey of Bangladesh Records, v. 2, p. 20 p.

Khan, M.A.M., and Husain, M., 1980, A look at the geology of Bangladesh gas fields: Oil & Gas Journal, p. 92-95.

Khan, M.A.M., Ismail, M., and Ahmad, M., 1988, Geology of hydrocarbon prospects of the Surma basin, Bangladesh: Seventh Offshore southeast Asia conference, Singapore, p. 364-387.

Khan, M.R., and Muminullah, M., 1980, Stratigraphy of Bangladesh, in petroleum and mineral resources of Bangladesh: Seminar and exhibition: Dhaka, Government of People's Republic of Bangladesh, p. 35-40.

Khandoker, R.A., 1989, Development of major tectonic elements of the Bengal basin: a plate tectonic appraisal: Bangladesh Journal of Scientific Research, v. 7, p. 221–232.

Khin, K., 2000, Sedimentary evolution of Miocene clastic sequences, western Myanmar, and its relation to unroofing of Himalayas: [Doctoral thesis]: Kyushu University, TOKYO, 245 p.

Klootwijk, C.T., Gee, J.S., Pierce, J.W., and Smith, G.M., 1992, An early India-Asea contact: Paleomagnetic constraints from Ninetyeast Ridge, ODP Leg 121: Geology, v. 20, p. 395-398.

Kononov, S.I., Fariduddin, M., Matin, M.A., and Boul, M.A., 1983, Possibility of oil discovery in Bangladesh- myth or reality: Bangladesh Journal of Geology, v. 2, p. 37-54.

Krishnamurthy, P., and Cox, K.G., 1977, Picrite basalts and related lavas from the Deccan Traps of western India: Contributions to Mineralogy and Petrology, v. 62, p. 53-75.

Kumar, P., 2004, Provenance History of Cenozoic Sediments near Digboi-Margherita Area, Eastern Syntaxis of the Himalayas, Assam, Northeast India: [Unpublished M.S. Thesis], Auburn University, p. 131.

Lee, T., and Lawver, L.A., 1995, Cenozoic plate reconstruction of Southeast Asia: Tectonophysics, v. 251, p. 85-138.

Le Fort, P., 1996, Evolution of the Himalaya, in Yin, A., and Harrison, M., eds., The tectonic evolution of Asia: New York, Cambridge University Press, World and Regional Geology Series, p. 95-109.

Lindsay, J.F., Holliday, D.W., and Hulbert, A.G., 1991, Sequence stratigraphy and the evolution of the Ganges– Brahmaputra Delta complex: American Association of Petroleum Geologists Bulletin, v. 75, p. 1233-1254.

Mahoney, J.J., Macdougall, J.D., Lugmair, G.W., Gopalan, K., and Krishnamurthy, P., 1985, Origin of contemporaneous tholeiitic and K-rich alkalic lavas: a case study from the northern Deccan Plateau, India: Earth and Planetary Science letters, v. 72, p. 39-53.

Mange, M.A., and Maurer, H.F.W., 1992, Heavy Minerals in Color: Chapman & Hall, London, p. 147.

McBride, E.F., 1985, Diagenetic processes that affect provenance determinations in sandstone: NATO ASI Series. Series C: Mathematical and Physical Sciences, v. 148, p. 95-113.

McDougall, I., and Harrison, T.M., 1988, Geochronology and thermochronology by the -p40-sAr/-p39-sAr method: Oxford University Press, p. 212 p.

McPherson, B.J.O.L., and Garven, G., 1999, Hydrodynamic and overpressure mechanisms in the Sacramento basin, California: American Journal of Science, v. 299, p. 429-466.

Milner, H.B., 1962, Sedimentary Petrography, George Allen and Unwin, London, 715 p.

Mirkhamidov, F.M., and Mannan, M.M., 1981, Nature of the gravity field and its relation with geotectonics at Bangladesh: Unpublished report, Petrobengla, Dhaka.

Mitchell, A.H.G., 1981, Phanerozoic plate boundaries in mainland SE Asia, the Himalayas and Tibet: Journal of Geological Society of London, v. 138, p. 109-122.

—, 1984, Post-Permian events in the Zangho suture zone, Tibet: Journal of the Geological Society, London, v. 141, p. 129-136.

—, 1993, Cretaceous-Cenozoic tectonic events in the western Myanmar (Burma)-Assam region: Journal of the Geological Society, London, v. 150, p. 1089–1102.

Molnar, P., 1984, Structure and tectonics of the Himalaya: Constraints and implications of geophysical data: Annual Review of Earth and Planetary Sciences, v. 12, p. 489-518.

Morton, A.C., 1985, Heavy minerals in provenance studies: in Zuffa, G.G., (ed.) Provenance of Arenites, NATO ASI Series, Cosenza, Italy, p. 249-277.

Morton, A.C., Davies, J.R., and Waters, R.A., 1992, Heavy minerals as a guide to turbidity provenance in the lower Palaeozoic southern Welsh Basin; a pilot study, Geological Magazine, v. 129, p. 573-580.

Morton, A.C., and Hallsworth, C.R., 1999, Processes controlling the composition of heavy mineral assemblages in sandstones: Sedimentary Geology, v. 124, p. 3-30.

Morton, A.C., and Taylor, P.N., 1991, Geochemical and isotopic constraints on the nature and age of basement rocks from Rockall Bank, NE Atlantic: Journal of the Geological Society, London, v. 148, p. 630-634.

Mukherjee, A.B., and Biswas, S., 1988, Mantle-derived spinel lherzolite xenoliths from the Deccan volcanic province (India): Implications for the thermal structure of the lithosphere underlying the Deccan Traps: Journal of Volcanology and Geothermal Research, v. 35, p. 269-276.

Murphy, R.W., 1988, Bangladesh enters the oil era: Oil and Gas Journal, v. 86, no. 9 p. 76-82.

Murthy, M.V.N., Chakrabarti, C., and C., T.S., 1976, Stratigraphic revision of the Cretaceous-Tertiary sediments of the Shillong Plateau: Geological Survey of India Records, v. 107, p. 80-90.

Najman, Y., and Garzanti, E., 2000, Reconstructing early Himalayan tectonic evolution and paleogeography from Tertiary foreland basin sedimentary rocks, northern India: Geological Society of America Bulletin, v. 112, p. 435-449.

Nanayama, F., 1997, An electron microprobe study of the Amazon Fan: Proceedings of the Ocean Drilling Program, Scientific Results, v. 155, p. 147-168.

Nandi, K., 1967, Garnets as indices of progressive regional metamorphism: Mineralogical Magazine, v. 36, p. 89-93.

Neuzil, C.E., 1995, Abnormal pressures as hydrodynamic phenomena: American Journal of Science, v. 295, p. 742-786.

Nixon, G.T., Cabri, L.J., and Laflamme, J.H.G., 1990, Platinum-group-element mineralization in lode and placer deposits associated with the Tulameen alaskan-type complex, British Columbia: The Canadian Mineralogist, v. 28, p. 503-535.

Osborne, M.J., and Swarbrick, R.E., 1997, Mechanisms for generating overpressure in sedimentary basins: a reevaluation: American Association of Petroleum Geologists Bulletin, v. 81, p. 1023-1041.

Plumley, W.J., 1980, Abnormally high fluid pressure: Survey of some basic principles: American Association of Petroleum Geologists Bulletin, v. 64, p. 414-430.

Powers, M.C., 1967, Fluid-release mechanisms in compacting marine mudrocks and their importance in oil exploration: American Association of Petroleum Geologists Bulletin, v. 51, p. 1240-1254.

Powley, D.E., 1990, Pressures and hydrogeology in petroleum basins: Earth Science Reviews, v. 29, p. 215-226.

Press, S., 1986, Detrital spinels from alpinotype source rocks in Middle Devonian sediments of the Rhenish Massif: Geologische Rundschau, v. 75, p. 333-340.

Rahman, M.J.J., 1999, Sedimentology of the subsurface Neogene Surma Group of the Sylhet Trough, Bengal Basin, Bangladesh: [Ph. D Thesis], University of Vienna, Vienna, 173 p.

Rahman, M.J.J., and Faupl, P., 2003, 40Ar/39Ar multigrain dating of detrital white mica of sandstones of the Surma Group in the Sylhet Trough, Bengal Basin, Bangladesh: Sedimentary Geology, v. 155, p. 383-392.

Rangarao, A., 1983, Geology and hydrocarbon potential of a part of Assam-Arakan Basin and its adjacent area: Petroleum Asia Journal, p. 127-158.

Reimann, K.U., 1993, Geology of Bangladesh: Gebruder Borntraeger, Berlin, 160 p.

Rochon, R.W., 1967, Relationship of mineral composition of shales to density: Transactions of Gulf Coast Association of Geological Societies, v. 17, p. 135-142.

Rowley, D.B., 1996, Age of initiation of collision between India and Asia: A review of stratigraphic data: Earth and Planetary Science Letters, v. 145, p. 1-13.

Sah, S.C.D., and Shah, S.C., 1974, Dubrajpur Formation and its biozones: Aspects and appraisals of Indian Paleobotany. In Surange, K.R., Lakhanpal, R.N. and Bharadwaj, D.C. (eds.), Birbal Sahni Inst., Lucknow, India, p. 447-451.

Salt, C.A., Alam, M.M., and Hossain, M.M., 1986, Bengal Basin: current exploration of the hinge zone area of southwestern Bangladesh: Proceedings of 6th Offshore Southeast Asia Conference, Singapore, p. 55-57.

Santosh, M., 1987, Cordierite gneisses of southern Kerala, India: Petrology, fluid inclusions and implications for crustal uplift history: Contributions to Mineralogy and Petrology, v. 96, p. 343-356.

Schmidt, G.W., 1973, Interstitial water composition and geochemistry of deep gulf coast shales and sandstones: American Association of Petroleum Geologists Bulletin, v. 57, p. 321-337.

Sclater, J.G., and Fisher, R.L., 1974, The evolution of the east central Indian Ocean, with emphasis on the tectonic setting of the Ninetyeast Ridge: Geological Society of America Bulletin, v. 85, p. 683-702.

Scowen, P.A.H., Roeder, P.L., and Helz, R.T., 1991, Reequilibration of chromite within Kilauea Iki lava lake, Hawaii, Contribution to Mineralogy and Petrology, v. 107, p. 8-20.

Sen, G., 1986, Mineralogy and petrogenesis of the Deccan Trap lava flows around Mahabalesh, India: Journal of Petrology, v. 27, p. 627-663.

Sengupta, S., Ray, K.K., Acharyya, S.K., and Smeth, J.B., 1990, Nature of ophiolite occurrences along the eastern margin of the Indian plate and their tectonic significance: Geology, v. 18, p. 439-442.

Sikder, A.M., and Alam, M.M., 2003, 2-D modeling of the anticlinal structures and structural development of the eastern fold belt of the Bengal Basin, Bangladesh: Sedimentary Geology, v. 155, p. 209-226.

Sinha, R.N., and Sastri, V.V., 1973, Correlation of the Tertiary geosynclinal sediments of the Surma valley, Assam, and Tripura state (India): Sedimentary Geology, v. 10, p. 107-134.

Sinha Roy, S., Mathai, J., and Narayanasamy, S., 1984, Structural and metamorphic characteristics of cordierite bearing gneiss of south Kerala: Journal of the Geological Society of India, v. 25, p. 231-244.

Spear, F.S., 1993, Metamorphic phase equilibria and pressure-temperature-time paths: Mineralogical Society of America, Washington, DC, 799 p.

Spear, F.S., and Cheney, J.T., 1989, A petrogenetic grid for pelitic schists in the system SiO (sub 2) -Al (sub 2) O (sub 3) -FeO-MgO-K (sub 2) O-H (sub 2) O: Contributions to Mineralogy and Petrology, vol.101, no.2, p.149-164.

Strut, B.A., 1962, The composition of garnets from pelitic schists in relation to the grade of regional metamorphism: Journal of Petrology, v. 3, p. 181-191.

Suttner, L.J., 1974, Sedimentary petrologic provinces; an evaluation: Special Publication-Society of Economic Paleontologists and Mineralogists, no. 21, p. 75-84.

Thompson, R.W., 1974, Mineralogy of sands from the Bengal and Nicobar Fans, Sites 218 and 211, eastern Indian Ocean: in von der Borch, C.C., Sclater, J.G., et al., eds. Initial Reports of the Deep Sea Drilling Project, Leg 22: Washington, D.C., U.S. Government Printing Office, p. 711-713.

Tucker, M., 1988, Techniques in Sedimentology: Blackwell Scientific Publications, London, 395 p.

Uddin, A., 1987, A geological evaluation of the hydrocarbon potential of the Ganges/Bengal Delta of Bangladesh: [unpublished M.S. thesis], University of Hawaii, 167 p.

Uddin, A., Burchfiel, B.C., Geissman, J.W., and Lundberg, N., 2002, Tectonic configuration of the Bengal Basin: Miocene juxtaposition with Assam, India: Geological Society of America - Abstracts with Programs, v. 34. p. 509.

Uddin, A., and Lundberg, N., 1998a, Cenozoic history of the Himalayan-Bengal system: Sand composition in the Bengal basin, Bangladesh: Geological Society of America Bulletin, v. 110, p. 497-511.

—, 1998b, Unroofing history of the Eastern Himalaya and the Indo-Burman ranges: Heavy-mineral study of Cenozoic sediments from the Bengal basin, Bangladesh: Journal of Sedimentary Research, v. 68, p. 465-472.

—, 1999, A paleo-Brahmaputra? Subsurface lithofacies analysis of Miocene deltaic sediments in the Himalayan–Bengal system, Bangladesh: Sedimentary Geology, v. 123, p. 239-254.

—, 2004, Miocene sedimentation and subsidence during continent–continent collision, Bengal basin, Bangladesh: Sedimentary Geology, v. 164, p. 131-146.

Van Andel, T.J., 1959, Reflections on the interpretation of heavy-mineral analysis: Journal of Sedimentary Petrology, v. 29, p. 153-163.

Van Orman, J.A., 1994, Provenance constraints on the Himalayan/Bengal systems: Mineral chemistry analysis of Sylhet through sandstone: [unpublished research project], Florida State University, 46 p.

Venkataramana, P., Dutta, A.K., and Acharya, S.K., 1986, Petrography and petrochemistry of the ophiolite: Geological Survey of India - Memoir, v. 119, p. 33-63.

Wallid, K.M., 1982, Palynostratigraphy of the Tertiary sediments as exposed along the Jaflong-Tamabil-Jaintapur roadcut in Sylhet district, Bangladesh: [masters thesis], University of Dhaka, 105 p.

Worm, H.-U., Ahmed, A.M.M., U., A., Islam, H.O., Huq, M.M., Hambach, U., and Lietz, J., 1998, Large sedimentation rate in the Bengal Delta: Magnetostratigraphic dating of Cenozoic sediments from northeastern Bangladesh: Geology, v. 26, p. 487-490.

Xie, X., Bethke, C.M., Li, S., Liu, X., and Zheng, H., 2001, Overpressure and petroleum generation and accumulation in the Dongying depression of the Bohaiwan basin, China: Geofluids, v. 1, p. 257-271.

Yokoyama, K., Taira, A., and Saito, Y., 1990, Mineralogy of silts from the Bengal Fan: Proceedings of Ocean Drilling Programs, Scientific Results, v. 116, p. 59-73.

Zhu, B., Delano, J.W., and Kidd, S.F.W., 2005, Magmatic compositions and source terranes estimated from melt inclusions in detrital Cr-rich spinels: An example from mid-Cretaceous sandstones in the eastern Tethys Himalaya: Earth and Planetary Science Letters, v. 233, p. 295-309.

APPENDIX A

Garnet microprobe data from the Bengal basin

	Garnet standard	Fench3 (Mio.)	Fench4 (Mio.)	Fench5 (Mio.)	Fench6 (Mio.)	Fench7 (Mio.)
SiO2	41.33	37.13	36.21	36.89	37.93	38.52
TiO2	0.66	0.03	0.06	0.00	0.02	0.06
Al2O3	21.61	21.53	21.45	21.83	22.22	22.25
FeO	9.75	32.80	36.46	37.18	29.30	28.04
MnO	0.38	2.97	1.76	1.79	1.20	0.60
MgO	20.82	3.10	3.35	3.51	8.84	9.31
CaO	4.25	3.44	0.73	1.43	1.26	1.75
Total	98.79	101.00	100.02	102.63	100.77	100.53
Si	5.98	5.92	5.86	5.83	5.86	5.92
Ti	0.07	0.00	0.01	0.00	0.00	0.01
Al	3.68	4.04	4.09	4.07	4.05	4.03
Fe	1.18	4.37	4.94	4.92	3.79	3.60
Mn	0.05	0.40	0.24	0.24	0.16	0.08
Mg	4.49	0.74	0.81	0.83	2.04	2.13
Ca	0.66	0.59	0.13	0.24	0.21	0.29
TOTAL	16.11	16.06	16.08	16.13	16.11	16.06
Endmembers						
Py	70.44	12.08	13.23	13.29	32.91	34.95
Alm	18.50	71.70	80.74	78.97	61.18	59.04
Gro	10.33	9.63	2.08	3.88	3.38	4.72
Sp	0.72	6.58	3.95	3.85	2.54	1.28
total	100.00	100.00	100.00	100.00	100.00	100.00

Garnet data continued..

	Fench8 (Mio.)	Fench9 (Mio.)	Fench10 (Mio.)	Fench11 (Mio.)	Fench12 (Mio.)	Bsr. 5.1 19(Oligo.)	Brs. 5.1 20(Oligo)
SiO2	36.55	37.20	36.41	37.61	37.25	37.63	36.53
TiO2	0.05	0.08	0.06	0.03	0.10	0.01	0.07
Al2O3	21.10	21.38	21.11	21.86	21.48	22.15	21.30
FeO	36.31	31.52	35.69	27.07	30.54	29.74	33.79
MnO	0.75	0.09	0.96	1.77	0.32	1.30	0.76
MgO	1.52	1.91	2.99	9.03	2.13	9.09	1.81
CaO	4.37	8.31	2.45	1.70	8.91	1.05	5.37
Total	100.65	100.48	99.67	99.06	100.73	100.98	99.64
Si	5.91	5.93	5.91	5.89	5.91	5.82	5.92
Ti	0.01	0.01	0.01	0.00	0.01	0.00	0.01
Al	4.02	4.02	4.04	4.03	4.02	4.04	4.07
Fe	4.91	4.20	4.84	3.54	4.05	3.85	4.58
Mn	0.10	0.01	0.13	0.23	0.04	0.17	0.10
Mg	0.37	0.45	0.72	2.11	0.50	2.10	0.44
Ca	0.76	1.42	0.43	0.28	1.52	0.17	0.93
TOTAL	16.07	16.05	16.07	16.09	16.06	16.16	16.04
Endmembers							
Py	5.96	7.44	11.82	34.16	8.23	33.34	7.23
Alm	80.02	69.04	79.07	57.43	66.29	61.18	75.64
Gro	12.34	23.32	6.96	4.61	24.78	2.76	15.40
Sp	1.67	0.19	2.15	3.80	0.71	2.71	1.72
total	100.00	100.00	100.00	100.00	100.00	100.00	100.00

APPENDIX B

Chrome spinel data from the Bengal basin

	Bsr. 5.1-13 (Oligo.)	Bsr. 5.1-14(Oligo.)	Bsr. 5.1-15(Oligo.)	Bsr. 5.1-16 (Oligo.)	Bsr. 5.1-17(Oligo.)	Bsr. 21.2-4 (Oligo.)
SiO2	0.01	0.08	0.07	0.08	0.09	0.01
TiO2	0.06	1.00	0.92	0.72	0.48	0.16
Al2O3	17.17	24.82	20.11	22.31	17.77	22.93
Cr2O3	49.8	38.36	44.78	43.51	49.48	37.5
V2O3	0	0	0	0	0	0
FeO	23.37	23.52	21.35	17.67	23.55	28.54
MnO	0.09	0.19	0.317	0	0.19	0.27
MgO	9.87	12.08	12.52	14.2	9.7	6.74
CaO	0.02	0	0.01	0	0.001	0
Zno	0	0	0	0	0	0
Total	100.41	100.07	100.09	98.50	101.27	96.16
Si	0.00	0.02	0.01	0.021	0.02	0.00
Ti	0.01	0.18	0.17	0.13	0.09	0.03
Al	5.16	7.14	5.88	6.48	5.29	7.13
Cr	10.04	7.40	8.78	8.48	9.89	7.82
V	0	0	0	0	0	0
Fe(ii)	4.98	4.80	4.43	3.64	4.98	6.29
Mn	0.02	0.03	0.06	0	0.04	0.06
Mg	3.75	4.39	4.63	5.22	3.65	2.65
Ca	0.00	0	0.00	0	0.00	0
Zn	0	0	0	0	0	0
TOTAL	24	24	24	24	24	24
Fe/Fe+Mg	0.57	0.52	0.48	0.41	0.57	0.70
Cr/Cr+Al	0.66	0.50	0.59	0.56	0.65	0.52
Fe(ii)	4.23	3.76	3.48	2.93	4.41	5.32
Fe(iii)	0.75	1.03	0.94	0.71	0.56	0.97
Fe2/(Fe2+Fe3)	0.84	0.78	0.78	0.80	0.88	0.84
Fe3/(Fe3+Fe2)	0.15	0.21	0.21	0.19	0.11	0.15

Chrome Spinel data continued..

	Bsr. 21.2-5 (Oligo.)	Bsr. 21.2-6 (Oligo.)	Bsr. 21.2-7 (Oligo.)	Bsr. 21.2-8 (Oligo.)	Bsr. 21.2-9 (Oligo.)	Bsr. 8.1-10(Oligo.)
SiO2	0.05	0.01	0.12	0.05	0.00	0.02
TiO2	0.04	1.44	1.40	0.59	0.03	0.28
Al2O3	7.03	12.44	24.12	31.31	29.69	46.72
Cr2O3	58.07	48.64	35.04	33.11	38.13	19.9
V2O3	0	0	0	0	0	0
FeO	23.38	23.92	25.54	17.84	17.43	14.23
MnO	0.43	0.29	0.17	0.21	0.07	0.13
MgO	6.4	10.19	11.74	15.83	13.57	18.08
CaO	0.03	0.00	0	0.02	0.02	0.05
Zno	0	0	0	0	0	0
Total	95.45	96.96	98.15	98.99	98.95	99.42
Si	0.01	0.00	0.03	0.01	0.00	0.00
Ti	0.00	0.29	0.26	0.10	0.00	0.04
Al	2.37	3.92	7.08	8.65	8.39	12.00
Cr	13.15	10.29	6.90	6.14	7.23	3.43
V	0	0	0	0	0	0
Fe(ii)	5.60	5.35	5.32	3.49	3.49	2.59
Mn	0.10	0.06	0.03	0.04	0.01	0.02
Mg	2.73	4.06	4.36	5.53	4.85	5.87
Ca	0.01	0.00	0	0.00	0.00	0.01
Zn	0	0	0	0	0	0
TOTAL	24	24	24	24	24	24
Fe/Fe+Mg	0.67	0.56	0.54	0.38	0.41	0.30
Cr/Cr+Al	0.84	0.72	0.49	0.41	0.46	0.22
Fe(ii)	5.17	4.16	3.89	2.53	3.13	2.13
Fe(iii)	0.42	1.19	1.42	0.96	0.36	0.45
Fe2/(Fe2+Fe3)	0.92	0.77	0.73	0.72	0.89	0.82
Fe3/(Fe3+Fe2)	0.07	0.22	0.26	0.27	0.10	0.17

Chrome Spinel data continued..

	Bsr. 8.1-12 (Oligo.)	Bsr. 8.1-13 (Oligo.)	Bsr. 8.1-14 (Oligo.)	Bsr. 8.1-15 (Oligo.)	Bsr. 20.2-16 (Oligo.)
SiO2	0.05	0.06	0.09	0.03	0
TiO2	3.12	1.64	0.95	1.85	0.05
Al2O3	15.66	10.02	25.7	16.06	18.24
Cr2O3	42.96	49.44	41.95	44.78	50.22
V2O3	0	0	0	0	0
FeO	31.52	28.3	17.11	20.81	19.79
MnO	0.23	0.18	0.13	0.04	0.23
MgO	6.19	8.53	13.45	12.6	10.87
CaO	0.01	0.01	0.02	0.03	0.00
Zno	0	0	0	0	0
Total	99.76	98.20	99.41	96.21	99.40
Si	0.01	0.01	0.02	0.00	0
Ti	0.62	0.33	0.17	0.36	0.00
Al	4.88	3.19	7.36	4.93	5.47
Cr	8.99	10.57	8.05	9.23	10.11
V	0	0	0	0	0
Fe(ii)	6.97	6.39	3.47	4.53	4.21
Mn	0.05	0.04	0.02	0.01	0.04
Mg	2.44	3.43	4.87	4.89	4.12
Ca	0.00	0.00	0.00	0.00	0.00
Zn	0	0	0	0	0
TOTAL	24	24	24	24	24
Fe/Fe+Mg	0.74	0.65	0.41	0.48	0.50
Cr/Cr+Al	0.64	0.76	0.52	0.65	0.64
Fe(ii)	6.13	4.86	3.28	3.45	3.83
Fe(iii)	0.84	1.53	0.18	1.08	0.38
Fe2/(Fe2+Fe3)	0.87	0.76	0.94	0.76	0.90
Fe3/(Fe3+Fe2)	0.12	0.23	0.05	0.23	0.09

APPENDIX C

Tourmaline data from the Bengal basin

	Tourmaline standard	Bsr. 11.1-22(Oligo.)	Bsr. 11.1-23(Oligo.)	Bsr. 11.1-24(Oligo.)	Bsr. 11.1-25(Oligo.)	Bsr. 11.1-26(Oligo.)
SiO2	40.16	35.36	34.45	36.43	34.63	35.89
TiO2	4.72	0.45	1.21	0.51	0.23	0.66
Al2O3	14.26	34.99	32.10	32.86	34.34	33.79
FeO	11.22	7.23	12.89	8.31	15.40	7.16
MnO	0.21	0.05	0.10	0.10	0.15	0.11
MgO	11.68	5.99	3.14	6.27	0.47	6.32
CaO	10.32	1.07	0.52	0.15	0.17	0.70
Na2O	2.50	1.68	1.90	2.30	1.89	1.78
K2O	2.00	0.07	0.06	0.01	0.06	0.03
Si	6.37	5.73	5.80	5.93	5.81	5.84
Ti	0.56	0.05	0.15	0.06	0.03	0.08
Al	2.66	6.69	6.37	6.30	6.79	6.48
Fe(ii)	1.48	0.98	1.82	1.13	2.16	0.97
Mn	0.02	0.01	0.01	0.01	0.02	0.01
Mg	2.76	1.45	0.79	1.52	0.12	1.53
Ca	1.75	0.19	0.09	0.03	0.03	0.12
Na	0.77	0.53	0.62	0.73	0.61	0.56
K	0.40	0.01	0.01	0.00	0.01	0.01
TOTAL	16.81	15.64	15.68	15.72	15.58	15.62
AL	--	6.28	5.98	5.92	6.37	6.09
Al50Fe(tot)50	--	3.60	3.84	3.49	4.20	3.50
Al50Mg50	--	3.82	3.36	3.67	3.24	3.76
Ca	--	0.17	0.09	0.02	0.03	0.11
Fe(tot)	--	0.92	1.70	1.06	2.03	0.91
Mg	--	1.36	0.74	1.43	0.11	1.44

Tourmaline data continued..

	Bsr. 11.1-27 (Oligo.)	Bsr. 11.1-28 (Oligo.)	Bsr. 17-32 (Oligo.)	Bsr. 17-33 (Oligo.)	Bsr. 17-34 (Oligo.)	Bsr. 17-35(Oligo.)
SiO2	35.68	34.58	35.45	33.32	35.39	34.86
TiO2	1.82	0.90	0.70	1.13	0.70	0.49
Al2O3	31.81	26.71	34.14	33.54	29.16	34.75
FeO	10.84	12.68	4.72	11.31	9.42	8.63
MnO	0.09	0.12	0.06	0.03	0.02	0.03
MgO	4.59	7.15	7.38	3.61	7.53	4.60
CaO	0.10	1.45	0.20	0.31	0.57	0.73
Na2O	1.90	2.13	2.05	2.08	2.44	1.61
K2O	0.01	0.05	0.00	0.06	0.02	0.05
Si	5.90	5.94	5.81	5.63	5.96	5.76
Ti	0.23	0.12	0.09	0.14	0.09	0.06
Al	6.19	5.40	6.59	6.68	5.79	6.76
Fe(ii)	1.50	1.82	0.65	1.60	1.33	1.19
Mn	0.01	0.02	0.01	0.00	0.00	0.00
Mg	1.13	1.83	1.80	0.91	1.89	1.13
Ca	0.02	0.27	0.04	0.06	0.10	0.13
Na	0.61	0.71	0.65	0.68	0.80	0.51
K	0.00	0.01	0.00	0.01	0.00	0.01
TOTAL	15.59	16.11	15.63	15.73	15.96	15.56
Al	5.82	5.07	6.19	6.27	5.43	6.35
Al50Fe(tot)50	3.61	3.39	3.40	3.89	3.34	3.73
Al50Mg50	3.44	3.39	3.94	3.56	3.60	3.71
Ca	0.02	0.25	0.03	0.05	0.10	0.12
Fe(tot)	1.41	1.71	0.61	1.50	1.25	1.12
Mg	1.06	1.72	1.69	0.85	1.77	1.06

Tourmaline data continued..

	Bsr. 17-36 (Oligo.)	Bsr. 17-37 (Oligo.)	Bsr. 17-38 (Oligo.)	Bsr. 17-39 (Oligo.)	Bsr. 21.2-3 (Oligo.)	Bsr. 1.2-17 (Oligo.)
SiO2	34.70	35.62	35.44	35.14	34.73	35.02
TiO2	0.52	0.53	0.34	0.54	0.90	0.65
Al2O3	35.20	30.01	32.03	27.02	28.68	34.98
FeO	10.65	8.12	9.70	10.34	13.15	8.18
MnO	0.00	0.04	0.04	0.04	0.31	0.01
MgO	2.71	8.33	6.22	8.84	4.83	5.09
CaO	0.18	2.06	0.48	3.51	0.93	1.00
Na2O	1.80	1.60	2.20	1.09	1.99	1.70
K2O	0.05	0.04	0.04	0.07	0.08	0.05
Si	5.77	5.89	5.86	5.91	5.95	5.72
Ti	0.07	0.07	0.04	0.07	0.12	0.08
Al	6.90	5.85	6.24	5.36	5.79	6.73
Fe(ii)	1.48	1.12	1.34	1.46	1.88	1.12
Mn	0.00	0.00	0.00	0.01	0.05	0.00
Mg	0.67	2.05	1.53	2.22	1.23	1.24
Ca	0.03	0.37	0.08	0.63	0.17	0.17
Na	0.58	0.51	0.71	0.36	0.66	0.54
K	0.01	0.01	0.01	0.02	0.02	0.01
TOTAL	15.51	15.88	15.83	16.02	15.87	15.61
Al	6.48	5.49	5.86	5.03	5.44	6.32
Al50Fe(tot)50	3.93	3.27	3.56	3.20	3.60	3.68
Al50Mg50	3.55	3.71	3.65	3.56	3.30	3.74
Ca	0.03	0.34	0.08	0.59	0.16	0.16
Fe(tot)	1.39	1.05	1.26	1.37	1.77	1.05
Mg	0.63	1.93	1.44	2.08	1.16	1.16

Tourmaline data continued..

	Bsr. 1.2-18 (Oligo.)	Bsr. 1.2-19 (Oligo.)	Bsr. 1.2-20 (Oligo.)	Bsr. 1.2-21 (Oligo.)
SiO2	35.71	35.13	34.66	35.84
TiO2	0.88	0.89	0.73	0.30
Al2O3	32.71	34.11	34.84	34.45
FeO	10.27	8.55	8.44	9.24
MnO	0.04	0.00	0.09	0.07
MgO	4.67	5.12	4.76	4.63
CaO	0.70	1.50	1.51	0.22
Na2O	1.51	0.70	0.87	1.90
K2O	0.01	0.02	0.04	0.04
Si	5.896	5.78	5.71	5.86
Ti	0.110	0.11	0.09	0.04
Al	6.365	6.61	6.76	6.64
Fe(ii)	1.418	1.18	1.16	1.26
Mn	0.006	0.00	0.01	0.01
Mg	1.150	1.26	1.17	1.13
Ca	0.124	0.26	0.27	0.04
Na	0.483	0.22	0.28	0.60
K	0.002	0.00	0.01	0.01
TOTAL	15.55	15.42	15.46	15.59
Al	5.98	6.21	6.35	6.23
Al50Fe(tot)50	3.65	3.65	3.72	3.71
Al50Mg50	3.53	3.69	3.72	3.65
Ca	0.12	0.25	0.25	0.04
Fe(tot)	1.33	1.10	1.09	1.19
Mg	1.08	1.18	1.10	1.06

APPENDIX D

Amphibole data from the Bengal basin

	Amphibole standard	Bsr. 11.1-21 (Oligo.)	Bsr. 11.1-29 (Oligo.)	Bsr. 11.1-30 (Oligo.)	Bsr. 11.1-31 (Oligo.)
SiO2	40.16	46.87	42.09	44.37	48.79
TiO2	4.72	0.28	0.47	1.11	0.29
Al2O3	14.26	9.79	12.95	11.51	7.25
Cr2O3	0.00	0	0	0	0
FeO	11.22	8.99	16.03	13.95	12.26
MnO	0.21	0.70	0.30	0.23	0.31
MgO	11.68	16.74	10.65	12.4	15.03
CaO	10.32	12.34	12.96	12.14	13.11
Na2O	2.50	1.79	1.10	1.17	0.65
K2O	2.00	0.14	0.42	0.54	0.15
ZrO2	0	0	0	0	0
Si	5.97	6.65	6.27	6.47	7.01
Ti	0.53	0.03	0.05	0.12	0.03
Al	2.50	1.64	2.27	1.98	1.23
Cr	0.00	0.00	0.00	0.00	0.00
Fe(ii)	1.39	1.07	2.00	1.70	1.47
Mn	0.03	0.08	0.04	0.03	0.04
Mg	2.59	3.54	2.37	2.70	3.22
Ca	1.64	1.87	2.07	1.90	2.02
Na	0.72	0.49	0.32	0.33	0.18
K	0.38	0.03	0.08	0.10	0.03
Zr	0.00	0.00	0.00	0.00	0.00
TOTAL	15.74	15.39	15.47	15.33	15.23
Fe3+/(Fe3++[6]Al)		0.51	0.60	0.36	0.69
Mg/(Mg+Fe2+)		0.83	0.65	0.66	0.77